I 2583
XVI
ESBA
1993

Visualization of Uptake and Processing of Lipoproteins by Various Liver Cell Types

E38

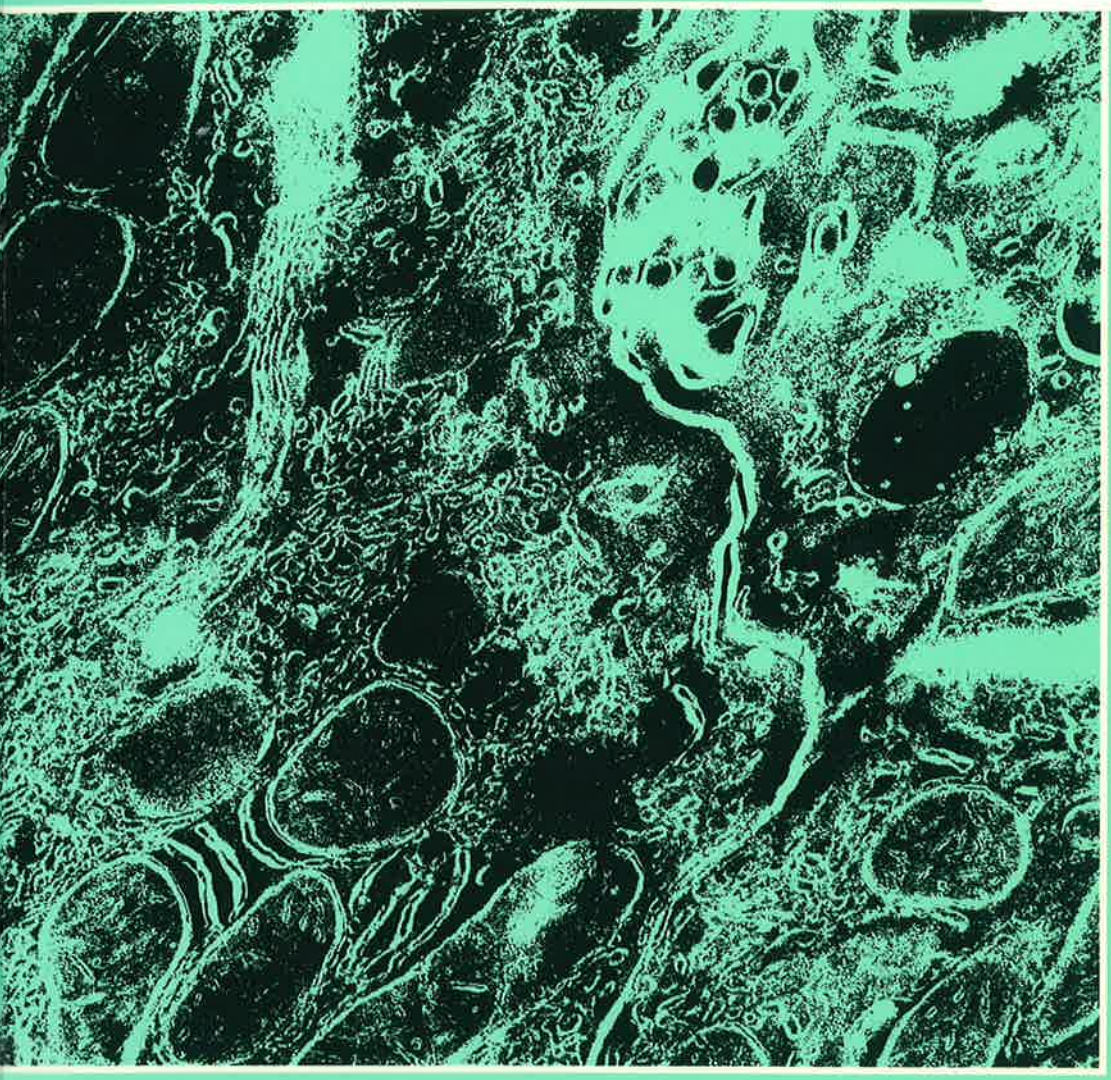

Bas Esbach

I 2583

Visualization of Uptake and Processing of Lipoproteins by Various Liver Cell Types

CIP-GEGEVENS KONINKLIJKE BIBLIOTHEEK, DEN HAAG

Esbach, Sebastiaan

Visualization of uptake and processing of lipoproteins by various liver cell types / Sebastiaan Esbach. - [S.l. : s.n.]. - Ill.
Proefschrift Leiden. - Met lit. opg.
ISBN 90-5412-016-9
Trefw.: lipoproteïnen / levercellen.

Stellingen

1. De complexe interactie van geoxideerde LDL-partikels met Kupffercellen leidt tot een zeer efficiënte galuitscheiding van de cholesterolesters van de partikels.
   (dit proefschrift)

2. Het fysiologische belang van de LDL-receptor voor de opname van VLDL-remnants door parenchymcellen lijkt gering.
   (dit proefschrift)

3. Gedurende een economische recessie zijn in analogie met de evolutietheorie van Darwin generalisten beter toegerust om te overleven dan specialisten.

4. De huidig vereiste flexibele inzetbaarheid van personeel is strijdig met de negatieve houding van personeelsfunctionarissen ten opzichte van "part-time" werken.
   (Intermediair 1993; 11: 47)

5. Financiële sancties lijken zwaarder te wegen dan de persoonlijke belangen van AIO's en OIO's om promotie-projecten binnen de gestelde termijn af te ronden.
   (Mediator 1993; 3: 3)

6. Het verschil tussen spel en sport bestaat uit het respectievelijk eindig en oneindig aantal statistische mogelijkheden.
   (Ing. Th.M. Laurman, wiskundige 1938-1988)
   Een belangrijk deel van de tijdsbesteding van werknemers moet dan ook als sport worden betiteld en niet als het spelen van spelletjes.

7. De houding ten opzichte van materiële zaken in een wegwerpmaatschappij mag niet los gezien worden van een verandering in de attitude ten opzichte van de waarde die toegekend wordt aan leven.

8. De kunde van mensen is vaak hun beperking.
   (J. Reeberg, oud-wereldkampioen karate)

Leiden, 13 december 1993

Sebastiaan Esbach

Visualization of Uptake and Processing of Lipoproteins by Various Liver Cell Types

Proefschrift

ter verkrijging van de graad van Doctor
aan de Rijksuniversiteit te Leiden,
op gezag van de Rector Magnificus Dr. L. Leertouwer,
hoogleraar in de faculteit der Godgeleerdheid,
volgens besluit van het College van Dekanen
te verdedigen op maandag 13 december 1993
te klokke 16.15 uur

door

Sebastiaan Esbach

geboren in 1963 te Goirle

Promotiecommissie:

Promotoren:	Prof.dr. D.L. Knook
	Prof.dr. Th.J.C. van Berkel
Co-promotor:	Dr. A. Brouwer (IVVO-TNO)
Referent:	Prof.dr. M.J. Hardonk (Rijksuniversiteit Groningen)
Overige leden:	Prof.dr. D.D. Breimer
	Prof.dr. B.J. Vermeer
	Prof.dr. E. Wisse (Vrije Universiteit Brussel)

The studies presented in this thesis were performed at the IVVO-TNO, Gaubius Laboratory, Leiden and at the former TNO Institute for Experimental Gerontology, Rijswijk. The studies were financially supported by the Dutch Foundation for scientific research (NWO-MEDIGON 900-523-091).

Financial support by the IVVO-TNO and by the Netherlands Heart Foundation for the publication of this thesis is gratefully acknowledged.

Aan Evelien

Contents

		page
Chapter 1	**General Introduction**	1
	1.1 Lipoproteins	1
	1.2 Lipoproteins and atherosclerosis	3
	1.3 Lipoproteins and liver	4
	1.3.1 Liver cells	6
	1.3.2 Lipoprotein binding sites	8
	1.3.3 Uptake and processing of lipoproteins by liver cells	10
	1.4 Methods of visualization	12
	1.5 Scope of the thesis	14
	1.6 References	14
Chapter 2	**Visualization of the Uptake and Processing of Oxidized Low Density Lipoproteins in Human and Rat Liver.** S. Esbach, M.N. Pieters, J. van der Boom, D. Schouten, M.N. van der Heyde, P.J.M. Roholl, A. Brouwer, Th.J.C. van Berkel and D.L. Knook.	19
Chapter 3	**Cholesteryl Esters from Oxidized Low Density Lipoproteins are *In Vivo* Rapidly Hydrolysed in Rat Kupffer Cells and Transported to Liver Parenchymal Cells and Bile.** M.N. Pieters, S. Esbach, D. Schouten, A. Brouwer, D.L. Knook and Th.J.C. van Berkel.	35
Chapter 4	**Morphological Characterization of Scavenger Receptor-Mediated Processing of Modified Lipoproteins by Rat Liver Endothelial Cells.** S. Esbach, M.F. Stins, A. Brouwer, P.J.M. Roholl, Th.J.C. van Berkel and D.L. Knook.	51
Chapter 5	**Visualization of the *In Vivo* Interaction of β-Migrating Very Low Density Lipoproteins with the Remnant Receptor in Rat Liver.** S. Esbach, J. van der Boom, M.N. Pieters, D. Schouten, P.J.M. Roholl, A. Brouwer, D.L. Knook and Th.J.C. van Berkel.	67

Chapter 6 **Visualization of the Interaction of β-Migrating Very Low Density Lipoproteins with Human Liver Cells: Involvement of Remnant- and LDL Receptors.** 83
S. Esbach, A. Bosma, A. Brouwer, Th.J.C. van Berkel and D.L. Knook.

Chapter 7 **The Fate of Recombinant Rat Bile Salt-Stimulated Cholesterol Ester Hydrolase *In Vivo*.** 93
D. Schouten, S. Esbach, M.N. Pieters, D.Y. Hui, A. Brouwer, D.L. Knook and Th.J.C. van Berkel.

Chapter 8 **General Discussion and Conclusions** 105
8.1 Visualization techniques 105
8.2 Uptake and processing of modified LDL 108
8.3 Uptake and processing of β-VLDL 111
8.4 Reverse cholesterol transport and selective uptake 113
8.5 Conclusions 114
8.6 References 115

Summary 117

Samenvatting 120

Abbreviations 124

Curriculum Vitae 125

Chapter 1

General Introduction

1 Introduction

Epidemiological data have indicated the relation between lipoproteins and the development of coronary artery disease, establishing the clinical relevance of these particles and their metabolism. In the last decade it appeared that especially the liver plays a prominent role in lipoprotein synthesis and metabolism. The present thesis is focused on the liver uptake and processing of atherogenic lipoproteins with special attention given to the role of the various liver cell types. Visualization techniques are used in order to obtain a detailed description of the mechanisms involved in binding, internalization and processing, both in human and rat liver. In this chapter some aspects of lipoproteins, liver cells and visualization techniques will be introduced.

1.1 Lipoproteins

Plasma lipoproteins are water soluble particles with a high molecular weight. Their function is to transport water insoluble lipids, such as triglycerides and cholesterol, from the site of synthesis or uptake through the blood and lymph to the site of degradation or storage (see for review 1). In order to transport lipophilic substances through a hydrophylic environment, the triglycerides and cholesteryl esters are localized in the core of the lipoprotein particles surrounded by a hydrophylic shell. The shell contains specific proteins, the so-called apolipoproteins, which are embedded in a monolayer of phospholipids. Unesterified cholesterol is present in the core as well as at the surface of the lipoprotein particles (2).

Four major classes of plasma lipoproteins can be distinguished based on the buoyant density of the particles as determined by ultracentrifugation (3,4). The classes differ in size and in the relative composition of cholesterol, triglyceride and apolipoproteins (Table 1) (5). The larger particles contain relatively more lipid, especially neutral lipids, explaining why the density of the particles decreases with increasing size. It is important to realize that the apolipoproteins do not only have a structural function in stabilizing the lipoproteins, but also perform a major role in mediating cell recognition (see 1.3.2), and enzyme activation (1).

Table 1. Physical properties and composition of human plasma lipoproteins.

	Lipoprotein			
	Chylomicrons	VLDL	LDL	HDL
Density (g/ml)	< 0.95	0.95 - 1.006	1.019 - 1.063	1.063 - 1.21
Size (nm)	80 - 1000	35 - 60	20 - 25	8 - 12
Triglycerides (%)	90	60	10	5
Phospholipids	5	15	22	25
Cholesterol esters	2	13	38	25
Cholesterol	1	7	8	4
Protein	2	5	22	41

Chylomicrons ($d < 0.950$) are the largest lipoproteins, varying in size from 80 to 1200 nm (6). Their function is the transportation of dietary lipids. Dietary lipids are taken up from the intestine by the enterocytes, which incorporate the fatty components into chylomicrons (7). These triglyceride-rich particles (Table 1) are secreted into the lymph and subsequently enter the blood compartment where they are metabolized into chylomicron remnants (8). During circulation the chylomicrons acquire apolipoprotein E and C (9), which are important for receptor recognition of the particles and activation of the enzyme lipoprotein lipase (LPL) (10). Lipoprotein lipase, which is located on the surface of vascular endothelial cells of extrahepatic tissues (11), hydrolyses the triglycerides of the chylomicrons. The free fatty acids are used as an energy source by muscle or taken up into adipose tissue were they are re-esterified and stored as triglycerides. The eventually-formed chylomicron remnants are rapidly internalized by the liver (12).

Very low density lipoprotein (VLDL) ($0.950 < d < 1.006$) is in comparison to chylomicrons a smaller triglyceride-rich fraction ranging in size from 35 to 60 nm (Table 1). VLDL is synthesized in the liver and carries endogenously synthesized triglyceride as well as cholesterol (13). Similar to the chylomicron metabolism, part of the VLDL particles is metabolized in the circulation into VLDL remnants, while some are metabolized into low density lipoprotein (LDL). Triglycerides are hydrolysed leading to VLDL remnants which contain relatively less triglyceride than VLDL, and to LDL which is almost completely depleted of triglycerides. VLDL remnants are rapidly removed from the circulation by the liver (14).

LDL ($1.019 < d < 1.063$) particles range in size from 20 to 25 nm. LDL predominantly contains cholesterol(esters) (Table 1) and only one apolipoprotein, apolipoprotein B-100. In man, LDL is the main cholesterol-carrying lipoprotein in the blood compartment. LDL is only slowly removed from the circulation; the circulatory period lasting a few days. The liver

is the predominant site of uptake of LDL (15,16).

High density lipoprotein (HDL) ($1.063 < d < 1.21$), the smallest of the lipoprotein classes (8-12 nm), forms a very heterogenous group of particles which originate from liver, intestine and also from the metabolism of triglyceride-rich particles (17-20). They are mainly synthesized as a discoidal precursor which is thereafter metabolized by the enzyme lecithin-cholesterol acyl transferase (LCAT), resulting in vesicular particles which transport cholesteryl esters in the circulation (see for review 20). Besides in cholesteryl esters, HDL particles are rich in protein and phospholipid (Table 1). There are strong indications that in general LDL transports cholesterol to the peripheral tissues, whereas HDL performs the opposite function. Several lines of evidence demonstrated that HDL is able to pick up cholesterol from cells (21-23) and to deliver cholesterol to the liver directly (24) or via an indirect pathway by transfer of cholesteryl esters to other lipoprotein subspecies.

1.2 Lipoproteins and atherosclerosis

Clinical and animal studies confirmed epidemiological studies that showed a strong positive correlation between serum cholesterol levels and the incidence of coronary artery disease in man. Especially the serum LDL cholesterol level was demonstrated to be an important risk factor in the development of atherosclerosis, while HDL cholesterol levels showed a negative correlation, although at first little attention was focused on the latter finding (see for review 25).

Atherosclerotic lesions, as they appear in man or as induced by high cholesterol diets in experimental animals, show many common properties. The narrowing of the vessel lumen is characterized by deposition of cholesterol in and around cells of the arterial wall. The cholesterol that accumulates in the arterial wall is derived from plasma lipoproteins (26,27). One of the early characteristics of the atherosclerotic lesion, both in human and animals, is the appearance of macrophage derived foam cells (28-31). *In vitro* studies showed that native lipoproteins, like LDL, did not provoke excessive accumulation of cholesteryl esters in tissue macrophages, even when exposed to high concentrations of LDL for prolonged periods (32,33). In the late 70's, Brown and Goldstein described a modified form of LDL, acetylated LDL, which was taken up by macrophages with high efficiency, leading to a massive cholesterol accumulation within the cells. This suggested that modification of LDL is an important prerequisite in order to become atherogenic (34). Various modifications of LDL were described, obtained by acetylation (34), malondialdehyde treatment (35), and oxidation (36), all leading to severe cholesterol accumulation in macrophages. The relevance of these modified forms of LDL was evidenced *in vivo* by the group of Steinberg who demonstrated that oxidized LDL was present in atherosclerotic lesions of rabbit and man (37).

Besides the modified forms of LDL mentioned above, another lipoprotein is of interest

because of its atherogenic potential, namely β-migrating VLDL. β-VLDL is a cholesterol-rich particle which has been demonstrated in patients with familial hypercholesterolemia type III and cholesterol-fed animals (38-40). β-VLDL is able to induce an excessive accumulation of cholesteryl esters in macrophages, inducing a foam like appearance (41). In patients with type III hypercholesterolemia an abnormal form of apolipoprotein E, disturbing the normal recognition through its binding site, seems responsible for the high serum levels noticed (42,43). In animals fed a cholesterol-rich chow over a prolonged period, overloading of the hepatic clearance system or increased synthesis may cause the accumulation of β-VLDL in the circulation.

To study the relation between lipoproteins and atherosclerosis several animal models have been used. Although similarity exists in the appearance of the (patho)physiology of atherosclerotic lesions, it is very important to analyze the relevance of animal studies in the human situation. Several differences have been reported between man and animals, not only with respect to the physicochemical characteristics of their plasma lipoproteins and apolipoproteins (see for review 44), but also with regard to receptor expression on cell types (45) and the presence of transfer proteins, like cholesteryl ester transferases. Although these differences may complicate the direct translation of animal studies to the human situation, they can also be of advantage in some aspects. The differences noticed between species in amino acid composition of certain apolipoproteins, which do not effect the receptor-mediated recognition of the apolipoprotein, allow the production of species-specific antibodies. With these antibodies, endocytotic pathways can be distinguished from exocytotic pathways by an experimental approach in which animals and lipoproteins from different species are used which do not show any immunological cross-reaction in their apolipoprotein profiles (see chapter 2).

1.3 Lipoproteins and liver

The most important organ in lipoprotein metabolism is the liver. The liver is involved in the catabolism of lipoproteins, involving uptake and degradation, while also lipoproteins and their constituents are synthesized. One of its unique properties is the ability to subtract cholesterol from the body by excretion into the bile. In Fig. 1 the central role of the liver in the lipoprotein metabolism and its relation to the different lipoprotein classes is schematically represented.

Chylomicrons which transport dietary lipids from the intestine, are after metabolic conversion to chylomicron remnants rapidly internalized by the liver following binding to specialized receptors (46,47). As mentioned before the chylomicrons loose most of their triglycerides to fat and muscle tissue before they reach the liver as relatively cholesterol-enriched particles (48).

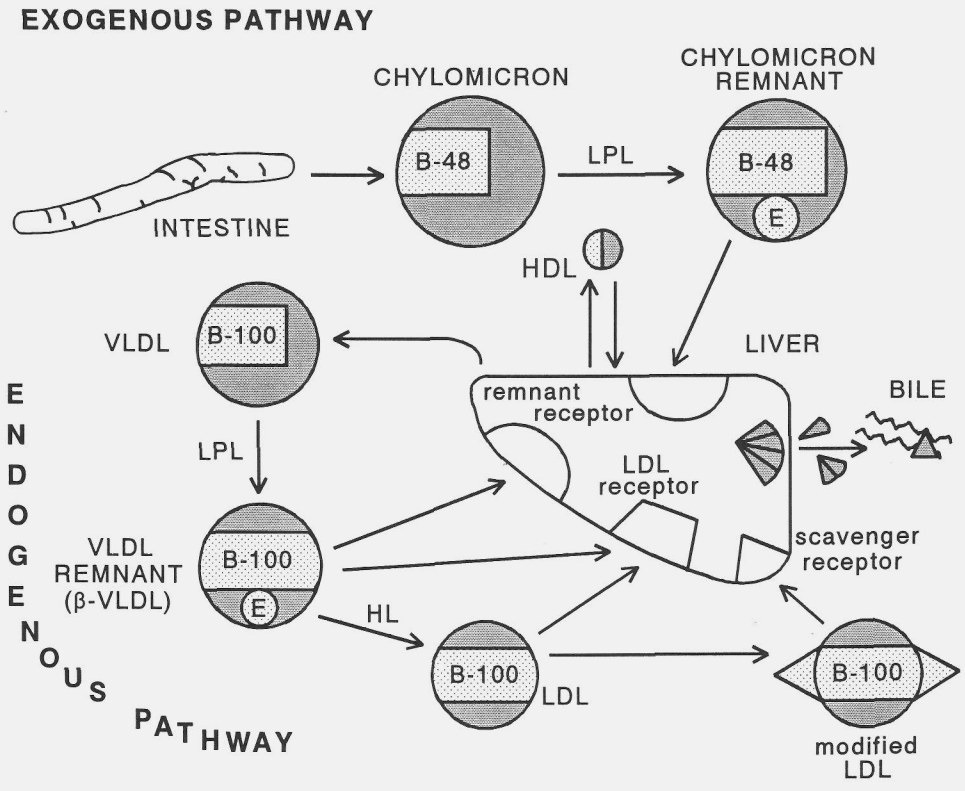

Figure 1. Schematic representation of the central role of the liver in lipoprotein metabolism and its relation to the different lipoprotein classes.

In the liver cholesterol can be excreted into the bile (mostly as bile acids) or repacked into VLDL particles (49,50). In addition to the package of cholesterol, the liver is responsible for the package of triglycerides and the synthesis of the apolipoproteins of VLDL. Subsequently, the different moieties of VLDL are joined together in VLDL particles which are excreted into the blood (49,50), entering the so-called endogenous pathway. VLDL particles are, in the same way as chylomicrons, metabolized into VLDL remnants which are then rapidly internalized by the liver. VLDL can also be metabolized into LDL particles, which process involves, in addition to lipoprotein lipase (LPL) activity, also the liver enzyme hepatic lipase. In man a relatively large portion of the VLDL is metabolized into LDL,

compared to the situation in most animals (see for review 44). There is a strong relation between the amount of LDL in the circulation and the number of LDL receptors expressed in the liver (51). In rabbits and dogs maintained on low-fat diets, the number of LDL receptors is high, while on a high cholesterol diet, a strong suppression of LDL receptor activity was noticed (51).

HDL metabolism also involves an important liver component. The liver plays a role in the synthesis and secretion of HDL precursors and is also involved in the binding of circulating HDL, as part of the so-called reverse cholesterol transport (52).

Besides the important role in synthesis and metabolism of native lipoproteins, the liver is also important for the removal of modified lipoproteins (52). In rat, oxidized LDL and acetylated LDL are rapidly cleared from the circulation by the liver, leading to lysosomal degradation of the particles (53,54). Synthesis, uptake and processing of lipoproteins by the liver can be considered as a highly complex multi-compartment system involving various liver cell types. Therefore, an introduction to some relevant aspects of the liver cells and lipoprotein binding sites will be presented. Current knowledge on the uptake and processing of the different lipoprotein classes by the various liver cells will be discussed in 1.3.3.

1.3.1 Liver cells

The smallest functional unit of the liver is generally considered to be the liver acinus. The major cell types of the liver acinus are parenchymal cells, endothelial cells, Kupffer cells, fat-storing cells and pit cells (Fig. 2). Parenchymal cells are the major cell type with respect to their contribution to cell number and protein mass of the liver which are respectively 67% and 90% in the rat, based on previous studies on volume contributions and protein/volume ratios (55-57). Parenchymal cells are arranged in one layer cords, separated by the sinusoids, radiating from portal veins to central veins. They are in direct contact with the bile canalicular system and perform a major role in most metabolic liver functions.

Non-parenchymal cells only contribute to a minor extent to liver protein mass but they contribute considerably to the total number of liver cells (30-35%) (57,58). Endothelial cells form a continuous lining which separates the parenchymal cells from the sinusoidal lumen (Fig. 2). The interaction of the parenchymal cells with the blood plasma is, however, optimalized by numerous pores in the liver endothelial cells, with a diameter of about 100 nm (59). Because of this pore size, chylomicrons with sizes up to 1200 nm have to be metabolized to smaller particles before they can interact with the parenchymal cells. Endothelial cells contain several morphological structures which point to involvement in uptake and processing, like pinocytotic, tubular and lysosomal structures (55). Micropinocytotic vesicles and macropinocytotic vesicles were described, and it was suggested that both directly arise from plasma membrane invaginations (59-61).

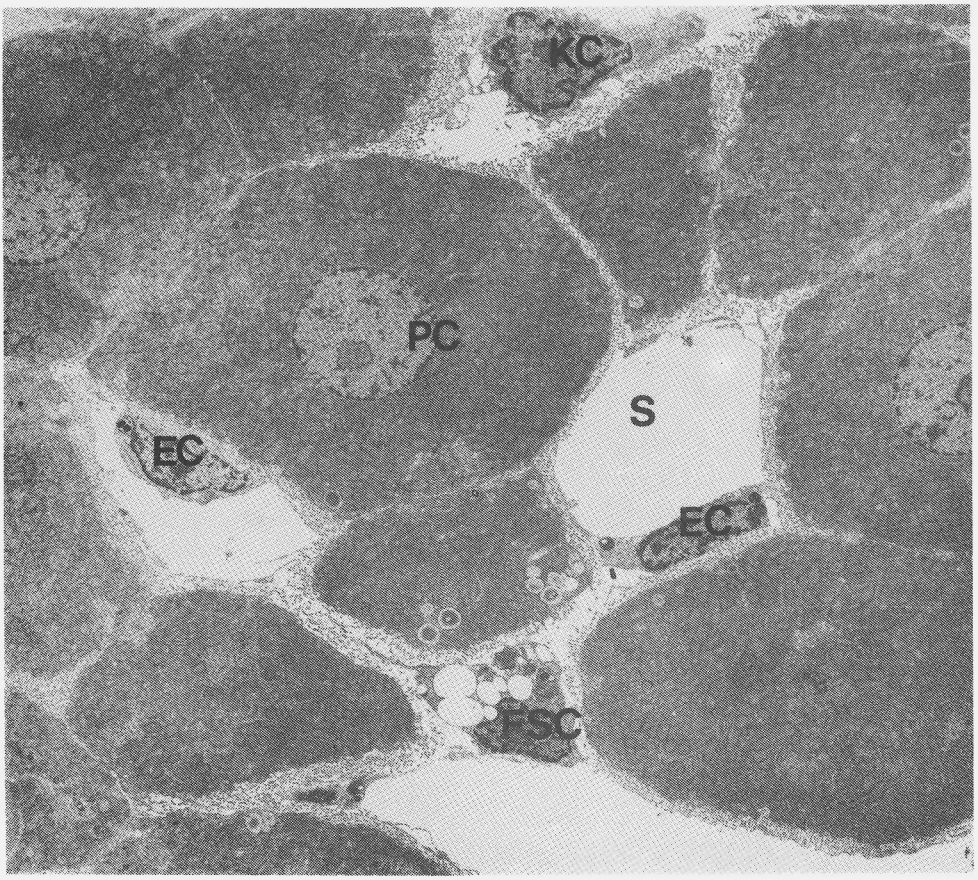

Figure 2. Electron micrograph of part of a rat liver acinus. PC = parenchymal cell, EC = endothelial cell, KC = Kupffer cell, FSC = fat-storing cell, and S = sinusoid. Magnification 2000x.

Kupffer cells are localized inside the sinusoidal lumen (Fig. 2), anchored to the endothelial and parenchymal cells. Their appearance is very characteristic by the presence of all kinds of endocytotic and lysosomal structures. Often in one Kupffer cell pseudopodia, micropinocytotic vesicles, coated macropinocytotic vesicles and worm-like structures are noticed, which are all involved in internalization (61-63).

Kupffer cells and endothelial cells both contribute to the so-called RES clearance system, which protects the organism against all kinds of circulating foreign substances, including bacteria, endotoxins and various macromolecules (64-66). Biochemical data obtained with isolated rat liver cells demonstrated the level of several lysosomal enzymes in endothelial

cells and Kupffer cells to be comparable, while the level of these enzymes in parenchymal cells is much lower (67-69). The diversity of endocytotic mechanisms noticed in the Kupffer and endothelial cells reflects the specialized function of these cell types in clearance from the blood compartment.

Fat-storing (Ito) cells and pit cells or large granular lymphocytes contribute to a minor extent to liver cell numbers and protein mass. Pit cells, localized in the sinusoidal lumen, are probably involved in the protection against metastatic cancer cells because of their natural cytotoxic activity against tumor cell lines (70-72). Fat-storing cells, localized in recesses between parenchymal cells (Fig. 2), contain characteristic fat droplets in their cytoplasm. The number and size of the fat droplets are directly related to the amount of vitamin A which is stored in this cell type (73). Furthermore, fat-storing cells synthesize extracellular matrix components (74), which under pathological conditions might lead to excessive collagen deposition, as noticed in liver fibrosis (see for review 75).

1.3.2 Lipoprotein binding sites

The LDL receptor is a cell surface protein which was first identified on cultured human fibroblasts (76). The receptor is a transmembrane glycoprotein with a molecular weight of 164 kD. It contains several domains involved in binding, clustering into coated pits and subsequent internalization (77,78). The receptor is able to recognize apo B-100 and apoE. The high affinity of lipoproteins containing apoE for the LDL receptor is thought to be caused by the multivalent binding of apoE to the receptor. Most apoE containing lipoproteins do contain several apoE molecules which may interact with several LDL receptors (79). Alternatively, since the LDL receptor contains several repeats which are thought to interact with apoE (80), several apoE molecules of one lipoprotein particle may bind to one receptor multivalently. *In vivo* studies demonstrated that LDL receptors are predominantly expressed in the liver as evidenced by LDL uptake (16,81-83). The expression of the receptor on the parenchymal cells is regulated by cellular cholesterol (84,85), as originally described for cultured human fibroblasts and other cultured cells (86). Studies on animals and humans with genetically deficient LDL receptors showed high blood cholesterol levels and severe atherogenesis at a young age (87,88).

Interestingly, studies performed in LDL receptor deficient animal strains showed that chylomicron clearance was unaffected (89). From these studies it was suggested that another receptor, the so-called remnant receptor, was involved in the clearance of chylomicron remnants. This receptor, localized in the liver, was demonstrated to interact with apoE (90-92), while opposing effects of apoC were noticed (93,94). The presence of apoC's on the lipoproteins probably induces conformational changes in the apoE, which will disturb the receptor recognition. Recently a protein which showed structural and biochemical similarities

to the LDL receptor, the so-called LDL-receptor related protein (LRP), was isolated and suggested to function as remnant receptor (95). Further characterization, however, demonstrated that this function is rather doubtful. The isolated protein appears to function as α2-macroglobulin receptor and α2-macroglobulin binding to rat liver parenchymal cells showed different characteristics as compared to the chylomicron and VLDL remnant binding (96-98). In chapter 5 and 6 the remnant receptor will be further characterized, both in human and rat liver using β-VLDL as a ligand.

Studies by Brown and Goldstein in the early 80's showed the existence of a third lipoprotein receptor, the so-called scavenger receptor (33). The apparent paradox that LDL was not able to cause a severe accumulation of cholesterol in macrophages, while epidemiological data showed a strong correlation between the incidence of coronary artery disease and LDL serum cholesterol levels, was explained by the fact that LDL has to be modified before it is recognized by the scavenger receptors leading to unregulated cholesterol accumulation in the cell. Several high-molecular mass ($\sim$ 250 kD) acetylated LDL (Ac-LDL) binding proteins were isolated by different groups (99-101). Since several binding proteins were identified and several ligands showed cross-reactivity with the binding proteins, the presence of a family of scavenger receptors is suggested, each with their specific characteristics (102).

Besides the involvement of scavenger receptors in the formation of foam cells, a beneficial role of this receptor system in the liver is suggested (53,54). *In vivo* Ac-LDL is rapidly cleared from the blood compartment by the liver by a scavenger receptor mediated mechanism (54,103). Recent evidence indicated that rather oxidative modified LDL (Ox-LDL) is the (patho)physiological representative of modified LDL (see for review 27). *In vitro* cross-competition studies with isolated liver cells demonstrated that two binding sites were involved in Ox-LDL recognition, one recognizing exclusively Ox-LDL, and another recognizing both Ox-LDL and Ac-LDL (53). Further characterization of the Ox-LDL and Ac-LDL scavenger receptors is the subject of study in chapters 2 and 4.

The HDL receptor or binding site is the most puzzling lipoprotein binding site. Specific high affinity binding sites for HDL were found on liver cells of various species (104-106). Binding to the putative receptor seems predominantly mediated by the apolipoprotein AI (24,107,108), the major apolipoprotein of HDL. From porcine liver, two HDL binding proteins were isolated (109). Histological localization of these binding proteins demonstrated that the 90 kD binding site was present in the bile canalicular area of the liver parenchymal cells, while the 180 kD binding protein was present at the plasma membrane. Purification and characterization of HDL binding sites from rat liver membranes also demonstrated two binding sites for HDL of 100 and 120 kD (110). Recently, Oram et al. described the cloning of an HDL binding protein with a molecular weight of 150 kD (111). Although the expression of this protein could be increased several fold when cells were loaded with cholesterol, the predicted structure does not conform to that of any known receptor,

suggesting that it does not function as a classic membrane receptor.

One of the interesting phenomena concerning the HDL interaction with cells is the preferential transfer of cholesteryl esters relative to apolipoprotein AI (112). Extracellular processing of HDL might facilitate such a selective uptake. In this respect we studied in chapter 7 the potential role of a recently described neutral cholesteryl ester hydrolase, which was synthesized by the liver and subsequently secreted into the blood compartment.

1.3.3 Uptake and processing of lipoproteins by liver cells

Three general intracellular routes are associated with receptor recognition.

1) The ligand can be transported through polarized cells without actual degradation. This process of transcytosis was demonstrated for polymeric IgA in endothelial cells and hepatocytes (113,114). Polymeric IgA appeared to be rapidly and actively secreted from blood to bile by rat liver (115).
2) The ligand can be taken up and exocytosed without degradation of the ligand-receptor complex as demonstrated for transferrin. Transferrin is an iron carrier which is endocytosed via a transferrin receptor-mediated mechanism (116). Following endocytosis, the iron is lost from the complex during acidification of the endocytic vesicles. The transferrin and receptor are subsequently recycled to the membrane from a prelysosomal compartment (117).
3) Ligand and receptor can be internalized and subsequently directed to lysosomes where both are degraded as demonstrated for epidermal growth factor (118), or solely the ligand is degraded and the receptor is returned to the plasma membrane for re-use. One of the model systems used to demonstrate the last pathway is the LDL receptor-mediated processing of LDL in cultured fibroblasts (119). Following endocytosis, LDL is transported to the lysosomes and degraded. After internalization, the LDL receptor is, however, recycled to the membrane from a prelysosomal compartment, functionally comparable to the Compartment for Uncoupling of Receptor and Ligand (CURL) as described by Geuze et al. in liver parenchymal cells (120).

With respect to the contribution of the different liver cell types to the uptake and processing of lipoproteins, several biochemical and some morphological studies have been reported.

In rats, chylomicron- and VLDL remnants are rapidly taken up from the circulation by the liver via a receptor-mediated mechanism (12,14). The lipoprotein remnants are predominantly taken up by the liver parenchymal cells and, to a small extent, by the non-parenchymal cells (14,47,121,122). Autoradiography and cell fractionation studies showed that remnants were internalized via coated pits, and subsequently transported via a CURL

compartment and multivesicular bodies into lysosomes (122,123). The protein part of the remnants was degraded while cholesteryl esters are hydrolysed and subsequently excreted into the bile, primarily as bile acids (124).

The major site of uptake of LDL is the liver (16,81-83). In rat and man, parenchymal cells and Kupffer cells are involved in the uptake of LDL. In contrast to man, in untreated rats LDL is predominantly taken up by Kupffer cells (16,83,125). Parenchymal cells internalize and process LDL via a similar intracellular pathway, as described for lipoprotein remnants, involving coated pits, CURL, multivesicular bodies and lysosomes (126,127). Biochemical experiments in estradiol-treated rats, leading to a marked upregulation of LDL receptors on the liver parenchymal cells, however, demonstrated that part of the administered LDL could be transferred into the bile without actual degradation, suggesting also a non-lysosomal intracellular pathway comparable to that described for IgA (127).

Ac-LDL and Ox-LDL are both rapidly cleared from the circulation by the liver (53,54). In rat, Ox-LDL is predominantly taken up by Kupffer cells, while Ac-LDL is predominantly taken up by endothelial cells. In both cell types a rapid degradation of the protein part of the particles occurs (53,54). It was suggested that the pathological deposition of cholesterol in arterial wall macrophages depends on the internalization of aggregated LDL by phagocytosis (128-130). *In vitro* experiments showed that modification of LDL led to an increased tendency to aggregate, especially when the concentration of the lipoproteins was high, ranging from 500 μg/ml up to 3 mg/ml.

Internalization of Ac-LDL by endothelial cells involves coated vesicle formation, but also macropinocytosis may facilitate the highly efficient uptake and degradation of this ligand (131). Cholesteryl esters from Ac-LDL are rapidly hydrolysed by liver endothelial cells, and subsequently appear in the parenchymal cells (132). Re-secretion of cholesterol into the circulation and association with HDL in the serum compartment indicated that transport of cholesterol from the endothelial cells to the parenchymal cells can be mediated by HDL (132). In this thesis the internalization mechanisms involved in the uptake of modified lipoproteins is addressed in chapters 2 and 4, whereas in chapter 3 the Ac-LDL processing by the liver endothelial cells and the Ox-LDL processing by Kupffer cells are compared with respect to the cholesterol handling.

HDL is predominantly taken up by the liver (24). Cell isolation procedures demonstrated that HDL interacts primarily with parenchymal cells and to a small extent with Kupffer and endothelial cells (133). Several mechanisms of binding and subsequent processing of HDL may be present. In bovine aortic endothelial cells and human skin fibroblasts HDL binding induced a cholesterol efflux from plasma membrane and intracellular cholesterol pools, while no actual HDL internalization was noticed (134). In peritoneal macrophages, gold-conjugated HDL was demonstrated to follow a non-lysosomal pathway and re-secretion was noticed from an endosomal compartment after close contact with lipid vacuoles (135-137). Morphological characterization of the interaction of apoE-free HDL with cultured human parenchymal cells

showed that HDL was only bound to the parenchymal cell plasma membrane without any evidence of internalization (138,139). In addition there is no biochemical evidence that binding of HDL to the high affinity binding site on the human parenchymal cells is coupled to internalization and lysosomal degradation (139).

1.4 Methods of visualization

Several morphological, biochemical and subcellular fractionation techniques can be applied to examine the uptake and processing of lipoproteins. In the present thesis we mainly focus on the use of microscopical techniques, which allow the visualization of tissue heterogeneity as well as a detailed analysis of the structures involved or directly related to binding, internalization and processing of the ligands. Although lipoprotein particles can be visualized directly by staining techniques (125,140), a specific localization at the light and electron microscopic level can only be achieved with the use of cytochemical markers. Such markers can be conjugated to a ligand before the actual processing, or applied to visualize the ligand after it has been physiologically handled.

The adequate utilization of a marker pre-conjugated to a ligand depends on the solubility and stability of the conjugate, and whether conjugation of the marker to the ligand interferes with receptor recognition or intracellular processing (141,142). When liver uptake is studied, special caution is needed, since introduced foreign substances can be rapidly cleared from the circulation by this organ (64-66).

Several markers can be associated with a number of ligands to allow a light microscopical localization. Horse radish peroxidase (HRP) produces in combination with diaminobenzidine (DAB) a visible, insoluble reaction product (143); radioactive labels can be detected by autoradiography (144), colloidal gold can be visualized by a silver enhancement technique (145); and fluorescent probes (146-148) can be applied. When HRP is used, endogenous peroxidatic activity should be considered (62). Autoradiography is the only method available which allows the specific detection of lipophilic substances like cholesterol and vitamin A (144,149). Localization of a fluorescent marker can be complicated due to autofluorescence, while some fluorescent markers rapidly fade out. However, fluorescent markers allow the visualization of structures even if they are below the light microscopic resolution limits.

All markers mentioned above can also be used for electron microscopical detection, with the exception of fluorescent probes. In addition, ferritin can be applied to allow the ultrastructural localization of a number of ligands (150,151). Ferritin, however, occurs also naturally in the liver and is, in comparison to gold label, more difficult to detect due to its relatively low electron density. Gold-conjugated ligands have the advantage that rather harsh fixation and embedding procedures may be used, which are not allowed when certain structural aspects of the tissue, as for immuno-histochemical detection, must be maintained.

Since the introduction of immuno-histochemical techniques in the early 40's (152) there is a wide spread use of this technique with all kinds of antibodies, visualization techniques and markers. The visualization techniques based on the use of antibodies can be separated into pre- and post-embedding labeling techniques.

Pre-embedding labeling implies that the labeling procedure is performed before the tissue is embedded, like in freeze etching and freeze fracturing. These techniques allow a detailed analysis of the lateral distribution of cell surface located antigens in combination with gold markers.

Post-embedding labeling techniques are performed on biological tissue which is embedded in plastics such as epon or lowicryl (153), or on frozen material (154). Several requirements have to be met with respect to tissue handling, like maintenance of antigenicity, immobilization of the antigen, preservation of the overall structure, accessibility of antigens, and fixation of fast processes. The basic problem is to compromise between maintenance of antigenicity and proper tissue preservation.

For analyzing the localization of antibodies, several techniques are available: 1) Direct labeling of the antibody, 2) an indirect labeling using labeled secondary antibodies to detect the primary antibody, and 3) three step labeling procedures, including avidin-biotin complexes and enzyme-anti-enzyme complexes (see for review 155). Commonly used markers are fluorescent probes, HRP, alkaline phosphatase (AP), ferritin, and colloidal gold. Each labeling technique and marker has its specific advantages and disadvantages concerning detection, sensitivity, and background labeling, as indicated above. At the EM level currently gold markers are preferred for their visibility and since gold particles of different sizes can be produced, double and even triple labeling experiments can be performed (120).

In the present thesis various strategies are used to visualize several aspects of uptake and processing. Tissue was fixed and embedded in plastic to study optimally preserved tissue for morphological characteristics related to uptake and processing. The cell types which were involved in the uptake of a certain lipoprotein were visualized by detection of fluorescently labeled lipoproteins or by immuno-histochemical detection of the lipoproteins. The LDL receptor was directly visualized by the use of a specific antibody, while the remnant receptor activity was demonstrated by the localization of its ligand, since no specific antibodies for this receptor are presently available. The specificity and nature of the binding were visualized by selective up-regulation of a specific receptor, like for the LDL receptor by estradiol treatment of rats and by competition experiments using unlabeled ligands. Tracer studies were used to visualize the different internalization and processing steps, while internalization mechanisms were visualized by specific membrane staining techniques which discriminated between extracellular and intracellular structures. Intracellular structures were characterized by morphological description and also by double-labeling procedures as for lysosomal enzymes (156).

1.5 Scope of the thesis

The present thesis focuses on the analysis of the processing of lipoproteins by various liver cell types in rat and man. To study the interaction of the lipoproteins with their binding sites, the internalization mechanisms and the intracellular handling, several complementary light microscopical, electron microscopical, biochemical and cell isolation techniques were employed. Modified LDL and β-VLDL were used as ligands because of their atherogenic nature. From biochemical studies it was already quantified to what extent the different liver cell types contributed to the uptake of these lipoproteins. Furthermore, from cross-competition studies, performed with isolated purified liver cells, the specificity of the receptors was already indicated. Experiments performed with isolated human parenchymal and Kupffer cells indicated that in principle the receptors demonstrated on the rat liver cells are also expressed on the human liver cells, although some differences in relative number of receptors per cell are evident.

The mechanisms of binding, internalization and cellular processing of Ox-LDL in Kupffer cells were hitherto unexplored, while the mechanisms of internalization and processing of Ox-LDL and Ac-LDL by the liver endothelial cells with respect to the involvement of the different scavenger receptors needed clarification. The handling of cholesterol of oxidized LDL by the liver is of clinical interest in order to verify if the predominant uptake of this atherogenic particle by the Kupffer cells can be considered as protective for the body. The mechanism of atherogenic β-VLDL handling may involve extracellular interaction with membrane bound apoE. Studies on the recognition and kinetics of uptake were aimed to clarify the potential extracellular processing and the relative importance of the remnant and LDL receptor for the uptake. Extracellular processing of HDL might facilitate selective cholesteryl ester delivery to liver parenchymal cells, leading to the potential possibility that a neutral cholesteryl ester hydrolase, as recently identified in the liver, might be involved. Localization and fate of this enzyme were studied in order to investigate its possible involvement in HDL-metabolism.

1.6 References

1. Gotto AM, Pownall HJ, Havel RJ. In: Segrest JP, Albers JJ. Methods in enzymology 1988;128:3-41.
2. Edelstein C, Kezdy F, Scanu AM, Shen BW. J Lipid Res 1979;20:143.
3. Gofman JW, Lindgren T, Elliott H. J Biol Chem 1949;179:973.
4. Redgrave TG, Roberts DCK, West CE. Anal Biochem 1975;65:42-49.
5. Assmann G. Lipid metabolism and atherosclerosis. Schattauer Verslag GmbH, Stuttgart 1982.
6. Haberbosch W, Poli A, Augustin J. Biochem Biophys Acta 1982;713:398-408.
7. Carey MC, Small DM, Bliss CM. Ann Rev Physiol 1983;45:651-77.
8. Tso P, Balint JA. Am J Physiol (Gastrointest Liver Physiol 13) 1986;250:g715-g726.

9. Imaizumi K, Havel RJ, Fainaru M, Vigne JL. J Lipid Res 1979;19:712-722.
10. LaRosa JC, Levy RI, Herbert R, Lux SE, Frederickson DS. Biochem Biophys Res Commun 1970;41:57.
11. Bengtson G, Olivecrona T. Eur J Bioch 1980;106:549-55.
12. Borensztjan J, Getz GS, Kotlar TJ. J Lipid Res 1988;29:1087-96.
13. Gibbons GF. Biochem J 1990;268:1-13.
14. Van Tol A, van Berkel ThJC. Biochim Biophys Acta 1980;619:156-66.
15. Pittman RC, Attie AD, Carew TE, Steinberg D. Proc Natl Acad Sci USA 1979;76:5345-49.
16. Harkes L, van Berkel ThJC. FEBS Lett 1983;154:75-80
17. Hamilton RL, Williams MC, Fielding CJ, Havel RJ. J Clin Invest 1976;58:667-80.
18. Marsh J. J Lipid Res 1974;15:544-50.
19. Forester GP, Tall AR, Bisgaler CL, Glickman RM. J Biol Chem 1983; 258:5938-43.
20. Eisenberg S. J lipid Res 1984;25:1017-58.
21. Aviram M, Bierman EL, Oram JF. J Lipid Res 1989;30:65-76.
22. Schmitz G, Robenek H, Assman G. Atherosclerosis reviews 1987;19:95-107.
23. Slotte JP, Oram JF, Bierman EL. J Biol Chem 1987;262:12904-07.
24. Glass C, Pittman RC, Civin M, Steinberg D. J Biol Chem 1985;260:744-50.
25. Gotto AM, LaRossa JC, Hunninghake D, Grundy SM, Wilson PW, Clarkson TB, Hay JW. Circulation 1990;81:1721-33.
26. Smith EB. Adv Lipid Res 1974;12:1-49.
27. Steinberg D. Atherosclerosis Rev 1988;18:1-23.
28. Fowler S, Shio H, Haley NJ. Lab Invest 1979;41:372-78.
29. Schaffner T, Taylor K, Bartucci EJ, Fischer-Dzoga K, Beeson JH, Glagov S, Wissler RW. Am J Pathol 1980;100:57-80.
30. Gerrity RG. Am J Pathol 1987;103:181-190.
31. Faggiotto A, Ross R, Harker L. Arteriosclerosis 1984;4:323-40.
32. Brown MS, Goldstein JL. Annu Rev Biochem 1983;52:223-261.
33. Brown MS, Basu SK, Falck JR, Ho YK, Goldstein JL. J Supramol Struct 1980;13:67-81.
34. Goldstein JL, Ho YK, Basu SK, Brown MS. Proc Natl Acad Sci USA 1979;76:333-37.
35. Fogelman AM, Schechter I, Saeger J, Hokom M, Chold JS, Edwards PA. Proc Natl Acad Sci USA 1980;77:2214-18.
36. Parthasarathy S, Steinbrecher UP, Barnett J, Witztum JL, Steinberg D. Proc Natl Acad Sci USA 1985;82:3000-04.
37. Ylä-Herttuala S, Palinski WF, Rosenfeld ME, Parthasarathy S, Carew TE, Butler S, Witztum JL, Steinberg D. J Clin Invest 1989;84: 1086-95.
38. Frederickson DS, Levy RI, Lindgren FT. J Clin Invest 1969;47:2446-57.
39. Shore VG, Shore B, Hart RG. Biochemistry 1979;13:1579-85.
40. Mahley RW. Atheroscler Rev 1979;5:1-34.
41. Goldstein JL, Ho YK, Brown MS, Innerarity TL, Mahley RW. J Biol Chem 1980;255:1839-48.
42. Utermann G, Jaeschke M, Menzel J. FEBS Lett 1975;56:352-55.
43. Schneider WJ, Kovanen PT, Brown MS, Utermann G, Weber W, Havel RJ, Kotite L, Kane JP, Innerarity TL,Mahley RW. J Clin Invest 1981;68:1075-85.
44. Chapman MJ. In: Segrest JP, Albers JJ. Methods in Enzymology 1988;128:70-143.
45. De Water R, Kamps JAAM, Van Dijk MCM, Hessels EMAJ, Kuiper J, Kruijt JK, Van Berkel ThJC. Biochem J 1992;281:41-48.
46. Windler E, Chao Y, Havel RJ. J Biol Chem 1980;255:5475-80.
47. Groot PHE, van Berkel ThJC, Tol A. Metabolism 1981;30:792-97.
48. Bergman EN, Havel RJ, Wolfe BM. J clin invest 1971;50:1831-39.
49. Alexander CA, Hamilton RL, Havel RJ. J Cell Biol 1976;69:241-63.
50. Hamilton RL. In: Glaumann H, Peters T, Redman C. Plasma protein secretion by the liver. 1984:357.

51. Brown MS, Goldstein JL. Scientific American 1984;251:58-66.
52. Glomset JA. J Lipid Res 1968;9:155-67.
53. Van Berkel ThJC, De Rijke YB, Kruijt JK. J Biol Chem 1991;5: 2282-89.
54. Nagelkerke FJ, Barto KP, Van Berkel ThJC. J Biol Chem 1983;258:12221-27.
55. Blouin A, Bolender RP, Weibel ER. J Cell Biol 1977;72:441-55
56. Knook DL. In: Christofalo VJ. handbook series in aging, biological sciences 1984.
57. Greengard O, Federman M, Knox WE. J Cell Biol 1972;52:261-72
58. Fabrikant JI. J Cell Biol 1968;36:551-65.
59. Wisse E. J Ultrastruc Res 1970;31:125-50.
60. Wisse E. J Ultrastruct Res 1972;38:528;62.
61. Wisse E. In: Wisse E, Knook DL. Kupffer cells and other liver sinusoidal cells. Elsevier/North Holland Biomedical Press Amsterdam, 1977:33-60.
62. Wisse E. J Ultrastruct Res 1974;46:393-426.
63. Wisse E. J Ultrastruct Res 1974;46:499-520.
64. Jones EA, Summerfield JA. In: Wisse E, Knook DL. Kupffer cells and other liver sinusoidal cells. Elsevier/North Holland Biomedical Press Amsterdam, 1977:507-23.
65. Praaning-Van Dalen DP, Brouwer A, Knook DL. Gastroenenterology 1981;81:1036-44.
66. Praaning-Van Dalen, Knook DL. FEBS Lett 1982;141:229-32.
67. Van Berkel THJC, Kruijt K, Koster JF. Eur J Biochem 1975;58:145-52.
68. Knook DL. Proc Soc Exp Biol Med 1980;165:170-77.
69. Knook DL, Sleyster ECh. Biochem Biophys Res Commun 1980;96:250-57.
70. Bouwens L, Remels L, Baekeland M,Van Bossuyt H, Wisse E. Eur J Immunol 1987;17:37-42.
71. Vanderkerken K, Bouwens L, Wisse E. Hepatology 1990;11:70-75.
72. Bouwens L, Jacobs R, Remels L, Wisse E. Cancer Immunol Immunother 1988;27:137-41.
73. Wake K. Int Rev Cytol 1980;66:303-53.
74. Kent G, Gay S, Inouye T, Bahu R, Minick OT, Popper H. Proc Natl Acad Sci 1976;73:3719-22.
75. Bissell D. In:Berk p, Lieber C, Schaffner F, Bissell D. Seminars in liver disease 1990;10:1-83.
76. Brown MS, Goldstein JL. Science 1974;185:61-63.
77. Yamamoto T, Davis CG, Brown MS, Schneider WJ, Casey ML, Goldstein JL, Russell DS. Cell 1984;39:27.
78. Lehrman MA, Schneider WJ, Suhof TC, Brown MS, Goldstein JL, Russell DW. Science 1985;277:140-146.
79. Havel RJ, Hamilton RL. Hepatology 1988;8:1689-704.
80. Brown MS, Goldstein JL. Science 1986;232:34-47.
81. Carew TE, Pittman RC, Steinberg D. J Biol Chem 1982;257:8001-08.
82. Bhattacharya S, Balabrasubramaniam S, Simons LA. Biochem J 1984;220:333-36.
83. Harkes L, van Berkel ThJC. Biochem J 1984;224:21-27.
84. Kosykh VA, Preobrazhensky SN, Ivanov VO, Tsibulsky VP, Repin VS, Smirnov VN. FEBS Lett 1985;183:17-20.
85. Edge SB, Hoeg JM, Trich T, Scneider PD, Brewer HB. J Biol Chem 1986;261:3800-06.
86. Brown MS, Goldstein JL. Science 1986;232:34-47.
87. Goldstein JL, Brown MS. In: Stanburry JB, Wyngarden JB, Frederickson DS, Goldstein JL Brown MS. The metabolic basis of inherited disease 1983:672-713.
88. Bilheimer DW, Watanabe Y, Kita T. Proc Natl Acad Sci USA 1982;257:7994-8000.
89. Kita T, Goldstein JL, Brown MS. Proc Natl Acad Sci USA 1982;9:3623-27.
90. Hui DY, Innerarity TL, Mahley RW. J Biol Chem 1981;256:5646-55.
91. Hoeg JM, Demosky SJ, Gregg RE, Schaeffer EJ, Brewer HB. Science 1985;227:759-61.
92. Rubinstein DC, Cohen JC, Berger GM, van der Westhuyzen DR, Coetzee GA, Gevers W. J Clin Invest 1990;86:1306-12.

93. Windler E, Havel RJ. J Lipid Res 1985;26:556-65.
94. Kowal RC, Herz J, Weisgraber KH, Mahley RW, Brown MS, Goldstein JL. J Biol Chem 1990;265:10771-79.
95. Herz J, Hanmann U, Rogne S, Myklebost O, Gausepohl H, Stanley KK. EMBO J. 1988;7:4119-27.
96. Strickland DK, Ashcom JD, Williams S, Burgess WH, Migliorini M, Argraves WS. J Biol Chem 1990;265:17401-404.
97. Van Dijk MCM, Ziere GJ,, Boers W, Linthorst C, Bijsterbosch MK, Van Berkel ThJC. Biochem J 1991;279:863-70.
98. Van Dijk MCM, Kruijt MCM, Boers W, Linthorst C, Van Berkel ThJC. submitted
99. Dresel HA, Friedrich EA, Via DP, Sinn H, Ziegler R, Schettler G. EMBO J 1987;6:319-26.
100. Via DP, Dresel HA, Cheng SL, Gotto AM. J Biol Chem 1985;260:7379-86.
101. Kodama T, Reddy P, Kishimoto C, Krieger M. Proc Natl Acad Sci USA 1988;85:9238-42.
102. Ottnad E, Via DP, Frubis J, Sinn H, Friedrich E, Ziegler R, Dresel HA. Biochem J 1992;281:741-51.
103. Blomhoff R, Drevon CA, Eskild W, Helgerud P, Norum KR, Berg T. J Biol Chem 1984;259:8898-903.
104. Van Berkel ThJC, Kruijt JK, Van Gent T, Van Tol A. Biochem Biophys Res Commun 1980;92:1002-1008.
105. Soltys PA, Portman OW, O'Malley JP. Biochim Biophys Acta 1982;713:300-14.
106. Bachorik PS, Franklin FA, Virgil DG, Kwiterovich PO. Biochemistry 1982;21:5675-84.
107. Chacko GK. Biochim Biophys Acta 1984;795:417-26.
108. Rifici VA, Eder HA. J Biol Chem 1984;259:13814-18.
109. De Crom RPG, Haperen RV, Willemsen R, Van der Kamp AWM. Arteriosclerosis and Thrombosis 1992;12:325-31.
110. Tozuka M, Fidge N. Biochem J 1989;261:239-44.
111. McKnight GL, Reasoner J, Gilbert T, Sundquist KO, Hokland B, McKernan PA, Champagne J, Johnson CJ, Bailey MC, Holly R, O'Hara PJ, Oram JF. J Biol Chem 1992;267:12131-41.
112. Glass C, Pittman RC, Weinstein DB, Steinberg, D. Proc Natl Acad Sci USA 1983;80:5435-39.
113. Brandtzaeg P. J Immunol 1974;112:1553-59.
114. Courtoy PJ, Limet JN, Quintart J, Schneider YJ, Vaerman JP, Baudhuin P. Ann NY Aad Sci 1983;409:799-802.
115. Jackson GDF, Lemaitre-Coelho I, Vaerman JP, Bazin H, Beckers A. Eur J Immunol 1978;8:123-26.
116. Octave JN, Schneider YJ, Crichton RR, Trouet A. Trends Biochem Sci 1983;8:217-19.
117. Harding C, Heuser J, Stahl P. J Cell Biol 1983;97:329-39.
118. Beguinot L, Lyall RM, Willingham MC, Pastan I. Proc Natl Acad Sci USA 1984;81:2384-88.
119. Goldstein JL, Anderson RGW, Brown MS. Nature 1979;279:679-85.
120. Geuze HJ, Slot JW, Strous GJAM, Lodish HF, Schwartz AL. Cell 1983;32:277-87.
121. Blomhoff R, Helgerud P, Rasmussen M, Berg T, Norum KR. Proc Natl Acad Sci USA 1982;79:7326-30.
122. Jones AL, Hradek GT, Hornick C, Renaud G, Windler E, Havel RJ. J lipid Res 1985;25:1151-58.
123. Jackle S, Rundquist E, Brady S, Hamilton RL. J Lipid Res 1991;32:485-98.
124. Van Dijk MCM, Pieters MN, Van Berkel ThJC. Eur J Biochem 1992;211:781.
125. Hamilton RL, Regen DM, Grey ME, LeQuire VS. Lab Invest 1967;16:305-19.
126. Jackle S, Brady SE, Havel RJ. Proc Natl Acad Sci USA 1989;86:1880-84.
127. Kleinherenbrink-Stins MF, Van der Boom J, Bakkeren HF, Roholl PJM, Brouwer A, Van Berkel ThJC, Knook DL. Lab Invest 1990;63:73-86.
128. Khoo JC, Miller E, McLoughlin P, Steinberg D. Arteriosclerosis 1988;8:348-58.
129. Heinecke JW, Suits AG, Aviram M, Chait A. Arteriosclerosis and Thrombosis 1990;11:1643-1651.
130. Hoff HF, Cole TB. Lab Invest 1991;64:254-63.
131. Mommaas-Kienhuis AM, Nagelkerke JF, Vermeer BJ, Daems WTh, Van Berkel ThJC. Eur J Cell Biol 1985;38:42-50.
132. Bakkeren HF, Kuipers F, Vonk RJ, van Berkel ThJC. Biochem J 1990;268:685-91.

133. Schouten D, Kleinherenbrink-Stins MF, Brouwer A, Knook DL, van Berkel ThJC. Biochem J 1988;256,615-21.
134. Oikawa S, Mendez AJ, Oram JF, Bierman EL, Cheung CM. Biochim Biophys Acta 1993;1165:327-34.
135. Robenek H, Schmitz G. Arteriosclerosis 1988;8:57-67.
136. Schmitz G, Robenek H, Beuck MN, Kranse R, Schurek A, Niemann R. Arteriosclerosis 1988;8:46-56.
137. Takata K, Horiuchi S, Torab A, Rahim A, Morino Y. J Lipid Res 1988;29:1117-26.
138. Kleinherenbrink-Stins MF, Van der Boom J, Schouten D, Roholl PJM, Van der Heijde MN, Brouwer A, Van Berkel ThJC, Knook DL. Hepatology 1991;13:79-90.
139. Schouten D, Kleinherenbrink-Stins MF, Brouwer A, Knook DL, van Berkel ThJC. Arteriosclerosis 1990;10:1127-35.
140. Hamilton RL, Wong JS, Luke S, Guo S Krisans S, Havel RJ. J Lipid Res 1990;31:1589-1603.
141. Willingham MC, Hanover JA, Dickson RB, Pastan I. Proc Natl Acad Sci USA 1984;81:175-79.
142. Kleinherenbrink-Stins MF, van der Boom J, Brouwer A, van Berkel ThJC, Knook DL. Ultramicroscopy 1988;24:439A.
143. Willingham MC, Pastan I. J Cell Biol 1982;94:207-12.
144. Hendriks HFJ, Elhanany E, Brouwer A, de Leeuw AM, Knook DL. Hepatology 1988;8:276-85.
145. Danscher D. Histochemistry 1981;71:81.
146. Pitas RE, Boyles J, Mahley RW, Bissell DM. J Cell Biol 1985;100:103-17.
147. Netland PA, Zetter BR, Via DP, Voyta JC. Histochemical J 1985;17:1309-20.
148. Kleinherenbrink-Stins MF, van der Boom J, Schouten D, Roholl PJM, van der Heyde MN, Brouwer A, van Berkel ThJC, Knook DL. Hepatology 1991;13:79-90.
149. Pieters MN, Blauw B, Esbach S, Brouwer A, Knook DL, Van Berkel ThJC, Roholl PJM. submitted.
150. Haigler HT McKanna JA, Cohen S. J Cell Biol 1979;81:382-95.
151. Willingham MC, Haigler HT, Fitzgerald DJP, Gallo MG, Rutherford AV, Pastan I. Exp Cell Res 1983;146:163-75.
152. Coons AH, Creech HJ, Jones RN. Proc Soc Exp Biol Med 1941;47:200-02.
153. Roth J, Bendayan M, Carlemalm E, Villigir W, Garavito M. J Histochem Cytochem 1981;29:663-71.
154. Tokuyasu KT. Histochem J 1980;12:381.
155. Bullock GR, Petrusz P. In: Techniques in Immunocytochemistry. Vol2 NY Acad Press 1983.
156. Geuze HJ, Stoorvogel W, Strous GJ, Slot JW, Bleekemolen JE, Mellman I. J Cell Biol 1988;107:2491-2501.

Chapter 2

Visualization of the Uptake and Processing of Oxidized Low-Density-Lipoproteins in Human and Rat Liver

Sebastiaan Esbach[1], Moniek N. Pieters[2], Johannes van der Boom[1], Donald Schouten[2], M. Niels van der Heyde[3], Paul J.M. Roholl[1*], Adriaan Brouwer[1], Theo J.C. van Berkel[2] and Dick L. Knook[1]

[1] TNO Institute of Ageing and Vascular Research, Gaubius Laboratories, Leiden, The Netherlands.

[2] Division of Biopharmaceutics, Center for Bio-Pharmaceutical Sciences, University of Leiden, Sylvius Laboratories, Leiden, The Netherlands.

[3] Academic Medical Centre, University of Amsterdam, Amsterdam, The Netherlands.

*present address RIVM, Bilthoven, The Netherlands.

Hepatology 1993; 18: 537-545.

Summary

The interaction of oxidized human low density lipoproteins (Ox-LDL) with human and rat liver was analyzed by light and electron microscopy. At the light microscopic level Ox-LDL was visualized by the fluorescent dye 1,1' dioctadecyl 3,3,3',3' tetramethyl indocarbocyanine perchlorate (DiI), whereas at the electron microscopic level, an indirect immuno-labeling procedure was used that detected the apoprotein B of the Ox-LDL. In rats, Ox-LDL was administered intravenously, while uptake by human liver was studied by perfusion of tissue blocks.

Both in human and in rat liver, DiI-Ox-LDL was mainly found to become concentrated in Kupffer cells, and, to a lesser extent, in endothelial cells. In both species the cell association of DiI-Ox-LDL could be inhibited by pre-administration of polyinosinic acid, indicating a scavenger receptor-mediated process.

At the electron microscopic level, Ox-LDL was found to bind mainly to areas of the plasma membrane of the Kupffer cells without clathrin coating, although binding to coated regions was also noticed. Internalization of the ligand occurred through coated vesicle formation, and through membrane folding of interacting lamellipodia and worm-like structures. No indication for phagocytosis of aggregated Ox-LDL particles was noticed. Following internalization, the immuno-reactive Ox-LDL was detected in relatively electron lucent endosomes, and, subsequently, in lysosomes. Endothelial cells internalized Ox-LDL solely through coated pits, after which the particles were transferred through endosomes into lysosomes. The endosomes often contained tubular extensions, which were devoid of immuno-label. In human Kupffer and endothelial liver cells, essentially the same organelles were demonstrated to be involved in the internalization and processing of Ox-LDL as in the rat.

Our morphological results confirm earlier biochemical data on the relative involvement of the various liver cell types in the uptake of Ox-LDL in rats, and the relevance of these data for the human situation is indicated. The uptake process, coupled to Ox-LDL recognition by Kupffer cells, as presently analyzed, indicates that both rat and human Kupffer cells are equipped with a similar removal system to protect the body against the occurrence of the atherogenic Ox-LDL particles in the blood.

Introduction

Macrophage-derived foam cell formation is characteristic in the early atherosclerotic lesion (1). Although the level of serum LDL cholesterol is positively correlated with the occurrence of atherosclerotic lesions, native LDL does not provoke excessive accumulation of cholesteryl esters in tissue macrophages, even when exposed to high concentrations of LDL for

prolonged periods (2, 3). Modified forms of LDL, however, are taken up with high efficiency by macrophages through interaction with the so-called scavenger receptor, resulting in massive cholesterol accumulation within the cells (4). Various types of modification of LDL have been described. These modifications include acetylation (4), malondialdehyde treatment (5) and oxidation (6).

In rats, it was previously demonstrated that acetylated LDL (Ac-LDL) is rapidly cleared from the circulation by the liver through the scavenger receptor on liver endothelial cells (7). More recently, evidence has been obtained which suggests that oxidized LDL is the real (patho)physiological form of modified LDL. Ox-LDL was detectable in, and even extractable from, rabbit and human atherosclerotic lesions (8). The possible mechanisms responsible for LDL oxidation and the atherogenic characteristics of Ox-LDL have been recently reviewed by Witztum and Steinberg (9).

On being injected into rats Ox-LDL is rapidly cleared from the circulation by the liver, as is Ac-LDL (10). However, biochemical data indicate that Kupffer cells rather than endothelial cells are responsible for the liver uptake of Ox-LDL (10). Studies with isolated endothelial and Kupffer cells showed evidence for the presence of an additional scavenger receptor, which is specific for Ox-LDL and highly concentrated on Kupffer cells (10). In our study we used a morphological approach with light and electronmicroscopical techniques to determine to what extent recognition by scavenger receptors uses a phagocytotic or another endocytotic mechanism. Furthermore, the morphological approach also allowed the visualization of the uptake of Ox-LDL in human liver tissue, which has hitherto not been described.

Materials and Methods

Materials

Human serum albumin (HSA) and polyinosinic acid were purchased from Sigma (St. Louis, MO, USA). Gelatin and glycine were obtained from Merck (Darmstadt, West Germany). Tylose (MH 300) was purchased from Fluka (Buchs, Switzerland) and gold-conjugated antibodies from Aurion (Wageningen, Netherlands). Dulbecco's DMEM was obtained from Flow Laboratories (Irvine, Scotland, UK) and DiI was obtained from Molecular Probes (Eugene, OR).

Lipoprotein isolation and modification

LDL ($1.024 < d < 1.055$) was isolated from human plasma plus 1 mM EDTA by density gradient centrifugation according to Redgrave et al. (11). LDL was dialysed against phosphate-buffered saline (PBS) containing 10 μM EDTA before being oxidized (200 μg of protein/ml) by exposure to CuSO4 (5 μM free Cu2+ concentration) as described by Van

Berkel et al. (10). Oxidation was arrested by cooling and addition of 200 μM EDTA. Oxidation of LDL was tested by assessing the electrophoretic mobility on agarose gel. In comparison to native LDL, the Rf value of Ox-LDL was increased from 0.21 ± 0.01 to 0.54 ± 0.01, in accordance to the data of Van Berkel et al. (10).

Oxidized LDL was fluorescently labeled with DiI according to Pitas et al. (12). The density of the DiI and lipoprotein mixture was subsequently raised to 1.21, and the lipoproteins were re-isolated according to the above described procedure. During the isolation of the labeled lipoproteins by density gradient centrifugation Ox-LDL was seen to be of a higher density in comparison to native LDL in accordance to previous data (13).

Animals and perfusion studies

For the visualisation studies on *in vivo* endocytosed Ox-LDL, 3-month-old male Wag/Rij rats were used, weighing about 200 grams. Following centrifugation (1 minute, 1200 g), oxidized LDL (50 μg/ml plasma) was injected into the vena cava inferior of overnight fasted rats under halothane anaesthesia and was allowed to circulate 2 or 10 minutes for light microscopical examination and 0.5, 2, 6 and 30 minutes for electron microscopic studies. For practical reasons Ox-LDL was injected into the portal vein to allow localization studies after 30 seconds of circulation. To study the involvement of the scavenger receptors in the uptake of Ox-LDL, polyinosinic acid, when indicated, was injected 1 minute prior to the lipoproteins in a concentration of 4 mg/kg body weight. Subsequently, rat livers were rinsed shortly with PBS up to 1 minute, or directly fixed with 4% paraformaldehyde (PF) and 0.1% glutaraldehyde (GA) in PBS by *in situ* perfusion via the portal vein for 10 minutes. Livers were stored in 2% PF in PBS. Rat livers that were only used for ultrastructural examination were fixed and stored according to the above described procedure using 2% GA in PBS.

Light- and electronmicroscopical studies

Fixed liver tissue was dissected and 200 μm vibratome slices were prepared. Specimens that were used for immuno-histochemical study were embedded in 5% gelatin, and immersed in 2.3 M sucrose in PBS, overnight. Specimens that were used for fluorescence microscopy were directly immersed in 2.3 M sucrose. To prepare cryosections, small pieces were placed on a specimen holder and frozen in liquid nitrogen. Semithin or ultrathin cryosections were cut using a Reichert FC-4D Ultracut cryomicrotome at a temperature of -100°C. To localize DiI-fluorescence, semithin sections were placed on a glass cover slip and after being mounted with glycerol viewed with a Leitz ortholux microscope with standard rhodamine excitation and emission filters. Ultrathin sections were placed on carbon coated nickel grids for immuno-labeling.

To differentiate between intracellular and extracellular compartments in order to study the internalisation mechanisms, 200 μm vibratome sections were stained *en bloc* with the membrane mordant stain ruthenium red according to Handley et al. (14) and, subsequently,

dehydrated in a graded series of ethanol and embedded in epon.

Livers that were used only for ultrastructural examination were postfixed in 1% OsO4 in 0.15 M sodium cacodylate buffer for 45 minutes, dehydrated, and, embedded in epon. Ultrathin sections were examined in a Philips EM 410 electron microscope.

Antibodies and immuno-labeling procedure

Antibodies against human apolipoprotein B (apoB), raised in rabbits, were kindly donated by Dr. L. Havekes (IVVO-TNO, Leiden, the Netherlands). The antibody was tested for reactivity with native and modified LDL using the double radial immuno-diffusion method as described by Crowle (15). Results showed that Ox-LDL had sufficiently retained antigenicity to allow use of the antibody against native LDL for immuno-cytochemical studies. Cross-reactivity with the rat lipoproteins LDL, VLDL and HDL, and lipoprotein-deficient rat serum was absent (16). In some cases, mouse antibodies against ED2 were used in double-labeling experiments to detect Kupffer cells. Antibodies against ED2 were kindly donated by Dr. C. Dijkstra (VU, Amsterdam, the Netherlands). The specificity has been described previously (17).

For the immuno-labeling procedure, antisera and gold conjugates were diluted in PBS containing 0.1% gelatin, 0.5% BSA and 0.1% Tween 20. The dilutions used were: anti-apoB, 600 fold, anti ED2, 100 fold, goat anti-rabbit IgG-gold (6nm), 30 fold, and protein A-gold (10 nm), 50 fold. For the washing steps the same medium was used, unless otherwise indicated.

Cryosections were incubated with 0.05 M glycine in PBS, washed, incubated with 10% non-immune rat serum followed by incubation with the primary antibody, washed, incubated with the secondary antibody coupled to colloidal gold, washed, washed again with aqua dest, stained with uranylacetate and covered with tylose according to Tokuyasu (18). Double-labeling experiments were done according to the procedure described by Slot et al. (19). In control sections, the primary antibodies were omitted from the procedure and, non-immune rabbit serum was used instead.

Processing and labeling of human liver tissue

Human liver tissue (n = 6, 4 female, 2 male, age between 44 and 74) was obtained from patients undergoing partial hepatic resection for liver tumors (Academic Medical Centre and Anthonie van Leeuwenhoek Hospital, Amsterdam, The Netherlands) under protocol of the Medical Ethical Commissions. Tissue blocks with apparently normal liver morphology were used for perfusion experiments within four hours after resection, while during this period liver tissue was preserved at 4°C. Fluorescently labeled Ox-LDL (20 μg/ml DMEM containing 1% HSA) was perfused (5 ml/min) through the pieces of liver via a portal vein for 2 or 10 minutes at 37°C, as previously described (20). To study the involvement of the scavenger receptor polyinosinic acid was perfused simultaneously, in some cases. The liver

pieces were shortly rinsed by perfusion with PBS and fixed with 4% PF and 0,1% GA in PBS for 12 minutes. Control tissue was only rinsed with PBS and subsequently fixed according to the above procedure. After fixation, liver tissue was processed for light and electron microscopic examination as described for rat tissue to allow respectively detection of fluorescence and immuno-detection of apoB.

Results and Discussion

Light microscopy

At 2 minutes after intravenous injection of DiI-Ox-LDL into rats, DiI-fluorescence is found to be mainly concentrated with Kupffer cells, whereas to a lesser extent, fluorescence is noticed with liver endothelial cells (Fig. 1a). At 10 minutes, the fluorescence intensity has increased with both cell types (Fig. 1b). Neither parenchymal cells nor fat-storing cells contain any fluorescent signal at the indicated time points. The intensity of fluorescence concentrated with Kupffer cells is in accordance to previous biochemical data (10), which showed Kupffer cells to be the major cell type in the rat liver involved in the uptake of Ox-LDL. The association of fluorescence is greatly reduced for both Kupffer and endothelial cells when, 1 minute before Ox-LDL administration, polyinosinic acid was pre-injected (Fig. 1c). This demonstrates that the association of fluorescence with both cell types is subject to inhibition by polyinosinic acid and can be defined as scavenger receptor-mediated (3, 10).

With human liver, a very similar visualization pattern is observed, showing DiI-Ox-LDL to be highly concentrated with Kupffer cells, while a less intensive fluorescent signal is found with endothelial cells (Fig. 1d, 1e). In contrast to rat liver, auto-fluorescence in human liver is found to be associated with lipid vacuoles of parenchymal cells. Perfusion of polyinosinic acid together with DiI-Ox-LDL strongly reduces fluorescent signal with both human liver Kupffer and endothelial cells (Fig. 1f), demonstrating the involvement of scavenger receptors. In addition to those in Fig. 1 liver tissue blocks from 5 other donors were analyzed. Although donors differed in gender, age and health status, the labeling pattern is very reproducible between the different donors. Earlier studies with human liver demonstrated considerable differences between donors in the relative uptake of the various liver cell types for native LDL (20). The amount of uptake of native LDL by human hepatocytes by a similar approach was found to correlate with the amount of LDL receptors (20). The receptors involved in the binding and uptake of Ox-LDL are, therefore, suggested to be consistently present in sufficient amounts on liver Kupffer and endothelial cells thereby allowing an adequate removal of Ox-LDL from the blood circulation. Our results with *ex situ* perfusion of human liver tissue blocks are sustained by recent biochemical data with isolated human Kupffer cells, which demonstrated that various recognition sites for modified LDL, including a specific Ox-LDL receptor, are present at a relatively high concentration (21).

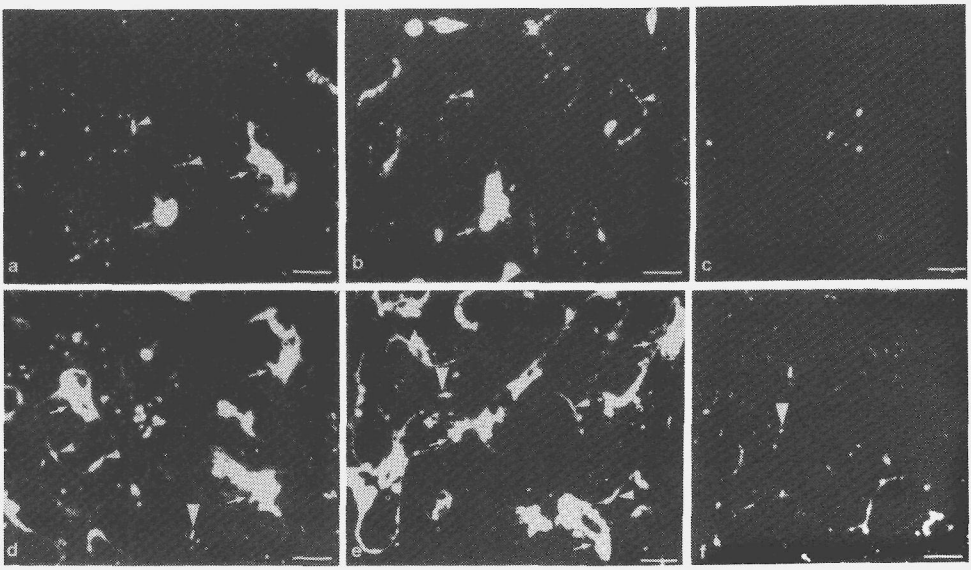

Figure 1. Fluorescence microscopy of rat (a, b) and human (d, e) liver respectively 2 and 10 minutes after intravenous injection or after *ex situ* perfusion of DiI-Ox-LDL. Fluorescence is mainly concentrated with Kupffer (arrow), and to a smaller extend with endothelial cells (arrowhead). Addition of polyinosinic acid clearly diminishes the amount of fluorescence present both in rat (c), and human liver (f). Some autofluorescence is present in fat vacuoles of human parenchymal cells (thick arrowhead). Bars = 6 μm.

Kupffer cells do not constitute a homogeneous population. Differences in size and endocytotic capacity of these cells in dependence of their position along the sinusoid have been reported (22, 23). In our experiments, Kupffer cells in portal as well as in central areas of the liver in both rat and human appear to participate in the uptake of Ox-LDL, suggesting that all liver macrophages do contain the receptor needed for the processing of Ox-LDL.

Electron microscopy

In rat liver, 30 seconds after portal vein injection, Ox-LDL, as demonstrated by immuno-labeling of apoB, is mainly bound to the exterior of the plasma membrane of Kupffer cells. Immuno-label is localized in small clusters at regions without clathrin coating (Fig. 2a), occasionally in coated membrane invaginations (Fig. 2b), and bound to lamellipodia (Fig. 2c). At this early time point, immuno-label is also found inside structures localized in the cell periphery that are surrounded by membranes in cross-sections (Fig. 2d). These apparent vacuoles in reality represent cross-sections of 'sponge-like' structures, in which channels of extracellular fluid are surrounded by complex associations of organelle-free lamellipodia. This becomes evident on staining with the membrane mordant stain ruthenium red, which

only stains the plasma membrane which is in direct contact with the extracellular medium (Fig. 2e). Although more than one type of scavenger receptor is present on Kupffer cells, as also demonstrated for other cell types (24-26), the majority of Ox-LDL binds to the Ox-LDL-specific receptor (10). The low frequency of label in clathrin coated structures suggests that the Ox-LDL-specific binding site on the Kupffer cells is predominantly localized outside coated pits.

Figure 3a shows that, besides the apparent vacuoles in the areas extended from the cell body, also tubular structures and apparent vesicles in the peripheral part of the cell body are surrounded by plasma membrane. The tubular structures are often demonstrated to be connected to the apparent vesicles. Similar structures are demonstrated to contain immuno-label at 6 minutes after the administration of Ox-LDL (Fig. 3b). It appears that, without actual internalization, bound ligand is transported into the cell body by movements of lamellipodia. In routinely plastic embedded liver tissue lamellipodia are demonstrated in continuity with worm-like structures (Fig. 4), suggesting that the lamellipodia arise from worm-like structures. The function of worm-like structures and their role in endocytosis of colloids have been debated previously (27). Our observations suggest that worm-like structures are involved in the formation of lamellipodia, and sponge-like structures by widening its enclosed space, and thereby allow binding and subsequent internalization of ligand.

Internalization of Ox-LDL occurs partly through coated vesicle formation, as demonstrated by the occasional presence of labeled coated vesicles 2 and 6 minutes after administration of Ox-LDL (Fig. 5a, inset). Coated vesicle formation is also involved in the uptake of other modified forms of LDL (24, 28-31). However, internalization of Ox-LDL predominantly seems to occur through membrane folding involving lamellipodia and worm-like structures on the basis of the amount of immuno-label associated with these structures. The ultrastructure of Kupffer cells was described in detail two decades ago with particular emphasis on endocytosis and phagocytosis (27, 32-35). Although involvement of lamellipodia in endocytosis has not yet been described, similar membrane folding and plasma membrane extensions have been described in peritoneal macrophages to be involved in the internalization of β-VLDL conjugated to colloidal gold (36, 37). The interaction of the lamellipodia with Ox-LDL is clearly different from pseudopodia engulfing particular matter during phagocytosis. Previous studies showed pre-aggregated modified LDL to be internalized by macrophages through phagocytosis (38, 39, 40). In these studies aggregates ranging in size up to several μm were demonstrated in different stages of engulfment. Phagocytosis of aggregates was never seen to occur *in vivo* in our studies.

At 6 minutes after injection of Ox-LDL, label is mainly demonstrated to be dispersed over vesicles ranging in size up to 0.6-0.7 μm. The label is associated with spherical particles of about 23 nm in diameter, probably representing still intact Ox-LDL (Fig. 5a). These particles are only observed in livers of animals that were injected with Ox-LDL, and

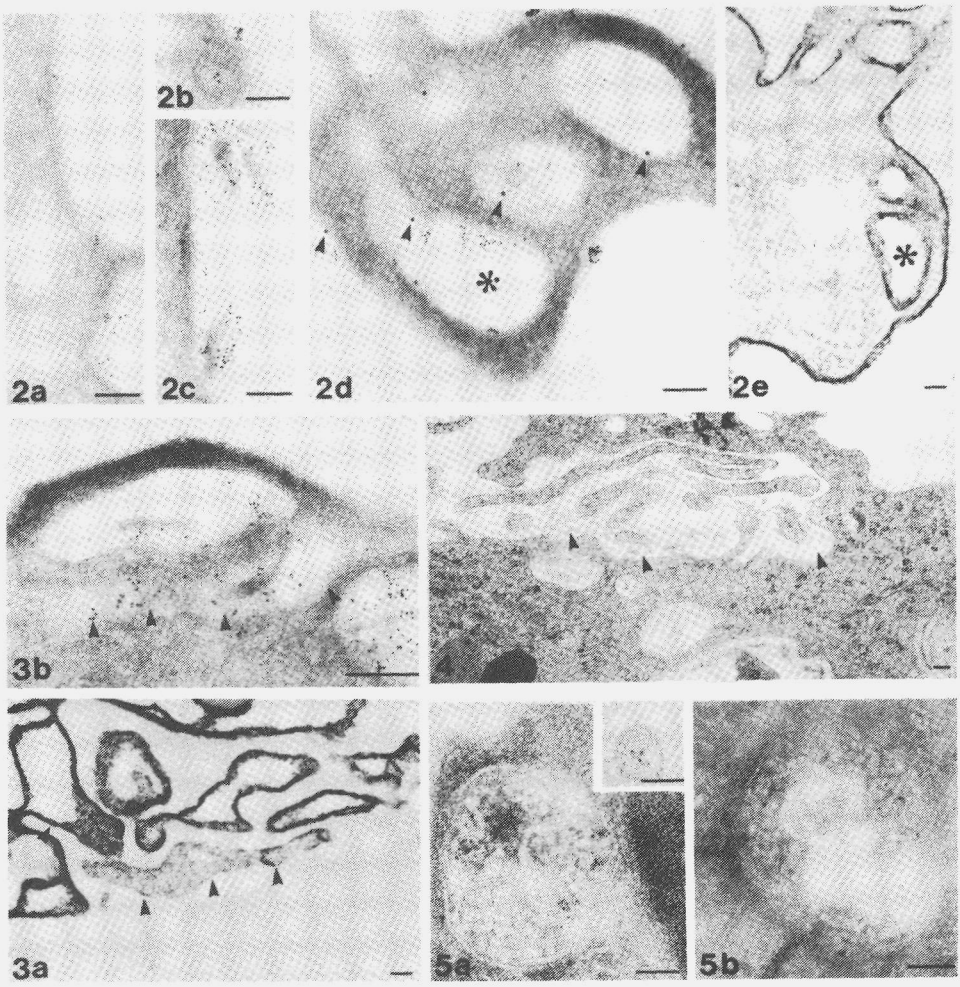

Figure 2. Immuno-labeling with anti-apoB of an ultrathin cryosection 30 seconds after injection of Ox-LDL (a-d). Immuno-gold is localized with Kupffer cells at regions of the plasma membrane without clathrin coating (a), in coated pits (b), bound to lamellipodia (c), and d-in close proximity to the membrane of apparent vacuoles (asterisk). The latter structures are demonstrated in Fig. 2e to be in contact with the extracellular space by ruthenium red stain of subsequently epon embedded specimens (asterisk). Large gold particles in Fig. 2d represent the Kupffer cell marker ED2 (arrowheads). Bars = 0.1 μm.

Figure 3. Electron micrograph of an ultrathin epon section of specimen contrasted with ruthenium red. Plasma membrane and membrane invaginations (arrowheads) of the Kupffer cell are stained (a). These structures (arrowheads) can be demonstrated in Kupffer cells on ultrathin cryosections to contain immuno-label 6 minutes after administration of Ox-LDL (b). Bars = 0.1 μm.

Figure 4. Electron micrograph of rat liver, after fixation with 2% GA. Worm-like structures characterized by the electron dense central line are demonstrated in continuity with lamellipodia (arrowheads). Bars = 0.1 μm.

Figure 5. Appearance of immuno-reactive apoB in Kupffer cells on ultrathin cryosections associated with lipoprotein-like particles in coated vesicles (a, inset), endosomes (a) and lysosomes, which also contain lipid inclusions (b), 6 minutes after injection of Ox-LDL. Bars = 0.1 μm.

not in untreated animals. Vesicles of this size are not stained by ruthenium red (not shown), suggesting that these structures represent the first intracellular compartment. The apparent detachment of particles and immuno-label from the vesicular membrane, may represent uncoupling of Ox-LDL from its receptor, a process that is known to take place in endosomes. Together with the ruthenium red exclusion and timing, we define this compartment as endosomal.

Transport of ligand through endosomes to lysosomes is apparent from the presence of immuno-reactive apoB in vesicles that contained not only label and ligand detached from the vesicle membrane, but also membranous material and lipid inclusions (Fig. 5b). Lysosomes as defined by their capacity to degrade biological material, are the final compartment of the Ox-LDL particles, as demonstrated by biochemical experiments (10). The appearance of labeled lysosomal structures already at 6 minutes after injection of Ox-LDL is in agreement with the rapid degradation of Ox-LDL by Kupffer cells (10). The appearance of lipid in the lysosomes has been previously demonstrated in peritoneal macrophages by Fukuda et al. (29). At 30 minutes after administration, immuno-label is exclusively localized in endosomes and lysosomes and is no longer bound to the plasma membrane or to apparent vesicular or tubular structures.

Ox-LDL is also observed in the endothelial cells of the rat liver. Thirty seconds after portal vein injection of Ox-LDL, some label is detectable bound to uncoated regions of the plasma membrane, but most label is present in coated pits (Fig. 6a). The scavenger receptors involved in binding of Ox-LDL by endothelial cells are apparently mainly localized in coated pits, comparable with the Ac-LDL scavenger receptor (31). At 2 minutes after injection less label is detectable at the plasma membrane than at 30 seconds, and most of the immuno-gold is present dispersed over large electron lucent vesicles ranging in size up to 0.7 μm (Fig. 6b). These structures are intracellular, because similar structures are excluded from the ruthenium red staining. In analogy to the Kupffer cells, these observations support the idea of the endosomal nature of these early label-containing vacuoles. These structures often show tubular membrane extensions, which are not labeled (Fig. 6b). This compartment might be functionally comparable to the Compartment of Uncoupling Receptor and Ligand (CURL), as described by Geuze et al. for liver parenchymal cells (41). Detachment of Ox-LDL particles from their receptor is indicated by the appearance of ligand in the vesicular lumen. The absence of immuno-label in the tubular extensions may indicate that the extensions are more likely to be involved in the recycling of the (scavenger) receptors to the plasma membrane than in ligand delivery. At 6 and 30 minutes after injection of Ox-LDL, the number of the vesicles that contain immuno-label increased. Besides in large electron lucent vesicles, immuno-label is present in more electron dense vesicles (Fig. 6c). The gradual increase in electron density of the endosomal structures is in accordance to the maturation of endosomes into lysosomes (27, 31, 42, 43), consistent with biochemical data that demonstrated lysosomal degradation of Ox-LDL (10) in liver endothelial cells.

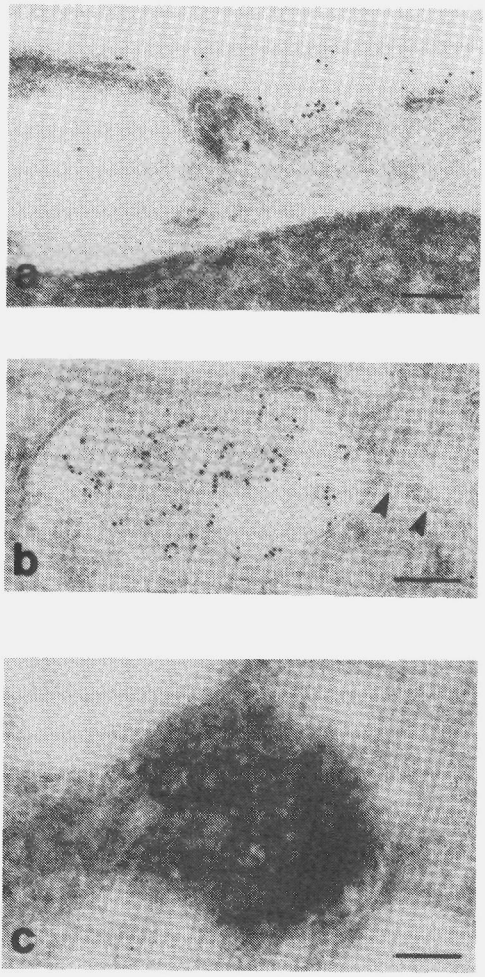

Figure 6. Ultrathin cryosections of rat liver endothelial cells after injection of Ox-LDL respectively for 30 seconds (a), 2 (b) and 6 minutes (c). Immuno-label is localized, 30 seconds after administration bound to uncoated and coated areas of the plasma membrane. After 2 minutes immuno-label is localized dispersed over vesicles, which often contained membrane extensions which were devoid of immuno-label (arrowheads). Increasing with time immuno-label is noticed dispersed over vesicles of a higher electron density (c). Bars = 0.1 μm.

Besides Kupffer and endothelial cells, no other cell types in the rat liver could be demonstrated to contain significant amounts of immuno-label.

In human liver, because anti-apoB antiserum recognizes also apoB from endogenous origin, parenchymal cells contained substantial amounts of immuno-label, also when the liver was not perfused with Ox-LDL. This endogenous apoB was mainly localized in the bile canalicular zone in multi-vesicular structures and associated with the Golgi-apparatus. Some label was also seen close to the plasma membrane in multi-vesicular structures and extracellularly (not shown). These observations are in accordance with synthesis of apoB and VLDL excretion as morphologically illustrated by Alexander et al. (44). Endothelial and Kupffer cells were never found to contain any immuno-label with control livers.

At 2 minutes after the beginning of Ox-LDL perfusion, immuno-reactive apoB was localized in Kupffer cells in small clusters bound to the plasma membrane, to lamellipodia

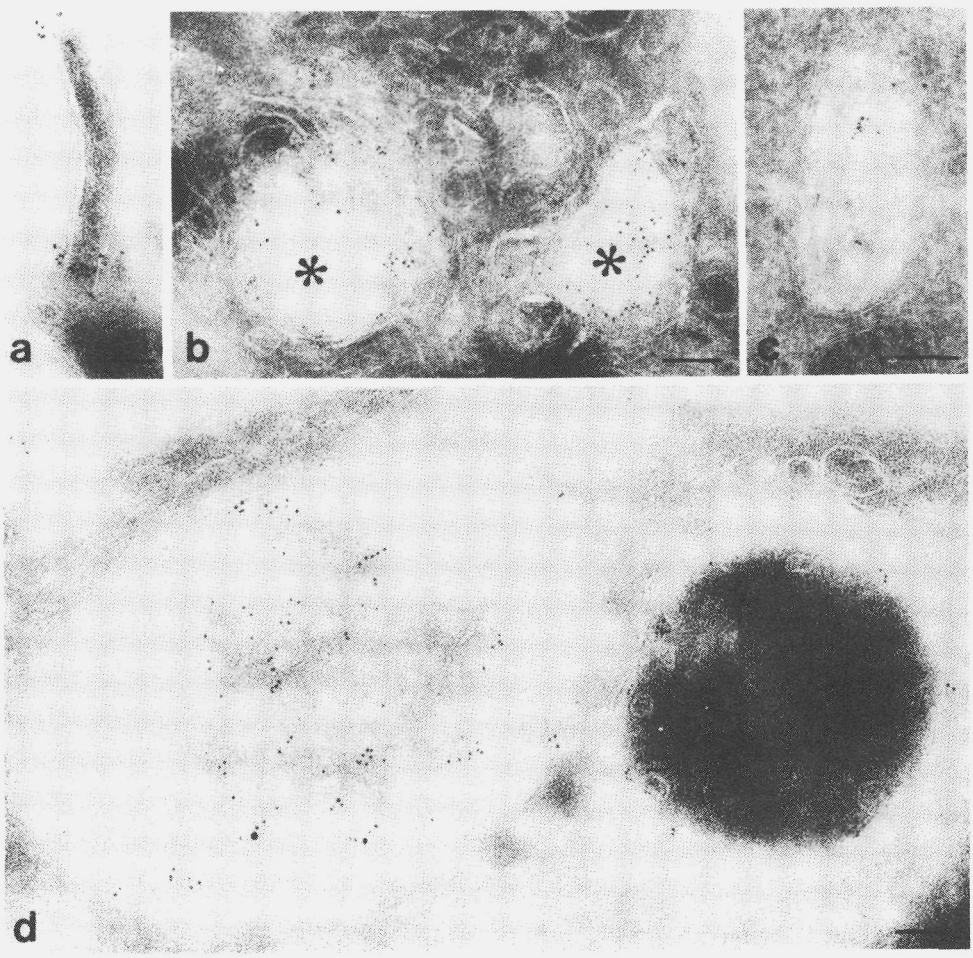

Figure 7. Electron micrograph of ultrathin cryosections of human liver cells 2 (a, b) and 10 minutes (c, d) after the beginning of perfusion. a-Immuno-gold is localized bound to the exterior of the plasma membrane of Kupffer cells to lamellipodia (a), and b-in close proximity to the membrane of apparent vacuoles, which are connected to more electron dense tubular structures (asterisk). c-At 10 minutes after perfusion immuno-label representing apoB is also localized in electron lucent vesicles in Kupffer cells. Endothelial cells contained immuno-reactive apoB, localized in vesicles of different electron densities (d). Bars = 0.1 μm.

(Fig. 7a), and in electron lucent roundish structures (Fig. 7b). The electron lucent roundish structures were often seen to continue into more electron dense, tubular-shaped structures, showing great similarity to the earlier described tubulo-vesicular structures from rat liver Kupffer cells (Fig. 2d). After 10 minutes, immuno-label is still localized in the above

mentioned structures, but is now also found dispersed over vesicles of a higher electron density (Fig. 7c). Lysosomes did not contain immuno-reactive apoB at any of the time points studied. Neither coated vesicles nor coated vesicle formation was noticed.

After 2 and 10 minutes of circulation, human liver endothelial cells showed immuno-staining, mainly dispersed over relatively electron lucent vesicles, whereas part of the label was also bound to the plasma membrane. After 10 minutes, low amounts of label were detectable at the plasma membrane, but immuno-label was mostly restricted to the relatively electron lucent vesicles and to some vesicles of a higher electron density (Fig. 7d), comparable with structures labeled in the rat endothelial cells (Fig. 6b-c).

Although not all described structures, that were found to be involved in the processing of Ox-LDL in rat liver Kupffer and endothelial cells, could be demonstrated in the human liver endothelial and Kupffer cells, all Ox-LDL-containing structures found in human liver, were also seen in rat liver. Coated pits and coated vesicles could not be demonstrated in human tissue, probably because some delay occured in actual fixation, which might have allowed some continuation of internalization after Ox-LDL has been removed from the perfusate. Immuno-label was not observed in lysosomal structures of human Kupffer cells, probably because of a slower processing of the Ox-LDL particles in this *ex situ* perfusion system. A more rapid degradation in human liver versus rat liver is not likely because lipid or membranous material would then be expected to accumulate in the lysosomes as noticed with rat liver (Fig. 5b).

In conclusion, our results show that Ox-LDL, intravenously injected into rats, or perfused through human liver tissue becomes rapidly concentrated in Kupffer cells and to a lesser extent in endothelial liver cells. Characterization of the *in vivo* interaction of Ox-LDL in rats by immuno-electron microscopy indicates that binding of Ox-LDL to Kupffer cells occurs primarily to regions of the plasma membrane without clathrin coating. For internalization, different mechanisms occurred simultaneously a) by coated vesicles, and b) by lamellipodia and worm-like structures. Subsequently immuno-reactive Ox-LDL was detected in relatively electron lucent endosomes, whereafter finally the lysosomal compartment was reached. For rat endothelial cells the mechanism of uptake exhibited a mechanism clearly different from that of Kupffer cells. Binding of Ox-LDL to liver endothelial cells is mainly observed in coated pits, whereas cellular processing involves large electron lucent endosomes (size up to 0.7 μm) before the lysosomal compartment is reached. The mechanism of uptake and processing of Ox-LDL by human liver involves similar ultrastructural features as observed with rat liver cells. These observations allow an extension of the animal studies to the human situation establishing that liver cells, particularly Kupffer cells, form a highly effective protective system against the occurrence of atherogenic Ox-LDL particles in the blood.

References

1. Gerrity RG. The role of the monocyte in atherogenesis. I. Transition of blood-borne monocytes into foam cells in fatty lesions. Am J Pathol 1987;103:181-190.
2. Brown MS, Goldstein JL. Lipoprotein metabolism in the macrophage: implications for cholesterol deposition in atherosclerosis. Annu Rev Biochem 1983;52:223-261.
3. Brown MS, Basu SK, Falck JR, Ho YK, Goldstein JL. The scavenger cell pathway for lipoprotein degradation: specificity of the binding site that mediates the uptake of negatively charged LDL by macrophages. J Supramol Struct 1980;13:67-81.
4. Goldstein JL, Ho YK, Basu SK, Brown MS. Binding site on macrophages that mediates uptake and degradation of acetylated low density lipoprotein, producing massive cholesterol deposition. Proc Natl Acad Sci USA 1979;76:333-337.
5. Fogelman AM, Schechter I, Saeger J, Hokom M, Chold JS, Edwards PA. Malondialdehyde alteration of low density lipoproteins leads to cholesterolester accumulation in human monocyte macrophages. Proc Natl Acad Sci USA 1980;77:2214-2218.
6. Parthasarathy S, Steinbrecher UP, Barnett J, Witztum JL, Steinberg D. Essential role of phospholipase A2 activity in endothelial cells induced modification of LDL. Proc Natl Acad Sci USA 1985;82:3000-3004.
7. Nagelkerke FJ, Barto KP, Van Berkel ThJC. In vivo and in vitro uptake and degradation of acetylated low density lipoprotein by rat liver endothelial, Kupffer and parenchymal cells. J Biol Chem 1983;258:12221-12227.
8. Ylä-Herttuala S, Palinski WF, Rosenfeld ME, Parthasarathy S, Carew TE, Butler S, Witztum JL, Steinberg D. Evidence for the presence of oxidatively modified low density lipoprotein in Atherosclerotic Lesions of Rabbit and Man. J Clin Invest 1989;84: 1086-1095.
9. Witztum JL, Steinberg D. Role of Low Density Lipoprotein in Atherogenesis. J Clin Invest 1991;88:1785-1792.
10. Van Berkel ThJC, De Rijke YB, Kruijt JK. Different fate in vivo of oxidatively modified low density lipoprotein and acetylated low density lipoprotein in rats. J Biol Chem 1991;5: 2282-2289.
11. Redgrave TG, Roberts DCK, West CE. Separation of plasma lipoproteins by density gradient centrifugation. Anal Biochem 1975;65:42-49.
12. Pitas RE, Boyles J, Mahley RW, Bissell DM. Uptake of chemically modified low density lipoproteins in vivo is mediated by specific endothelial cells. J Cell Biol 1985;100:103-117.
13. Steinbrecher UP, Witztum JL, Parthasarathy S, Steinberg D. Decrease in reactive amino groups during oxidation or endothelial cell modification of low density lipoprotein: correlation with changes in receptor mediated catabolism. Arteriosclerosis 1987;7:135-143.
14. Handley DA, Arbeeny CM, Witte LD, Goodman DS, Chien S. Ultrastructural visualization of low-density lipoproteins during receptor binding and cellular endocytosis. J Ultrastruct Res 1983;83:43-47.
15. Crowle AJ. In: Immunodiffusion, New York, Academic Press, 1961
16. Kleinherenbrink-Stins MF, Van der Boom J, Bakkeren HF, Roholl PJM, Brouwer A, Van Berkel ThJC, Knook DL. Light- and immunoelectron microscopic visualization of in vivo endocytosis of low density lipoprotein by hepatocytes and Kupffer cells in rat liver. Lab Invest 1990;63:73-86.
17. Dijkstra CD, Dopp EA, Joling P, Kraal G. The heterogeneity of mononuclear phagocytes in lymphoid organs: distinct macrophage subpopulations in the rat recognized by monoclonal antibodies ED1, ED2, ED3. Immunology 1985;54:589-591.
18. Tokuyasu KT. Immunochemistry on ultrathin frozen sections. Histochem J 1980;12:381-403.
19. Slot JW, Geuze HJ, Freeman BA, Crapo JD. Intracellular localization of the copper-zinc and manganese superoxide dismutases in rat liver parenchymal cells. Lab Invest 1986;55:363-371.
20. Kleinherenbrink-Stins MF, Van der Boom J, Schouten D, Roholl PJM, Van der Heyde MN, Brouwer A, Van Berkel ThJC, Knook DL. Visualization of the interaction of native and modified lipoproteins with parenchymal, endothelial and Kupffer cells from human liver. Hepatology 1991;14:79-90.

21. Kamps JAAM, Kruijt JK, Kuiper J, Van Berkel ThJC. Characterization of the interaction of acetylated and oxidatively modified LDL with human liver parenchymal and Kupffer cells in culture. Arterioscler Thromb 1992;12:1079-1087.
22. Sleyster EC, Knook DL. Relation between localization and function of rat liver Kupffer cells. Lab Invest 1982;47:484-490.
23. Bouwens L, Baekeland M, De Zanger R, Wisse E. Quantitation, tissue distribution and proliferation kinetics of Kupffer cells in normal rat liver. Hepatology 1986;6:718-722.
24. Robenek H, Schmitz G, Assmann G. Topography and dynamics of receptors for acetylated and malondialdehyde-modified low-density lipoprotein in the plasma membrane of mouse peritoneal macrophages as visualized by colloidal gold in conjunction with surface replicas. J Histochem Cytochem 1984;32:1017-1027.
25. Sparrow CP, Parthasarathy S, Steinberg D. A macrophage receptor that recognizes oxidized low density lipoprotein but not acetylated low density lipoprotein. J Biol Chem 1989;264:2599-2604.
26. Kume N, Arai H, Kawai C, Kita T. Receptors for modified low-density lipoproteins on human endothelial cells: different recognition for acetylated low-density lipoprotein and oxidized low-density lipoprotein. Biochim Biophys Acta 1991;1091:63-67.
27. Wisse E. Ultrastructure and function of Kupffer cells and other sinusoidal cells in the liver. In: Wisse E, Knook DL, eds. Kupffer cells and other liver sinusoidal cells. Elsevier/North Holland Biomedical Press Amsterdam, 1977;33-60.
28. Traber MG, Kallman B, Kayden HJ. Localization of the binding sites of native and acetylated low density lipoprotein (LDL) in human monocyte derived macrophages. Exp Cell Res 1983;145:95-103.
29. Fukuda S, Horiuchi S, Tomita K, Murakami M, Morino Y, Takahashi K. Acetylated low-density lipoprotein is endocytosed through coated pits by rat peritoneal macrophages. Virchows Arch [B] 1986;52:1-13.
30. Mommaas-Kienhuis AM, Van der Schroef JG, Wijsman MC, Daems WTh, Vermeer BJ. Conjugates of colloidal gold with native and acetylated low density lipoproteins for ultrastructural investigations on receptor mediated endocytosis by cultured human monocyte derived macrophages. Histochemistry 1985;83:29-35.
31. Mommaas-Kienhuis AM, Nagelkerke JF, Vermeer BJ, Daems WTh, Van Berkel ThJC. Visualization of the interaction of native and modified low density lipoproteins with isolated rat liver cells. Eur J Cell Biol 1985;38:42-50.
32. Fahimi HD. The fine structural localization of endogenous and exogenous peroxidase activity in Kupffer cells of rat liver. J Cell Biol 1970;47:247-262.
33. Wisse E. Observations on the fine structure and peroxidase cytochemistry of normal rat liver Kupffer cells. J Ultrastruct Res 1974;46:393-426.
34. Wisse E. Kupffer cell reactions in rat liver under various conditions as observed in the electron microscope. J Ultrastruct Res 1974;46:499-520.
35. Fahimi HD. In: Arias I, Popper H, Schachter D. et al. eds. The liver: Biology and Pathology Raven Press, New York 1982;495-498.
36. Robenek H, Schmitz G, Greven H. Cell surface distribution and intracellular fate of human b-VLDL in cultured peritoneal mouse macrophages: a cytochemical and immunocytochemical study. Eur J Cell Biol 1987;43:110-120.
37. Jones NL, Allen NS, Lewis JC. Beta VLDL uptake by pigeon monocyte-derived macrophages: correlation of binding dynamics with three-dimensional ultrastructure. Cell Motil Cytoskeleton 1991;19:139-151.
38. Khoo JC, Miller E, McLoughlin P, Steinberg D. Enhanced macrophage uptake of low density lipoprotein after self-aggregation. Arteriosclerosis 1988;8:348-58.
39. Heinecke JW, Suits AG, Aviram M, Chait A. Phagocytosis of lipase aggregated low density lipoprotein promotes macrophage foam cell formation. Arteriosclerosis and Thrombosis 1990;11:1643-1651.

40. Hoff HF, Cole TB. Macrophage uptake of LDL modified by 4- hydroxynonenal an ultrastructural study. Lab Invest 1991;64:254-263.
41. Geuze HJ, Slot JW, Strous GJ, Lodish HF, Schwartz AL. Intracellular site of asialoglycoprotein receptor-ligand uncoupling: Double label immunoelectron microscopy during receptor-mediated endocytosis. Cell 1983;32:277-287.
42. Wisse E. An ultrastructural characterization of the endothelial cell in the rat liver sinusoid under normal and various experimental conditions, as a contribution to the distinction between endothelial and Kupffer cells. J Ultrastruc Res 1972;38:528-562.
43. Stoorvogel W, Strous GJ, Geuze HJ, Oorschot V, Schwartz AL. Late endosomes derive from early endosomes by maturation. Cell 1991;65:417-427.
44. Alexander CA, Hamilton RL, Havel RJ. Subcellular localization of apoB apoprotein of rat plasma lipoproteins in rat liver. J Cell Biol 1976;69:241-263.

Chapter 3

Cholesteryl Esters from Oxidized Low Density Lipoproteins are *In Vivo* Rapidly Hydrolysed in Rat Kupffer Cells and Transported to Liver Parenchymal Cells and Bile

Moniek N. Pieters[1], Sebastiaan Esbach[2], Donald Schouten[1], Adriaan Brouwer[2], Dick L. Knook[2] and Theo J.C. van Berkel[1]

[1] Division of Biopharmaceutics, Center for Bio-Pharmaceutical Sciences, Sylvius Laboratory, Leiden, The Netherlands

[2] TNO Institute of Ageing and Vascular Research, Gaubius Laboratories, Leiden, The Netherlands

Submitted for publication.

Summary

Human low density lipoprotein (LDL) was labeled in its cholesteryl ester moiety with ^{3}H-cholesteryl oleate or ^{3}H-cholesteryl oleoyl ether and oxidized by exposure to 10 μM of $CuSO_4$. The *in vivo* metabolism of cholesteryl esters of oxidized LDL (Ox-LDL) was determined after injection into rats. When Ox-LDL was labeled with ^{3}H-cholesteryl oleoyl ether, a non-hydrolysable analog of cholesteryl oleate, Kupffer cells contributed for 55.1 $\pm$ 4.1% to the total liver uptake at 10 min after injection. When ^{3}H-cholesteryl oleate labeled Ox-LDL was injected, the radiolabeled cholesteryl esters were nearly completely hydrolysed within 1 h after injection. Within this time, the Kupffer cell associated radioactivity declined to 32% of the maximal uptake value. In serum the highest specific resecreted ^{3}H-cholesterol (esters) were associated with the serum HDL fraction, thus suggesting a role for HDL as an *in vivo* cholesterol acceptor. The kinetics of biliary secretion were studied in rats equipped with catheters in the bile, duodenum and heart. At 1 h after injection of ^{3}H-cholesteryl oleate labeled Ox-LDL, 4.15 $\pm$ 0.67% of the injected dose was secreted in the bile, mainly as bile acids. At 6 h after injection this value was 19.2 $\pm$ 1.2%. These values are 3-fold higher than for injected ^{3}H-cholesteryl oleate labeled Ac-LDL, which is initially mainly taken up by liver endothelial cells. The rapid processing of cholesteryl esters derived from Ox-LDL to bile acids, indicate that Kupffer cells form an efficient protection system against the atherogenic action of Ox-LDL in the blood compartment.

Introduction

It has been well established that *in vitro* modification of LDL by acetylation (1), acetoacetylation (2), malondialdehyde treatment (3) or oxidation (4) all lead to the formation of atherogenic particles. In the artery wall, the uptake of modified LDL by macrophages mediated by the scavenger receptor leads to lipid accumulation (5) and eventually to the formation of foam cells, an important event in the developing atherosclerotic plaque.

We have shown previously by using iodinated oxidized LDL (Ox-LDL), that in the rat the liver is highly effective in removing Ox-LDL from the circulation. We provided evidence that on various liver cell types different scavenger receptors do exist, recognizing acetylated LDL (Ac-LDL), Ox-LDL or both (6). By scavenging atherogenic particles from the blood compartment, the liver forms a major protection system of the body. It has been established that oxidized LDL rather than acetylated LDL is the physiological representative for modified LDL (7). Therefore, in this study, we focused on the *in vivo* fate of the cholesterol ester moiety from Ox-LDL in the rat.

The possible involvement of high density lipoproteins (HDL) as transport vehicles for intercellular transport of cholesterol (esters) was also studied. The potential role of HDL in

the so-called "reverse cholesterol transport", the transport of peripheral cholesterol to the liver as proposed by Glomset (8), is generally accepted. The exact mechanism however, by which HDL removes cholesterol from the cells is still not clear. It has been stated that cholesterol efflux from the cell is based on passive diffusion ((9), for review see (10)). It has also been reported that binding of HDL induces the activation of a signal-transduction pathway which results in the translocation of intracellular cholesterol to the plasma membrane (11,12). Recently, it has been suggested that in cells cholesterol is present in slow and fast kinetic pools. Increased cholesterol efflux from cells upon binding of apoAI was proposed to be linked to a higher participation of the fast kinetic cholesterol pool in the efflux (13).

In a study with Ac-LDL we have shown previously (14) that the uptake of radiolabeled cholesterol esters by liver endothelial cells is followed by a resecretion of radiolabeled free cholesterol into the serum. The results indicated that HDL is necessary for an efficient transport of cholesterol from liver endothelial cells to parenchymal cells, thus providing evidence for the role of HDL in reverse cholesterol transport. HDL has been shown to selectively deliver its cholesteryl ester moiety to hepatic (15-17), steroidogenic (16,17) and extrahepatic tissues (18). We have provided evidence that hepatic selective delivery of HDL cholesteryl esters is restricted to the liver parenchymal cells and efficiently coupled to bile acid formation and secretion (19). In the present study we investigated therefore also the role of HDL as an *in vivo* cholesterol acceptor for Kupffer cell associated cholesterol (esters). Furthermore we followed the kinetics of appearance of radiolabeled bile in order to test the efficiency of biliary secretion of metabolized cholesteryl esters initially associated with Kupffer cells.

Materials and Methods

Isolation, labeling and oxidation of LDL

Human LDL was isolated from plasma of healthy volunteers as described by Redgrave et al. (20). After density ultracentrifugation LDL ($1.024 < d < 1.055$) and lipoprotein deficient serum (LPDS, $d > 1.21$) were collected and dialysed against 8 mM-phosphate-buffered saline/1 mM EDTA, pH 7.4. ^{3}H-Cholesteryl oleate was incorporated into LDL according to Blomhoff et al. (21). In short, 25 μCi of [1α,2α(n)-^{3}H]-cholesteryl oleate (Amersham, USA) was dried under N_2 and dissolved in 100 μl acetone. 1 ml of human LPDS was added, placed under a stream of N_2 for 10 min, and incubated for 10 min at 37°C. Then, 1 ml of LDL was added and incubated at 37°C during 5 h. ^{3}H-Cholesteryl oleate labeled LDL was re-isolated by density ultracentrifugation and dialysed against phosphate-buffered saline containing 10 μM EDTA, pH 7.4. LDL (0.2 mg/ml) was then oxidized by exposure to $CuSO_4$ (10 μM of free copper ions) during 20 h at 37°C. The oxidation of LDL was stopped by the addition of EDTA (1 mM final concentration). ^{3}H-Cholesteryl oleate labeled LDL was filtrated

through a Millipore Millex-GV4 0.4 μm filter to remove possible aggregates and its relative electrophoretic mobility checked on agarose gelelectrophoresis (Ox-LDL: $R_f = 0.52 \pm 0.01$ ($n = 6$, $\pm$ S.E.M.; Control LDL: $R_f = 0.21 \pm 0.01$ ($n = 6$, $\pm$ S.E.M.). Specific activity of ^{3}H-Ox-LDL was 12.5 $\pm$ 1.5 dpm/ng ($n = 6$, $\pm$ S.E.M.). 79.4 $\pm$ 3.6% of the radiolabel could be recovered as ^{3}H-cholesteryl esters as determined by Bligh and Dyer extraction (22) and thin layer chromatography (23). For some experiments ^{3}H-cholesteryl oleoyl ether, a non-hydrolysable analog of cholesteryl oleate, was incorporated into LDL, similarly to described above, and subsequently oxidized (specific activity 7.9 dpm/ng, $R_f = 0.54$). ^{3}H-Ox-LDL was used for experiments within 3 weeks after oxidation. Acetylation of ^{3}H-cholesteryl oleate labeled LDL was carried out as described by Basu et al. (24). Specific activity of ^{3}H-Ac-LDL was 15.2 $\pm$ 1.7 dpm/ng ($n = 3$, $\pm$ S.E.M.). 95.8 $\pm$ 0.9% of the radiolabel could be recovered as cholesteryl esters after lipid extraction and thin layer chromatography.

Serum decay and liver association

Throughout this study 12 week old male Wistar rats were used. Rats were anaesthetized by an intraperitoneal injection of Nembutal (1 ml/kg body wt.). The abdomen was opened and ^{3}H-cholesteryl oleate labeled Ox-LDL was injected in the vena penis. At the indicated time points blood and liver samples were taken. Corrections were made for the contribution of entrapped serum to the liver uptake (90 μl serum/g wet tissue) as described previously (25). In order to separate ^{3}H-cholesteryl esters from ^{3}H-free cholesterol, liver lobules were put on fluid nitrogen immediately after excision in order to stop further hydrolysis. Liver samples were homogenized and extracted according to Bligh and Dyer (22). To separate free cholesterol from cholesteryl esters, the lipid fraction of the Bligh and Dyer extraction was subjected to thin layer chromatography with n-heptaan/di-ethylether/glacial acetic acid as eluens (60:40:1 by vol.) (23). To determine serum radioactivity at time points longer than 1 h after injection, rats were anaesthetized with diethylether and injected in the vena penis. Blood samples were taken by capillary puncture of the orbital plexus.

Cell Isolation

For determination of the hepatic cellular distribution *in vivo*, ^{3}H-cholesteryl oleate or ^{3}H-cholesteryl oleoyl ether labeled Ox-LDL were injected into the vena penis. At the indicated time points the vena porta was cannulated and the liver perfused with oxygenated Hanks' buffer plus Hepes (2.4 g/l), pH 7.4 at 8°C. In order to determine the total liver uptake a liver lobule was tied off after 8 min perfusion (flow rate 14 ml/min). The various liver cell types were then isolated by a low temperature (8°C) perfusion method with 0.05% collagenase in Hanks'/Hepes buffer. The separation of parenchymal cells was carried out as described earlier (26). The non-parenchymal liver endothelial and Kupffer cells were isolated by centrifugal elutriation (27). The purity of isolated cell fractions (> 90%) was checked

light microscopically after staining for peroxidase activity. Calculation of the contribution of the different cell types to total liver uptake was performed as described previously (27). In these calculations parenchymal cells contributed for 92.5%, liver endothelial cells for 2.5% and Kupffer cells for 3.3% to the total liver uptake.

Bile sampling

Bile was collected from unrestrained 3-month-old male Wistar rats (28). Rats received tap water and standard chow *ad libitum*. Rats were equipped with permanent catheters in the bile duct, the duodenum and the heart. Bile duct and duodenum catheters were connected immediately after surgery in order to maintain an intact enterohepatic circulation. Rats were allowed to recover from surgery for 1 week. 40-50 μg ^{3}H-cholesteryl oleate labeled Ox-LDL (app. 500,000 dpm) was injected via the heart catheter. The bile duct catheter was then connected to a fraction collector and bile samples were collected hourly. 100 μl bile was de-colorized by adding 10 μl 30% H_2O_2 solution. The samples were counted for radioactivity after addition of hionic fluor scintillation fluid (Packard) in a Packard Liquid Scintillation Analyzer. To separate bile acids from the lipid fraction, bile samples were extracted according to Bligh and Dyer (22). The aqueous layer containing the bile acids was counted for radioactivity. Cholesterol and cholesterol esters were separated by thin layer chromatography as described above.

Protein was determined as described by Lowry et al. (29), with BSA as standard. Cholesterol and cholesteryl esters were quantified by using a commercial kit (Boehringer, Mannheim).

Results

Serum decay and liver association

The serum decay and liver association of ^{3}H-cholesteryl oleate-labeled Ox-LDL is shown in Fig. 1. The rapid decay of ^{3}H-cholesteryl oleate labeled Ox-LDL from the serum resembles the clearance of iodinated Ox-LDL (6). At two min after injection 91.8 $\pm$ 0.2% of the injected dose has been removed from the serum. Radioactivity of ^{3}H-cholesteryl oleate labeled Ox-LDL was almost quantitatively recovered in the liver. At 15 min after injection 89.6 $\pm$ 7.0% of the injected dose was liver associated. At later time points the liver associated radioactivity decreased, indicating processing of the Ox-LDL derived ^{3}H-cholesteryl esters. Figure 2 shows the percentage of ^{3}H-free cholesterol in the liver at different times after injection of ^{3}H-cholesteryl oleate labeled Ox-LDL. At 5 min after injection already 50% of the liver associated radioactivity was present as free cholesterol. Subsequently, the percentage of free cholesterol in the liver increased up to 80% at 45 min

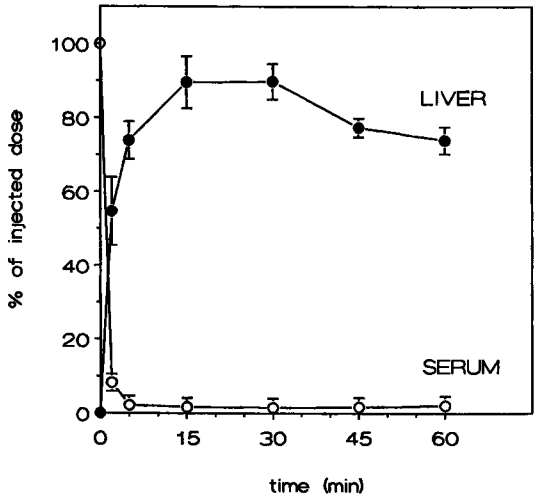

Figure 1. Serum decay and liver association of ^{3}H-cholesterol oleate labeled oxidized LDL. 40-50 μg (app. 500,000 dpm) of ^{3}H-cholesteryl oleate Ox-LDL was injected into the vena penis of anaesthetized rats. At the indicated time points serum was drawn from the vena cava inferior and serum decay (o) was calculated. In order to determine liver association (•) a liver lobule was tied off, weighed, combusted in a Hewlett Packard sample oxidizer 306 and counted for radioactivity. A correction was made for the contribution of serum to the total liver associated radioactivity (25). Data are expressed as percentage of injected dose ± S.E.M. (n = 4).

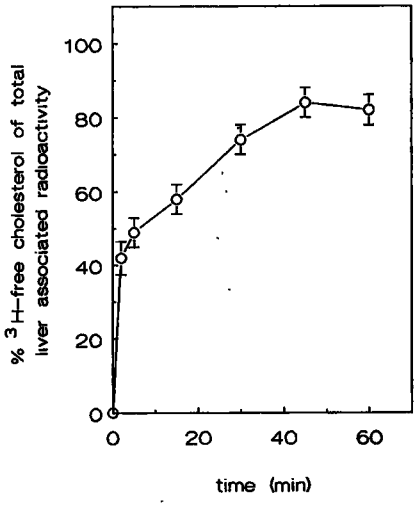

Figure 2. Percentage of free cholesterol of total liver associated radioactivity. Anaesthetized rats were injected with 40-50 μg ^{3}H-cholesteryl oleate labeled Ox-LDL. At the indicated time points liver lobules were tied off and immediately put in fluid nitrogen in order to stop hydrolysis. Liver samples were extracted according to Bligh and Dyer (22) and subjected to thin layer chromatography. Spots corresponding with free cholesterol and cholesterol esters were scraped off and counted for radioactivity. Data are presented ± S.E.M. (n = 4).

after injection. The data also indicate that the liver is still able to hydrolyse cholesteryl esters of LDL after oxidation.

Cellular distribution studies of ^{3}H-Ox-LDL in the liver

We have shown previously that Ox-LDL iodinated on its apolipoprotein moiety is mainly taken up by Kupffer cells (6). When ^{3}H-cholesteryl oleate labeled Ox-LDL is injected into the rat the highest specific activity is also found to be associated with Kupffer cells (Fig. 3). At first sight, a discrepancy between Kupffer cell involvement seems to exist in the uptake of the apolipoprotein and the cholesteryl ester moiety of Ox-LDL. At 10 min after injection the specific activity (% of injected dose (ID) *10^{3}/mg cell protein) of Kupffer cells is 1163 ± 202 and 764 ± 65 for the apolipoprotein and cholesteryl ester part respectively.

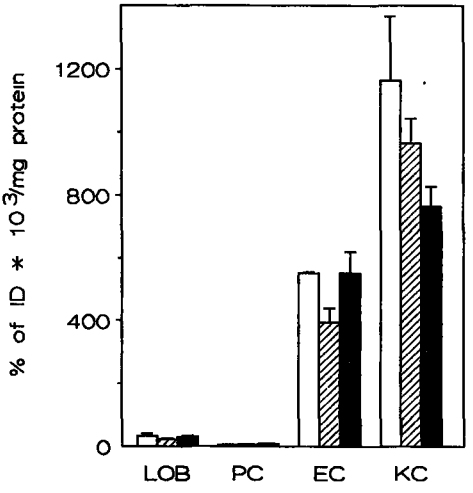

Figure 3. Cellular distribution of Ox-LDL in the liver. 40-50 ug of Ox-LDL labeled on the apolipoprotein (^{125}I, open bars, from (6)) or cholesteryl ester moiety (cholesteryl oleoyl ether, hatched bars or cholesterol oleate, filled bars) was injected into rats and a low temperature perfusion was carried out at 10 min after injection. Cells were separated into parenchymal cells (PC), liver endothelial cells (EC) and Kupffer cells (KC). LOB represents the total liver uptake. Data are expressed as specific activity ± S.E.M. (n = 4).

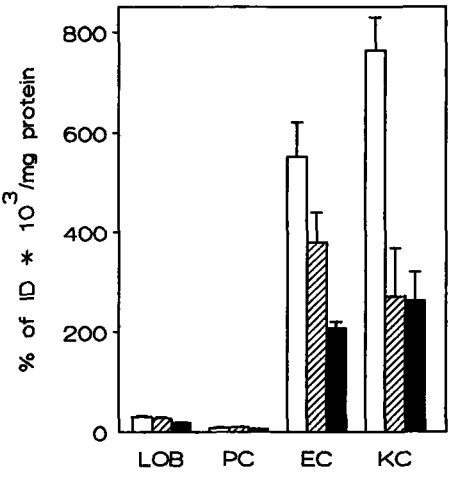

Figure 4. Cellular distribution of ^{3}H-cholesteryl oleate labeled Ox-LDL at different times after injection. 40-50 μg cholesteryl oleate labeled Ox-LDL was injected into rats and parenchymal cells (PC), liver endothelial cells (EC) and Kupffer cells (KC) were isolated at 10 (open bars), 60 (hatched bars) and 120 min (filled bars) after injection. LOB represents the total liver uptake. Data are expressed as specific activity ± S.E.M. (n = 4).

Consequently the calculated relative contribution of the Kupffer cells to the total liver radioactivity is less for ^{3}H-cholesteryl ester labeled Ox-LDL than for ^{125}I-Ox-LDL (Table 1). However, when LDL is labeled with a non-hydrolysable cholesteryl ester analog (cholesteryl oleoyl ether), the involvement of Kupffer cells (966 ± 77) is similar as for the iodinated Ox-LDL. The significant difference ($p < 0.05$, Student's t-test) between the ^{3}H-cholesteryl ester and ^{3}H-cholesteryl oleoyl ether uptake suggests a rapid hydrolysis of cholesteryl esters and a rapid secretion of ^{3}H-free cholesterol by the Kupffer cells. Within 1 h after injection a further reduction of Kupffer cell associated radioactivity can be observed (Fig. 4). At 60 min after injection of ^{3}H-cholesteryl oleate labeled Ox-LDL the specific activity of Kupffer cells declined to 32% of the maximal uptake as determined with ^{3}H-cholesteryl oleoyl ether labeled Ox-LDL. After the rapid secretion of ^{3}H-free cholesterol from Kupffer cells in the first hour, the Kupffer cell associated radioactivity remained constant upto 2 h after injection.

Table 1. Relative contribution of the different liver cell types to the total liver uptake of Ox-LDL labeled in its apolipoprotein or cholesteryl ester moiety at 10 min after injection
Parenchymal cells (PC) contribute for 92.5 % to the total liver, endothelial cells (EC) for 3.3 % and Kupffer cells (KC) 2.2 %. The amount of radioactivity per mg cell protein was multiplied with the amount that each cell type contributes to the total liver volume in order to calculate the relative contribution (27). Values represent the mean of 4 experiments ± S.E.M.

	Ox-LDL labeled with		
cell type	^{125}I	^{3}H-chol. oleate	^{3}H-chol. oleoyl ether
PC (%)	6.9 ± 1.2	16.8 ± 3.5	12.7 ± 2.4
EC (%)	36.3 ± 4.2	40.3 ± 3.1	31.9 ± 2.4
KC (%)	6.8 ± 3.0	43.0 ± 2.2	55.1 ± 4.1

Resecretion of ^{3}H-radioactivity into the serum

When the serum radioactivity was determined at different time points after injection of ^{3}H-cholesteryl oleate labeled Ox-LDL, the initial rapid decay is followed by a re-appearance of

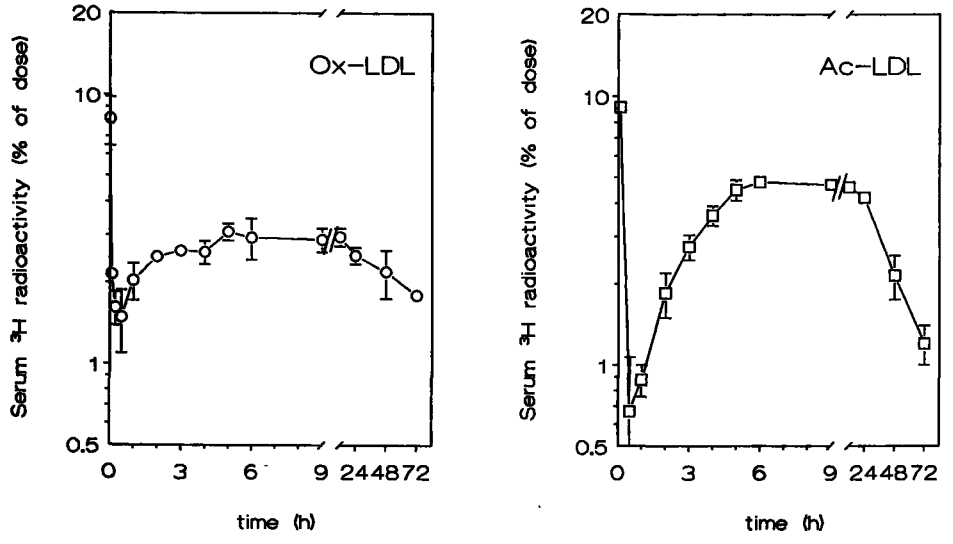

Figure 5. Serum radioactivity after the injection of ^{3}H-cholesteryl oleate labeled Ox-LDL or Ac-LDL. ^{3}H-Ox-LDL (Fig. 5A) or ^{3}H-Ac-LDL (Fig. 5B) (120-160 μg, 2,000,000 dpm) was injected into rats via the vena penis. At the indicated time points blood was drawn from the orbital plexus. Serum was counted for radioactivity and serum decay was calculated. Results are the mean of 4 experiments ± S.E.M.

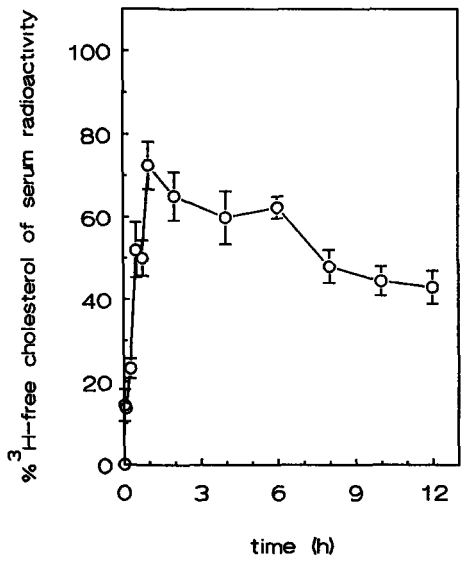

Figure 6. Percentage of free cholesterol in serum after injection of ^{3}H-cholesterol oleate labeled Ox-LDL. Serum of rats injected with ^{3}H-cholesterol oleate labeled Ox-LDL was extracted according Bligh and Dyer (22). Free cholesterol was separated from cholesterol esters by thin layer chromatography. Spots were scraped off and counted for radioactivity. Data are presented ± S.E.M. (n = 4).

radioactivity (Fig. 5). In Fig. 5 the serum radioactivity upto 72 h after injection of ^{3}H-cholesteryl oleate labeled Ox-LDL or ^{3}H-cholesteryl oleate labeled Ac-LDL can be compared. At 30 min after injection of ^{3}H-cholesteryl oleate labeled Ox-LDL only 1.5 ± 0.4% of the injected dose was present in the serum. Subsequently, serum radioactivity increased up to 3% of the injected dose (significantly different from 1.5% at 30 min after injection, ($p < 0.01$, Student's t-test) and remained constant for upto 12 h after injection. When ^{3}H-cholesteryl oleate labeled Ac-LDL was injected, the serum radioactivity decreased to 0.7% of the injected dose and subsequently increased upto 5%. In the serum the re-appearance of radiolabel after injection of ^{3}H-cholesteryl oleate labeled Ox-LDL (Fig. 6) was initially mainly in the form of free cholesterol. This indicates that after hydrolysis of cholesteryl esters in the liver, ^{3}H-free cholesterol is secreted into the serum compartment. Serum density ultracentrifugation at 3 h after injection (Fig. 7A) revealed that 55.5 ± 1.1% of the radioactivity could be recovered in the HDL density range ($1.05 < d < 1.13$). For LDL and VLDL these values were 11.9 ± 2.0 and 11.2 ± 2.8%, respectively (n = 4 ± S.E.M.). Evidence for re-esterification in the serum compartment can be derived from the relative decrease of free cholesterol associated radioactivity at the later time points (Fig. 6). The specific activity of radioactivity of free cholesterol and cholesteryl esters in the different lipoprotein fractions is indicated in Fig. 7B. The specific radioactivity of free cholesterol is similar for HDL, LDL and VLDL. The specific radioactivity of cholesteryl esters however, was in HDL 3.7-fold and 3.5-fold higher than for LDL and VLDL respectively.

Biliary secretion of ^{3}H radioactivity

In order to study the kinetics of biliary secretion after injection of ^{3}H-cholesteryl ester labeled

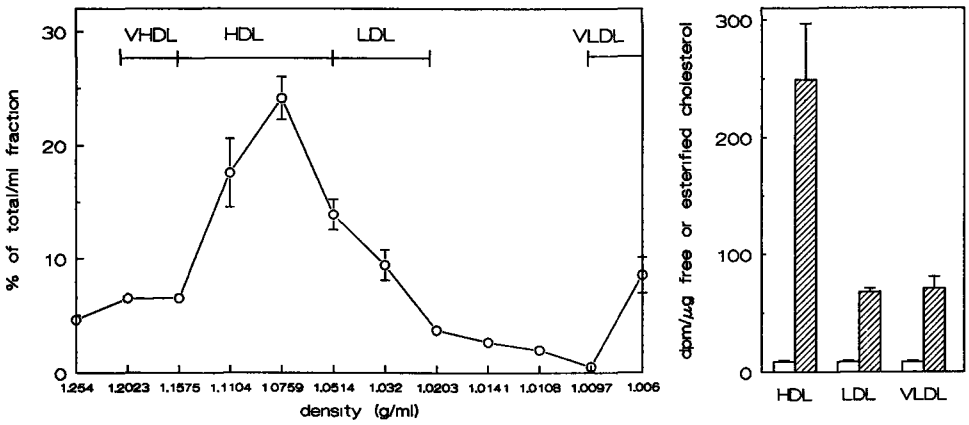

Figure 7. Density gradient distribution of ^{3}H radioactivity in the serum and specific activities in serum fractions at 3 h after injection of ^{3}H-cholesteryl oleate labeled Ox-LDL. ^{3}H-cholesteryl oleate labeled Ox-LDL (150-200 µg) was injected into the vena penis of a rat. At 3 h after injection, serum was obtained and subjected to KBr density-gradient centrifugation at 4°C. The gradient was subdivided into 500 µl fractions, starting from the bottom (7A). The profile is a representative for 4 experiments. Specific activity of ^{3}H in the different serum fractions were measured and expressed as dpm/µg free (open bars) or esterified cholesterol (hatched bars) (7B).

Ox-LDL, we used rats catheterized in bile duct, duodenum and heart. Immediately after the administration of ^{3}H-Ox-LDL via the heart catheter, bile collection was started. The biliary secretion of ^{3}H-radioactivity is illustrated in Fig. 8. Figure 8A shows the kinetics of biliary secretion expressed as percentage of injected dose secreted per hour. The immediate rapid secretion of radiolabeled bile resulted in a high initial peak during the first hours after injection of ^{3}H-cholesteryl ester labeled Ox-LDL. At 6 h after injection already 19.2% of the injected dose could be recovered in the bile. For ^{3}H-cholesteryl oleate labeled Ac-LDL the initial biliary secretion rate was much lower. Upto 6 h after injection only 6.3% of the injected dose was secreted into the bile (14). Most of the biliary radioactivity (91.3 ± 2.6%) could be recovered in the aqueous layer after Bligh and Dyer extraction (12), indicating that radioactivity was present as bile acids. The remainder was recovered as labeled free cholesterol. When the biliary secretion is expressed cumulatively (Fig. 8B), it appears that the great initial difference in biliary secretion after injection of ^{3}H-cholesteryl oleate labeled Ox-LDL or Ac-LDL is diminished at later time points. Especially in the first 24 h after injection, the biliary output of ^{3}H-cholesteryl oleate labeled Ox-LDL derived radioactivity is higher than with ^{3}H-cholesteryl oleate labeled Ac-LDL. At 72 h after injection of Ox-LDL 56.8 ± 1.5% of the injected dose has been secreted in the bile while for ^{3}H-cholesteryl oleate labeled Ac-LDL this value is 50.5 ± 2.2%.

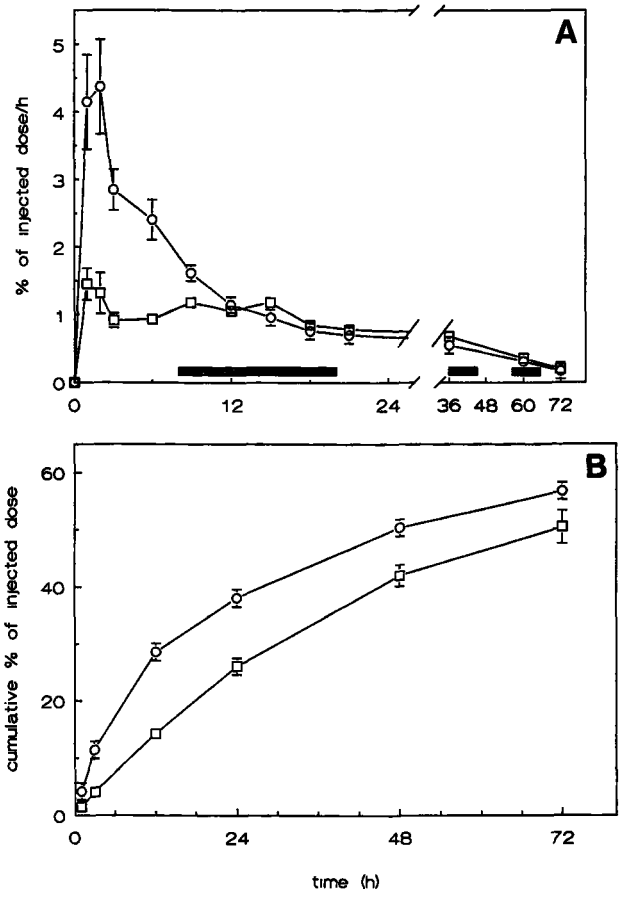

Figure 8. Biliary secretion of ^{3}H radioactivity after injection of ^{3}H-cholesteryl oleate labeled Ox-LDL (○) or Ac-LDL (□). Bile was collected for 72 hour in 1 hour time intervals after injection of 40-50 μg of ^{3}H-cholesteryl oleate labeled Ox-LDL or Ac-LDL in unrestrained cannulated rats. Values are expressed as percentages of injected dose per hour (8A) or as cumulative percentage of injected dose (8B) and represent the mean of 4 experiments ± S.E.M. Black horizontal bars indicate the dark periods.

Discussion

In a previous study with Ac-LDL we provided evidence for the role of HDL in reverse cholesterol transport *in vivo*. It appeared that HDL could act as an acceptor for liver endothelial cell associated cholesterol with subsequently transport of cholesterol to liver parenchymal cells and bile (14). Since oxidized LDL rather than acetylated LDL is the (patho)physiological representative for atherogenic LDL particles, we investigated in the present study the *in vivo* fate of ^{3}H-cholesteryl oleate labeled Ox-LDL.

^{3}H-cholesteryl oleate labeled Ox-LDL was rapidly cleared from the serum and almost quantitatively recovered in the liver. The appearance of ^{3}H-free cholesterol in the liver indicated that the liver rapidly hydrolyzed the cholesteryl esters derived from Ox-LDL. Ox-LDL particles are taken up as integral particles from the blood circulation as indicated by the similar cellular distribution of the apolipoprotein and cholesteryl ether moiety. When Ox-LDL labeled with ^{3}H-cholesteryl oleate was injected, it appeared that already in the first 10 min after injection cholesteryl esters were processed and some ^{3}H-free cholesterol was released from the Kupffer cells. The specific radioactivity of Kupffer cells at 10 min after injection of ^{3}H-cholesteryl oleate labeled Ox-LDL was 79% of the specific activity after injection of ^{3}H-cholesteryl oleoyl ether labeled Ox-LDL. At 1 h after injection of ^{3}H-cholesteryl oleate Ox-LDL the Kupffer cell associated radioactivity was declined to 32% of the maximal uptake value. The rapid hydrolysis and rapid secretion of ^{3}H-free cholesterol was reflected by a modest increase in serum radioactivity. The increase in serum radioactivity reached a value of approximately 3% of the injected dose and remained at this level during 12 h after injection. The ratio of radiolabeled free cholesterol to cholesteryl esters in the serum initially rapidly increased, which indicates that free cholesterol is secreted into the serum compartment. By gradient ultracentrifugation most of the radioactivity could be recovered in the HDL range. Subsequently the relative proportion of cholesteryl esters to the total radioactivity increased, a process consistent with serum conversion of cholesterol to cholesteryl esters by the enzyme lecithin cholesteryl acyl transferase. The specific radioactivity of HDL was 3.7- and 3.5-fold higher than for other lipoproteins which supports the role of high density lipoproteins as initial cholesterol acceptors and serum site for conversion into cholesteryl esters. We have shown previously, that HDL cholesteryl esters are *in vivo* selectively delivered to liver parenchymal cells and efficiently processed into bile acids (19). In the present study, the rapid secretion of ^{3}H-free cholesterol from Kupffer cells appeared to be linked to a rapid biliary secretion of radioactivity. Almost all of the radioactivity could be recovered in the aqueous phase after extraction, indicating an almost complete intracellular processing into bile acids in the parenchymal cells. Collection of bile at shorter time intervals showed that the lag-phase of biliary secretion of radioactivity was only 15 min (data not shown). After this time point biliary secretion rapidly increased. Upto 6 h after injection, the biliary secretion of radioactivity from ^{3}H-cholesteryl oleate labeled Ox-LDL was much higher than for ^{3}H-cholesteryl oleate labeled Ac-LDL. It thus appears that the Kupffer cell mediated uptake as compared to liver endothelial cells, is more efficiently coupled to bile acid formation. The molecular mechanism for this more efficient appearance of bile acids radioactivity from ^{3}H-cholesteryl oleate labeled Ox-LDL might be explained in two ways.

In case of ^{3}H-cholesteryl oleate labeled Ac-LDL, the minimal serum value (at 30 min after injection) is two times lower than after injection of ^{3}H-cholesteryl oleate labeled Ox-LDL (0.7% versus 1.5%). Furthermore, resecretion percentages in the serum are higher for

Ac-LDL as for Ox-LDL (5% versus 3%). Comparing the kinetics of biliary secretion, it is clear that radiolabeled bile acids derived from Ox-LDL are secreted at an initially 3-fold higher rate than for Ac-LDL. Anatomically, biliary secretion is linked to liver parenchymal cells. Thus, cholesterol transport from liver endothelial cells and Kupffer cells to parenchymal cells is obligatory. It is possible that Kupffer cells secrete vesicles containing cholesterol and other lipids, which are rapidly taken up by liver parenchymal cells. It has been reported that mouse macrophages and human monocyte-macrophages secrete apolipoprotein E (apoE), which can be incorporated in lipoproteins (30). Increases in cellular cholesterol content markedly stimulate the apoE production (31). Immunogold labeling of rat liver showed that also Kupffer cells do stain for apoE (32). ApoE, secreted by Kupffer cells, may be associated with a lipid vesicle and evoke an apoE-mediated uptake by parenchymal cells. A high turnover of these vesicles would explain the pattern of serum radioactivity for Ox-LDL. We tried to test this hypothesis by blocking apoE-mediated parenchymal cell uptake by lactoferrin (33). However, no effect of lactoferrin on the biliary secretion rate was noticed (M.N. Pieters et al., unpublished). The second explanation is related to the difference in localisation of liver endothelial cells and Kupffer cells. Liver endothelial cells are separated from parenchymal cells by the space of Disse. Therefore, cholesterol from liver endothelial cells has to be transported through the serum compartment in order to reach the parenchymal cells. Kupffer cells are located in the sinusoids, but micropodia of Kupffer cells are able to penetrate through the endothelial fenestrae and can be in direct contact with the microvilli of parenchymal cells. This would enable the Kupffer cell to directly transport cholesterol from the Kupffer cell to the parenchymal cell. To discriminate between these possibilities and to explain the molecular mechanisms of the rapid cholesterol transport from Kupffer cells to parenchymal cells further experiments will be necessary.

In conclusion, cholesteryl esters from oxidized LDL are *in vivo* mainly taken up by Kupffer cells and rapidly hydrolyzed to free cholesterol. Resecretion of cholesterol to serum HDL occurs, supporting a role of HDL in reverse cholesterol transport. A relative rapid secretion of radiolabeled bile acids is noticed after injection of ^{3}H-Ox-LDL which was 3-fold higher than for ^{3}H-Ac-LDL. The rapid processing of cholesteryl esters from Ox-LDL by Kupffer cells and the efficient conversion to bile acids and secretion into bile indicate that Kupffer cells form an efficient major protection system against the atherogenic action of Ox-LDL in the blood compartment.

References

1. Goldstein, J.L., Ho, Y.K., Basu, S.K. and Brown, M.S. Binding site on macrophages that mediates uptake and degradation of acetylated low density lipoprotein, producing massive cholesterol deposition. Proc. Natl. Acad. Sci. U.S.A. 1979;76:333-337

2. Mahley, R.W., Innerarity, T.L., Weisgraber, K.H. and Oh, S.Y. Altered metabolism (in vivo and in vitro) of plasma lipoproteins after selective chemical modification of lysine residues of the apoproteins. J. Clin. Invest. 1979;64:743-750
3. Fogelman, A.M., Schlechter, I., Seager, J., Hokom, M., Child, J.S. and Edwards, P.H. Malondialdehyde alteration of low density lipoproteins leads to cholesterol ester accumulation in human monocyte macrophages. Proc. Natl. Acad. Sci. U.S.A. 1980;77:2214-2218
4. Parthasarathy, S., Steinbrecher, U.P., Barnett, J., Witztum, J.L. and Steinberg, D. Essential role of phospholipase A_2 activity in endothelial cells induced modification of LDL Proc. Natl. Acad. Sci. U.S.A. 1985;82:3000-3004
5. Brown, M.S., and Goldstein, J.L. Lipoprotein metabolism in the macrophage: Implications for cholesterol deposition in atherosclerosis. Annu. Rev. Biochem 1983;52:223-261
6. Van Berkel, Th.J.C. De Rijke, Y. B., and Kruijt, J.K. Different fate in vivo of oxidatively modified low density lipoprotein and acetylated low density lipoprotein in rats. Recognition by various scavenger receptors on Kupffer and endothelial cells. J. Biol. Chem. 1991;266:2282-2289
7. Steinberg, D. Metabolism of lipoproteins and their role in the pathogenesis of atherosclerose. Atheroscl. Rev 1988;18:1-23
8. Glomset, J.A. The plasma lecithin:cholesterol acyltransferase reaction. J.Lipid Res. 1968;9:155-167
9. Phillips, M.C., McLean, L.L., Stoudt, G.W. & Rothblath, G.H. Mechanism of cholesterol efflux from cells. Atherosclerosis 1980;36:409-422
10. Johnson, W.J., Mahlberg, F.H., Rothblat, G.H., and Phillips, M.C. Cholesterol transport between cells and high-density lipoproteins. Biochim. Biophys. Acta 1991;1085: 273-298
11. Oram J.F., Johnson C.J., Aulinskas-Brown T. Interaction of high density lipoprotein with its receptor on cultured fibroblasts and macrophages. Evidence for reversible binding at the cell-surface without internalization. J. Biol. Chem. 1987;262:2405-2410
12. Slotte J.P., Oram J.F., Bierman E.L. Binding of high density lipoproteins to cell receptors promotes translocation of cholesterol from intracellular membranes to the cell surface. J. Biol. Chem. 1987;262:12904-12907
13. Mahlberg, F.H., and Rothblat, G.H. Cellular cholesterol efflux: Role of cell membrane kinetic pools and interaction with apolipoproteins A-I, A-II and Cs. J. Biol. Chem. 1992;267:4541-4550
14. Bakkeren, H.F., Kuiper, F., Vonk, R.J. & Van Berkel, Th.J.C. Evidence for reverse cholesterol transport in vivo from liver endothelial cells to parenchymal cells and bile by high-density-lipoprotein. Biochem. J. 1990;268:685-691
15. Pittman, R.C., Knecht, T.P., Rosenbaum, M.S., and Taylor, C.A. Jr. A non-endocytotic mechanism for the selective uptake of high density lipoprotein associated cholesteryl esters. J.Biol.Chem. 1987;262:2443-2450
16. Glass, C., Pittman, R.C., Weinstein, D.B., and Steinberg, D. Dissociation of tissue uptake of cholesterol ester from that of apoprotein A-I of rat plasma high density lipoprotein: Selective delivery of cholesterol ester to liver, adrenal, and gonad. Proc. Natl. Acad. Sci. U.S.A. 1983;80:5435-5439
17. Leitersdorf, E., Stein, O., Eisenberg, S. & Stein, Y. Uptake of rat plasma HDL fractions labeled with cholesteryl oleoyl ether or with ^{125}I by cultured rat hepatocytes and adrenal cells. Biochim. Biophys. Acta 1984;796:72-82
18. Rinniger, F. & Pittman, R.C. Regulation of the selective uptake of high density lipoproteins-associated cholesteryl esters. J. Lipid Res. 1987;28:1313-1325
19. Pieters, M.N., Schouten, D., Bakkeren, H.F., Esbach, S., Brouwer, A., Knook, D.L., and van Berkel, Th.J.C. Selective uptake of cholesteryl esters from apolipoprotein E-free high density lipoproteins by rat parenchymal cells in vivo is efficiently coupled to bile acid synthesis. Biochem. J. 1991;280:359-365
20. Redgrave, T.G., Roberts, D.C.K. & West, C.E. Separation of plasma lipoproteins by density gradient ultracentrifugation. Anal. Biochem. 1975;65:42-49

21. Blomhoff, R., Drevon, C.A., Eskild, W., Helgerud, P., Norum, K.R. and Berg, T. Clearance of acetyl low density lipoprotein by rat liver endothelial cells J. Biol. Chem. 1984;259:8898-8903
22. Bligh, E.G. & Dyer, W.J. A rapid method of total lipid extraction and purification. Can. J. Biochem. Physiol. 1959;37:911-917
23. Nagelkerke, J.F. and van Berkel, Th.J.C. Rapid transport of fatty acids from rat liver endothelial cells to parenchymal cells after uptake of cholesteryl-ester labeled acetylated LDL. Biochim. Biophys. Acta 1986;875:593-598
24. Basu, S.K., Goldstein, J.L., Anderson, R.G.W., Brown, M.S. Degradation of cationized low density *lipoprotein and regulation of cholesterol metabolism in homozygous familial hypercholesterolemia* fibroblasts. Proc. Natl. Acad. Sci. U.S.A. 1976;72:3178-3182
25. Van Berkel, Th.J.C., Kruijt, J.K. & Kempen, H.J.M. Specific targeting of high density lipoproteins by incorporating of a Tris-galactoside-terminated cholesterol derivative. J. Biol. Chem. 1985;260:12202-12207.
26. Van Berkel, Th.J.C., Kruijt, J.K., Spanjer, H.H., Nagelkerke, J.F., Harkes, L. and Kempen, H.-J.M. The effect of a water-soluble tris-galactoside terminated cholesterol derivative on the fate of low-density lipoproteins and liposomes. J. Biol. Chem 1985;260:2694-2699
27. Nagelkerke, J.F., Barto, K.P. and van Berkel, Th.J.C. In vivo and in vitro uptake and degradation of acetylated low density lipoprotein by rat liver endothelial, Kupffer and parenchymal cells. J. Biol. Chem. 1983;258:12221-12227
28. Kuipers, F., Havinga, R., Bosschieter, H., Toorop, G.P., Hindriks, F.R. & Vonk, R.J. Enterohepatic circulation in the rat. Gastroenterology 1985;88:403-411
29. Lowry, O.H., Rosebrough, N.J., Farr, A.L. & Randall, R.J. Protein measurement with the Folin phenol reagent. J. Biol. Chem. 1951;193:265-275
30. Basu, S., Ho, Y., Brown, M., Bilheimer, D., Anderson, R. & Goldstein, J. Biochemical and genetic studies of the apoprotein E secreted by mouse macrophages and human monocytes. J. Biol. Chem. 1982;257:9788-9795
31. Mazzone, T., Gump, H., Diller, T. & Getz, G.S. Macrophage free cholesterol content regulates apo E production. J. Biol. Chem. 1987;262:11657-11662
32. Hamilton, R.L., Wong, J.S., Guo, L.S.S., Krisans, S. & Havel, R.J. Apolipoprotein E localization in rat hepatocytes by immunogold labeling of cryothin sections J. Lipid Res. 1990;31:1589-1603
33. Van Dijk, M.C.M., Ziere, G.J., Boers, W., Linthorst, C., Bijsterbosch, M.K. & Van Berkel, Th.J.C. Recognition of chylomicron remnants and ß-migrating very low density lipoproteins by the remnant receptor of parenchymal cells is distinct from the liver α_2-macroglobulin recognition site. Biochem. J. 1991;279, 863-870

Chapter 4

Morphological Characterization of Scavenger Receptor-Mediated Processing of Modified Lipoproteins by Rat Liver Endothelial Cells

Sebastiaan Esbach[1], Monique F. Stins[1]*, Adriaan Brouwer[1], Paul J.M. Roholl[1#], Theo J.C. van Berkel[2] and Dick L. Knook[1].

[1] TNO Institute of Ageing and Vascular Research, Gaubius Laboratories, Leiden, The Netherlands.

[2] Division of Biopharmaceutics, Center for Bio-Pharmaceutical Sciences, University of Leiden, Sylvius Laboratories, Leiden, The Netherlands.

present address:

* Childrens Hospital of L.A., Los Angeles, USA.

\# RIVM, Bilthoven, The Netherlands.

Accepted for publication in Experimental Cell Research

Summary

Scavenger receptor-mediated processing by rat liver endothelial cells *in vivo* is studied by using acetylated and oxidized low density lipoproteins (LDL) as ligands. The cellular localization of acetylated LDL (Ac-LDL) is visualized both by immuno-histochemistry, and by silver enhancement of ultra small gold particles conjugated to Ac-LDL.

Scavenger receptor-mediated internalization by the endothelial cells only involves coated vesicle formation. Subsequently, three stages of processing are noticed, as represented by 1) large electron lucent vesicles, with ligand in close association to the membrane, 2) relatively electron lucent structures, with Ac-LDL dispersed over the vesicular lumen, while tubular membrane extensions did not contain ligand, and, 3) electron dense vesicles in which the non-degradable gold particles of the conjugate accumulate, while the immuno-reactivity for Ac-LDL is low. Addition of chloroquine, an inhibitor of lysosomal degradation, demonstrated that the relatively electron lucent and electron dense structures represent subsequent stages of the lysosomal pathway of Ac-LDL, which was also verified by detection of the lysosomal enzyme cathepsin D. Evaluation of the processing of Ac-LDL and oxidized LDL, labeled with different fluorochromes, demonstrated that both ligands follow apparently the same intracellular pathway in the liver endothelial cells, since the fluorescent probes are predominantly localized in the same structures.

It is concluded that the scavenger receptor-mediated processing of modified LDL by rat liver endothelial cells involves four morphologically distinguishable stages which represent a highly effective catabolic route, sustaining the important role of the liver endothelial cells in the protection against circulating atherogenic lipoproteins.

Introduction

Liver endothelial cells have been demonstrated to be responsible for the uptake of several ligands, including modified low density lipoproteins (1-4). Modification of LDL is considered to be of great importance in the development of atherosclerosis. In contrast to native LDL, modified LDL is able to provoke foam cell formation, which is an early characteristic of the atherosclerotic lesion (5). Several modifications of LDL have been described including acetylation (6), biological modification (7), and oxidation (8).

Ac-LDL is demonstrated to be rapidly cleared from the blood by the liver by a receptor-mediated mechanism (1,2). This so-called scavenger receptor is predominantly localized on liver endothelial cells (1,2), and is suggested to form an important protection against the occurrence of atherogenic lipoproteins in the circulation. More recently, the (patho)physiological representative of modified LDL was suggested to be oxidized LDL (Ox-LDL) (9). Ox-LDL is rapidly cleared from the circulation by the liver, but in contrast to Ac-

LDL, mainly by Kupffer cells, although the liver endothelial cells still account for about 40% of the uptake of Ox-LDL (4). Cross-competition experiments showed that two scavenger receptors are present on liver endothelial cells and Kupffer cells, one recognizing exclusively Ox-LDL, and another receptor recognizing both Ox-LDL and Ac-LDL (4).

We recently visualized the uptake and processing of Ox-LDL in the rat liver by immuno-electron microscopy, and noticed in the liver endothelial cells, scavenger receptor-mediated uptake via coated vesicle formation. Subsequently Ox-LDL is processed via a compartment in which uncoupling of receptors and ligands seemed to occur, before the lysosomes are reached (10). Earlier studies suggested that the uptake of a number of ligands, including Ac-LDL, by the liver endothelial cells can result from direct invagination of the plasma membrane, leading to macropinocytotic vesicles (11-13). The position and shape of these macropinocytotic structures would allow a rapid transport of the internalized receptors to the plasma membrane.

In the present work we address the question whether macropinocytosis does explain the extremely rapid processing of scavenger receptor-mediated uptake of Ac-LDL by the liver (1,2). Two independent labeling techniques, immuno-staining and recently developed ultra small (1 nm) gold particles (14) conjugated to Ac-LDL were used to describe the intracellular processing of Ac-LDL. Furthermore, a specific staining technique, which allows the discrimination between intracellular and extracellular compartments is used to identify the early stages of Ac-LDL processing at the ultrastructural level. At the light microscopical level we evaluated by a direct comparison whether Ac-LDL and Ox-LDL are processed via different intracellular pathways, using a double-labeling fluorescence technique.

Materials and Methods

Materials

Bovine serum albumin (fraction V), polyinosinic acid (PIA), and chloroquine were purchased from Sigma (St. Louis, MO, USA). Gelatin and glycine were obtained from Merck (Darmstadt, Germany). Tylose (MH 300) was purchased from Fluka (Buchs, Switzerland). Gold-conjugated antibodies were purchased from Aurion (Wageningen, Netherlands), and the monoclonal antibodies mouse anti-rabbit and rabbit anti-mouse peroxidase from Dakopatts (ITK Diagnostics, Netherlands). 1,1'-dioctadecyl-3,3,3',3'-tetramethyl indocarbocyanine perchlorate (DiI) and 3,3' dioctadecyloxacarbo-cyanine perchlorate (DiO) were obtained from Molecular Probes (Eugene, OR, USA).

Lipoprotein isolation, acetylation and oxidation

LDL ($1.024 < d < 1.055$) was isolated from human plasma plus 1 mM EDTA by density gradient centrifugation according to Redgrave et al. (15). LDL was dialysed against

phosphate-buffered saline (PBS) plus 1 mM EDTA and acetylated by repetitive addition of acetic anhydride as described by Basu et al. (16). LDL was dialysed against PBS containing 10 μM EDTA before being oxidized (200 μg of protein/ml) by exposure to $CuSO_4$ (5 μM free Cu2+ concentration) as described by Van Berkel et al. (4). Oxidation was arrested by cooling and addition of 200 μM EDTA. Acetylation and oxidation of LDL were tested by assessing the electrophoretic mobility on agarose gel. In comparison to native LDL, the Rf value of Ac-LDL and Ox-LDL were increased from 0.21 $\pm$ 0.01 to 0.52 $\pm$ 0.01 and 0.54 $\pm$ 0.01 respectively, in accordance to the data of Van Berkel et al. (4).

Conjugation of fluorescent- and gold probes to modified LDL

Ac-LDL and Ox-LDL were fluorescently labeled with DiI or DiO according to Pitas et al. (17). The density of the fluorescent dye and lipoprotein mixture was subsequently raised to 1.21, and the lipoproteins were re-isolated by ultracentrifugation according to the above described procedure.

Conjugation of Ac-LDL to ultra small gold (1 nm) was performed by Aurion (Wageningen, Netherlands). The Ac-LDL particles conjugated to colloidal gold will be referred to as Ac-LDL-Au. To study whether conjugation of the colloidal gold to the Ac-LDL particles interfered with the specific cell-recognition of Ac-LDL, non-parenchymal cell fractions, isolated according to the below described procedure, were incubated with Ac-LDL-Au in the absence or presence of excess unlabeled Ac-LDL.

Non-parenchymal liver cell suspensions from untreated rats, containing about 20% Kupffer cells, 45% endothelial cells and 29% lymphoid cells as determined by morphological characterization at the electron microscopic level, were obtained by the warm collagenase method described previously (21). Non-parenchymal cells were separated from parenchymal cells by differential centrifugation (0.5 min., 50 g, three times). The viability of the cell suspensions was more than 90% as determined from trypan blue exclusion.

The cell suspensions (0.5 x 10^6/ml) were incubated at 37°C with 30 μg Ac-LDL-Au/ml for 10 minutes. When indicated 500 μg/ml unlabeled Ac-LDL was added to the medium 5 minutes prior to the incubation with Ac-LDL-Au. Cells were fixed with 4% paraformaldehyde (PF) and 0.1% glutaraldehyde (GA) in phosphate-buffered saline (PBS) for 10 minutes at 4°C. Following centrifugation the cell pellets were post-fixed in OsO_4 and subsequently dehydrated and embedded in epon.

Ac-LDL-Au preferentially bound to the liver endothelial cells and only to a small extent to Kupffer cells, confirming previous biochemical data (1). Binding of the Ac-LDL-Au particles to endothelial cells (Fig. 1a) was strongly reduced by 17 fold excess of unlabeled Ac-LDL (Fig. 1b), demonstrating the interaction to be scavenger receptor-mediated. Gold-conjugation has been described previously to influence receptor recognition (18,19), and also to interfere with intracellular processing (20), probably due to the net negative charge and size of the conjugates. The size of the conjugate depends on the ratio of gold particles and

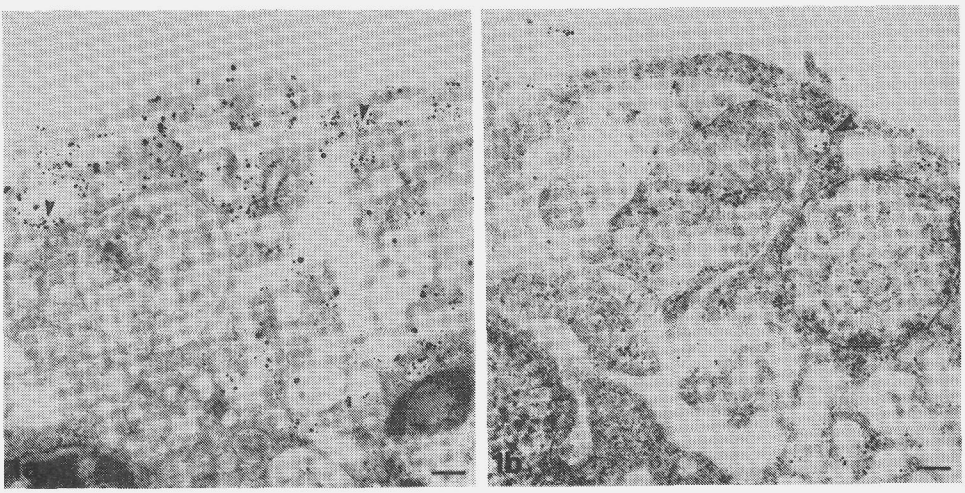

Figure 1. Electron micrographs of isolated liver endothelial cells. Cells were incubated for 10 minutes with Ac-LDL-Au in the absence (a) or presence of excess unlabeled Ac-LDL (b). Ac-LDL-Au particles were visualized by silver enhancement. Incubation with Ac-LDL-Au results in an association of label to the plasma membrane, and vesicles. The latter in close proximity to the vesicle membrane (arrowheads)(a). In the presence of excess unlabeled Ac-LDL a clear overall decrease of labeling of the endothelial cells is observed (b). Note the presence of gold label in coated pits (large arrowhead). Bars = 2 μm.

lipoprotein particles, and the size of the gold particles used. For example conjugation of 1 nm gold to Ac-LDL (ø 23 nm) leads to a conjugate with a size of approximately 24 nm. The use of 20 nm gold particles leads to Ac-LDL conjugates of about 66 nm in diameter, since several lipoprotein particles will bind to one gold granule (13). It can be concluded from the competition studies depicted in Fig. 1 that Ac-LDL-Au used in our experiments still interacts with its original binding site.

Animals and perfusion studies

For the visualisation studies on *in vivo* endocytosed Ac-LDL, 3-month-old male Wag/Rij rats were used, weighing about 200 grams. When indicated rats were pre-treated with chloroquine according to Hornick et al. (22). As confirmed by routine electron microscopy, pre-treatment of rats with chloroquine resulted in an increase in the number of (pre-)lysosomal structures in endothelial cells.

Ac-LDL or Ac-LDL-Au (50 μg/ml plasma) was injected into the vena cava inferior of overnight fasted rats under halothane anaesthesia and was allowed to circulate 2, 10 and 30 minutes. For practical reasons Ac-LDL was injected into the portal vein to allow localization studies after 30 seconds of circulation. To study the co-localization of Ac-LDL and Ox-LDL

both were labeled with DiI or DiO, injected simultaneously in an equal dose, and allowed to circulate for 10 minutes. Control liver was obtained from rats intravenously injected with PBS only, following a 10 minute incubation. Subsequently, rat livers were rinsed with PBS (1 minute), or directly fixed with 4% PF and 0.1% GA in PBS by *in situ* perfusion via the portal vein for 10 minutes at room temperature. Livers were stored in 2% PF in PBS at 4°C.

Light- and electron microscopical studies

Ruthenium red staining. To differentiate between intracellular and extracellular compartments in order to study the internalisation mechanisms, 200 μm vibratome sections of fixed liver tissue were stained *en bloc* with the membrane mordant stain ruthenium red according to Handley et al. (23) and, subsequently, dehydrated in a graded series of ethanol and embedded in epon. Ultrathin sections were viewed in the electron microscope without further contrasting.

Fluorescence microscopy. Liver tissue which was used for fluorescence microscopy was after fixation dissected, and 200 μm vibratome slices were immersed in 2.3 M sucrose. To prepare cryosections, small pieces of liver tissue were placed on a specimen holder and frozen in liquid nitrogen. Semithin cryosections were cut using a Reichert FC-4D Ultracut cryomicrotome at a temperature of -100°C. To localize DiI- and DiO-fluorescence, semithin sections were placed on a glass cover slip and after being mounted with glycerol viewed with a Leitz ortholux microscope with standard rhodamine and FiTC excitation and emission filters.

Visualization of Ac-LDL-Au. Livers that were used for ultrastructural localization of Ac-LDL-Au were postfixed in 1% OsO_4 in 0.15 M sodium cacodylate buffer for 45 minutes, dehydrated, and, embedded in epon. Silver enhancement (10 minutes) of ultrathin sections was performed according to the procedure of Danscher (24). Subsequently, sections were contrasted with lead citrate and examined in a Philips EM 410 electron microscope. Control silver enhancement on liver tissue injected with unlabeled Ac-LDL showed no label at all after the indicated silver enhancement time.

Immuno-histochemistry. Antibodies against human apolipoprotein B (apoB), raised in rabbits, were kindly donated by Dr. L. Havekes (IVVO-TNO, Leiden, the Netherlands) (25). The antibody was tested for reactivity with native and modified LDL using the double radial immuno-diffusion method as described by Crowle (26). Results showed that Ac-LDL had sufficiently retained antigenicity to allow use of the antibody against native LDL for immuno-cytochemical studies (27). Cross-reactivity with the rat lipoproteins LDL, VLDL and HDL, and lipoprotein deficient rat serum was absent (27). Rabbit antibodies against cathepsin D was kindly given by R. Willemsen (Dept. of Cell Biology, Erasmus University, Rotterdam the Netherlands). Their specificity has been described by Reuser et al. (28).

Specimens that were used for immuno-histochemical studies were embedded in 5% gelatin, and immersed in 2.3 M sucrose in PBS, overnight. Semithin or ultrathin cryosections

were cut of small pieces of liquid frozen liver tissue a temperature of -100°C. Semithin and ultrathin sections were placed on glass cover slips and carbon coated nickel grids respectively.

For the immuno-labeling procedure, antibodies and gold conjugates were diluted in PBS containing 0.1% gelatin, 0.5% BSA and 0.1% Tween 20. The dilutions used were: anti-apoB, 600 fold, anti cathepsin D, 100 fold, goat anti-rabbit IgG gold (6 nm), 30 fold, mouse anti-rabbit, 100 fold, rabbit anti-mouse peroxidase, 100 fold. For the washing steps the same medium was used, unless otherwise indicated.

Cryosections were incubated with 0.05 M glycine in PBS, washed, incubated with 10% non-immune rat serum followed by incubation with the primary antibody, washed, incubated with the secondary antibody coupled to colloidal gold, washed, washed again with aqua dest, stained with uranylacetate and covered with tylose according to Tokuyasu (29), or following the primary antibody, washed, incubated with the secondary antibody, washed again, incubated with the peroxidase conjugated antibody, washed, incubated with diaminobenzidine and H_2O_2, washed with aqua dest, counterstained with hematoxyline, washed again with aquadest, and finally embedded in entellan. Endogenous peroxidatic activity was quenched by a 10 minute incubation in 0.3% H_2O_2 in methanol preceding the light microscopical incubation procedure. Control incubations with non-immune rabbit serum resulted in a low number of randomly distributed gold label over the liver endothelial cells, seemingly not associated with particular structures. With respect to the light microscopical procedure, no reaction product was noticed.

Results and Discussion

Immuno-electron microscopical detection of Ac-LDL showed that 30 seconds after administration Ac-LDL is bound to the plasma membrane of liver endothelial cells, mainly in coated membrane invaginations (Fig. 2a). Similar findings were noticed in epon-embedded liver tissue after the enhancement of Ac-LDL-Au at the same time interval (Fig. 2b). The initial binding of Ac-LDL to the plasma membrane is in agreement with previous data which demonstrated that Ac-LDL binds in coated pits but also to uncoated areas of the plasma membrane of endothelial cells and macrophages (30,31), suggesting that the scavenger receptor is localized inside, but also outside coated pits. Sometimes two or more coated pits are in close proximity to each other, thereby forming "multiple coated pits" (Fig. 2 insets). Multiple coated pits were demonstrated in liver endothelial cells of isolated perfused livers, involved in the uptake of latex beads (ø 230 nm) (32). Ac-LDL (ø 23 nm), is 10 fold smaller and did not appear to be aggregated. It might be that the concentration of scavenger receptors on the liver endothelial cells is so high that simultaneous coated vesicle formation in close proximity of each other leads to the observed coalescence. On negatively stained cryo-

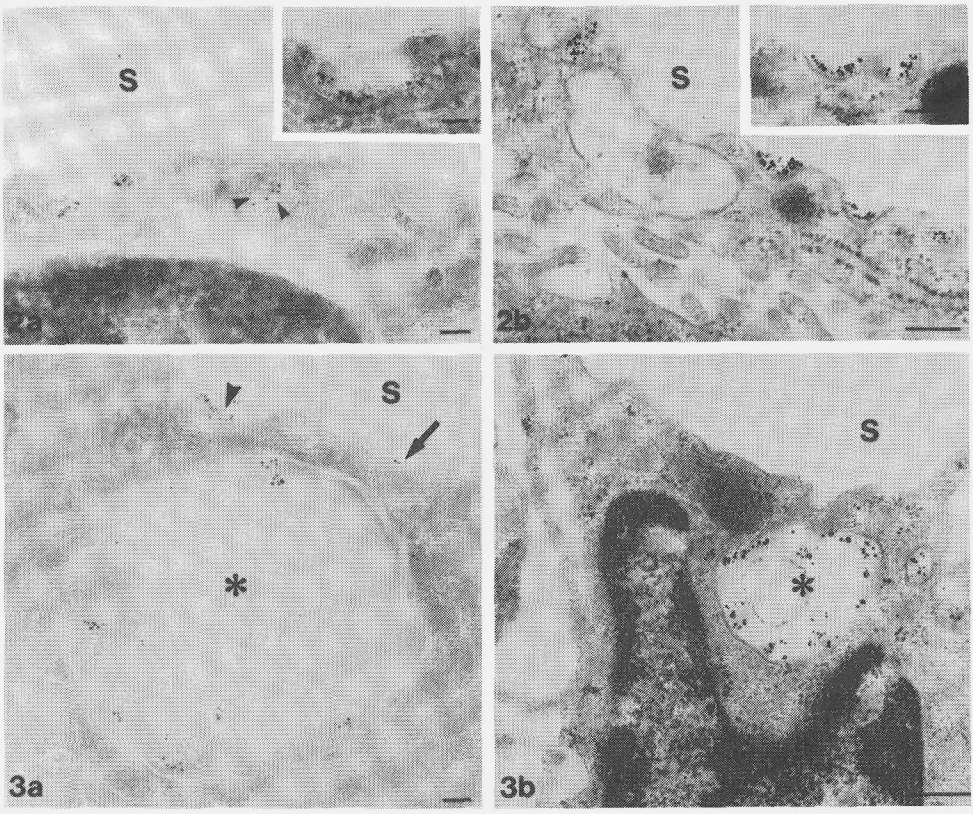

Figure 2. Cryosection (a) and epon section (b) of rat livers 15 seconds after injection of Ac-LDL or Ac-LDL-Au respectively. Gold particles representing immuno-reactive apoB (a)or Ac-LDL-Au (b) are located in coated pits, which are in different stages of vesicle formation. Due to negative staining, labeled Ac-LDL particles can be noticed in the cryosection (arrowheads)(a). Inset; Gold particles, representing Ac-LDL (a) or Ac-LDL-Au (b), are also noticed in multiple coated pits. S = sinusoid. Bars = 0.05 μm.

Figure 3. Electron micrographs of liver endothelial cells 2 minutes after injection of Ac-LDL (a) or Ac-LDL-Au (b) respectively. Immuno-localization of Ac-LDL (a) and localization of Ac-LDL-Au both show that Ac-LDL is present in close proximity to the membrane of large electron lucent vesicles (asterisks). Some Ac-LDL is noticed at the plasma membrane bound to coated (arrowhead) and uncoated areas (arrow)(a). S = sinusoid. Bars = 0.05 μm.

sections, immuno-reactive lipoprotein-like particles with an average diameter of 23 nm are recognizable in the coated pits (Fig. 2a). In accordance to their size, the immuno-reactivity, and the fact that these particles are only detectable in livers of animals that were injected with Ac-LDL, these particles most probably represent intact Ac-LDL.

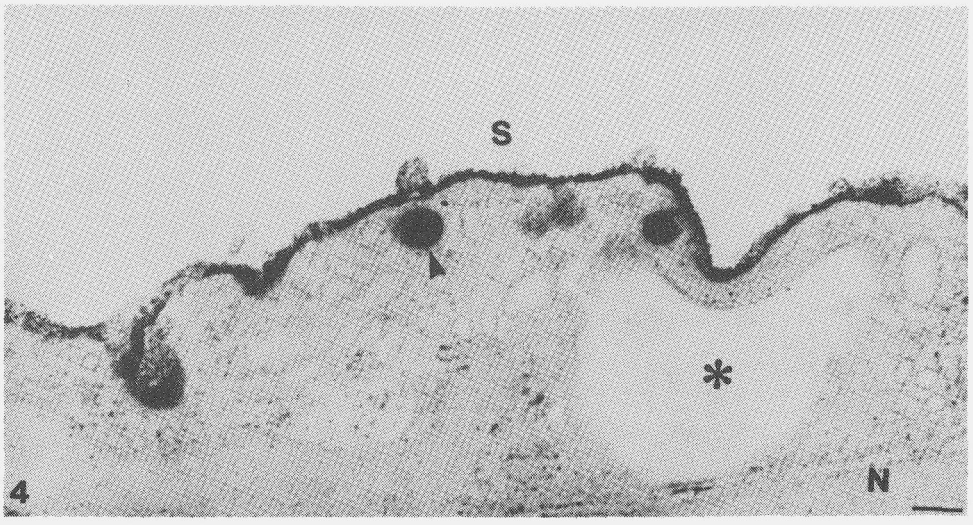

Figure 4. Electron micrograph of a liver endothelial cell, 2 minutes after injection of Ac-LDL, contrasted with ruthenium red and subsequently embedded in epon. Plasma membrane and membrane invaginations are stained, surprisingly, even when the structure is completely surrounded by cytosol (arrowhead). The membrane of large electron lucent vesicles (asterisk) is not contrasted. N = cell nucleus, S = sinusoid. Bars = 0.1 μm.

At two minutes after injection of Ac-LDL, immuno-detection of Ac-LDL demonstrated that Ac-LDL is still detectable at te plasma membrane but also in large electron lucent vesicles, in close proximity to the vesicle membrane (Fig. 3a), and inside vesicles of a higher electron density. Similar observations were made following the fate of the Ac-LDL-Au in the plastic-embedded tissue (Fig. 3b). In order to verify whether the electron lucent structures are really intracellular, the extracellular membrane mordant stain ruthenium red was used. As shown in Fig. 4 only the plasma membrane and few small vesicles are stained, while large electron lucent vesicles are not contrasted by ruthenium red. No indications of invagination of large areas of plasma membrane were noticed, strongly suggesting that the large electron lucent vesicles represent the first intracellular compartment involved in the Ac-LDL processing. Internalization of Ac-LDL by liver endothelial cells therefore seems to occur only by coated vesicle formation, in accordance with previous indications of Pitas et al. (17). The immuno-localization of Ac-LDL (Fig. 3a) and silver enhancement of Ac-LDL-Au (Fig. 3b) demonstrated that Ac-LDL was present close to the membrane of electron lucent vesicles suggesting that the particles are still associated with their receptor.

At 10 minutes after injection of the ligand, only few Ac-LDL particles are associated with the plasma membrane of the liver endothelial cells as demonstrated by immuno-histochemistry, and, occasionally, the previously described electron lucent vesicles were noticed

to contain immuno-label (not shown). The majority of Ac-LDL, as identified by immuno-histochemistry is present in roundish relatively electron lucent vesicles at 10 minutes after injection (Fig. 5a). The immuno-gold particles are not in close association with the membrane, but are dispersed over the vesicles associated with Ac-LDL particles. The detachment of the Ac-LDL, as shown by immuno-histochemistry, from the vesicular membrane indicates uncoupling of Ac-LDL from its receptor. The vesicles sometimes showed tubular membrane extensions, in which no Ac-LDL was observed by immuno-histochemical detection (Fig. 5a). Similar observations were made in the plastic embedded tissue; following silver enhancement, Ac-LDL-Au could be demonstrated dispersed over the vesicles, and also the tubular membrane extensions, which were devoid of Ac-LDL-Au were clearly detectable (Fig. 5b). Tubular structures in liver endothelial cells have been suggested to be involved in the early processing of several ligands like ferritin, a nonspecific fluid-phase marker (33), horse-radish-peroxidase (HRP) which is specifically endocytosed via its mannose-terminated oligosaccharide chains (34), and ovalbumin also internalized by the mannose receptor (35). Tubular structures which contained ovalbumin were suggested to be involved in retro-endocytosis (35), since, biochemical experiments showed that a substantial amount of ovalbumin was retro-endocytosed from an early endocytotic compartment (36). It is, therefore, conceivable that the relatively electron lucent vesicular structures with the tubular membrane extensions noticed in the present study, represent a compartment, which is functionally comparable to CURL as described by Geuze et al. (37). The dispersed labeling of the vesicular part of the structure supports the idea of uncoupling of receptor and ligand, the tubular structures devoid of ligand may suggest sorting of receptors and ligand, and from the experiments of Geuze et al. (37) it is known that morphologically similar tubular extensions were involved in the recycling of receptors to the plasma membrane. Future experiments, detecting the scavenger receptors by specific antibodies could confirm whether sorting of receptor and ligand actually takes place in these tubulo-vesicular structures.

At 30 minutes after injection of Ac-LDL, Ac-LDL, as evidenced by immuno-histochemical detection, is present inside the liver endothelial cells dispersed over the previously described relatively electron lucent vesicles, but also over more electron dense vesicles (Fig. 6a). The electron dense vesicles were smaller than the relatively electron lucent structures. The size of the electron dense vesicles varied considerably ranging from 250 nm up to 500 nm. Both structures contain the lysosomal marker cathepsin D as evidenced by immuno-histochemistry (Fig. 6b), demonstrating them both to be involved in the lysosome-directed pathway of Ac-LDL. In the more electron dense vesicles, the intact Ac-LDL particles could be detected less clearly by negative staining, suggesting loss of integrity due to degradation. The gradual increase in concentration of the Ac-LDL-Au in the more electron dense structures of epon-embedded tissue (Fig. 6c), sustains this notion, since it suggests a lysosomal accumulation of the non-degradable gold particles of the Ac-LDL-Au (Fig. 6c inset). The gradual increase of the electron density of the Ac-LDL containing vesicles, is in

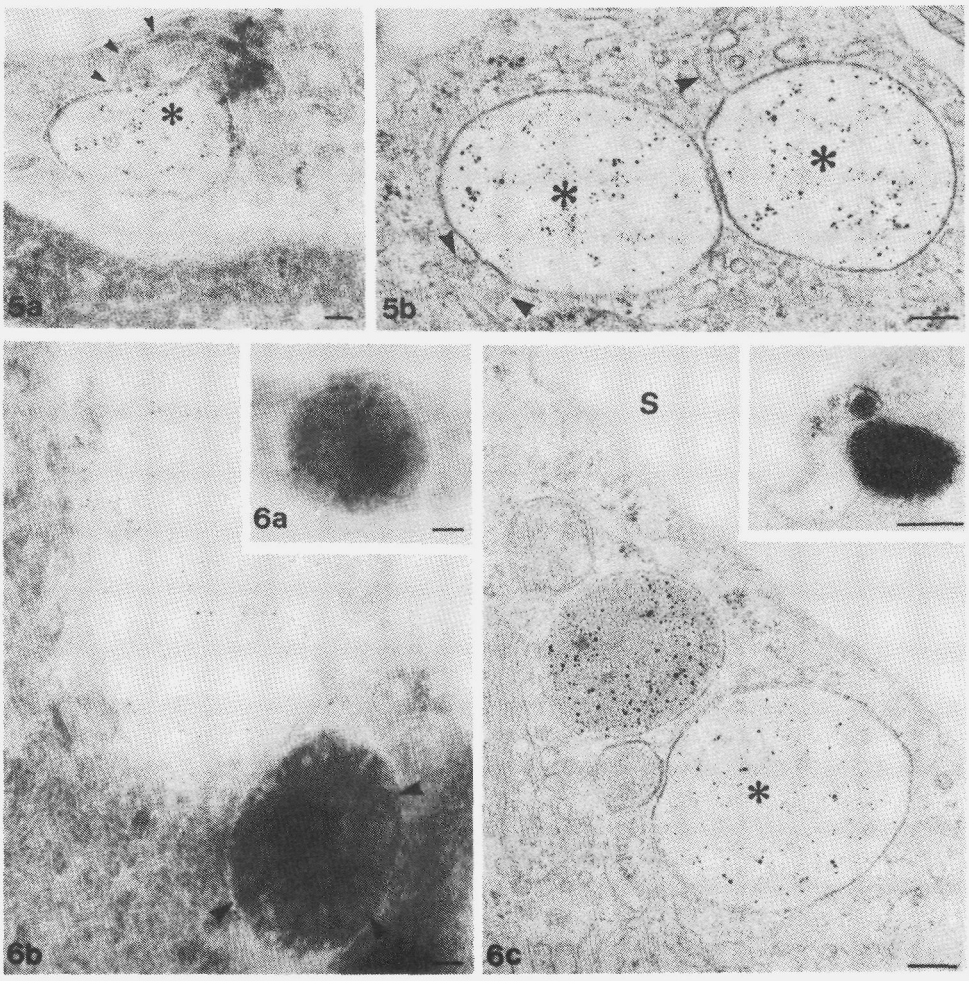

Figure 5. Localization of Ac-LDL in liver endothelial cells, 10 minutes after injection of Ac-LDL (a) or Ac-LDL-Au (b). Immuno-localization of Ac-LDL and silver enhancement of Ac-LDL-Au show that Ac-LDL is dispersed over relatively electron lucent vesicles (asterisks). Unlabeled tubular membrane extensions are noticed in connection to these vesicles (arrowheads). Bars = 0.05 μm.

Figure 6. Cryosections (a, b) and epon section (c) of rat livers 30 minutes after injection of Ac-LDL (a, b) or Ac-LDL-Au (c). Gold particles representing Ac-LDL or Ac-LDL-Au are present dispersed over vesicles, of which the electron density ranges from relatively electron lucent (asterisk) to electron dense (a, c). In comparison to the relatively electron lucent vesicles the electron dense vesicles contain less immuno-reactive apoB, while the non-degradable gold particles of Ac-LDL-Au get concentrated inside these vesicles (c inset). Immuno-localization experiments with the same livers show structures with similar electron densities to contain cathepsin D (arrowheads) (b). S = sinusoid. Bars = 0.05 μm.

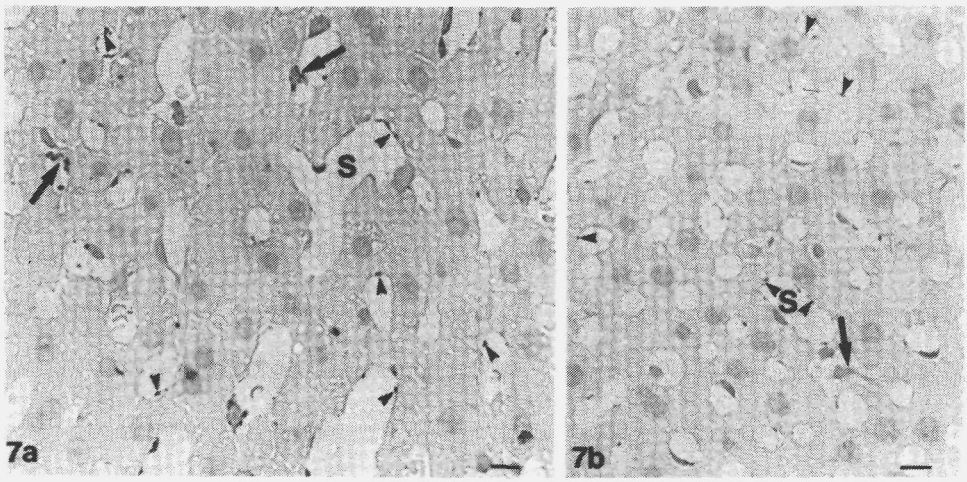

Figure 7. Micrographs of livers of chloroquine treated (a) and untreated (b) rats, 30 minutes after injection of Ac-LDL. An overall increase in staining product representing immuno-reactive apoB (arrowheads), is noticed following chloroquine treatment in the liver endothelial cells in comparison to untreated rats. Note the presence of reaction product in Kupffer cells (arrows) following chloroquine treatment. S = sinusoid. Bars = 30 μm.

agreement with morphological studies of Wisse (11,12), who described the transitional stages between endosomal and lysosomal structures in liver endothelial cells with other ligands. Pretreatment with chloroquine, an inhibitor of lysosomal degradation, strongly increases the amount of immuno-reactive apoB in the liver endothelial cells at 30 minutes, as is shown at the light microscopic level by an indirect immuno-peroxidase staining technique (Fig. 7). At the electron microscopic level, treatment with chloroquine results in an increase in the size of the relatively electron lucent structures and a concomitant increase in the amount of apoB as evidenced by immuno-histochemical detection, while only few electron dense structures are noticed to contain immuno-label (not shown). The increase of immuno-staining for apoB at the light microscopic level confirms that the lysosomal degradation of Ac-LDL is delayed by chloroquine. This is also in accordance with studies by Hornick et al. (22) and Kleinherenbrink-Stins et al. (23), who examined the effect of chloroquine on degradation in liver parenchymal and Kupffer cells. It is, therefore, suggested that the electron dense structures are lysosomes which represent the final destination for Ac-LDL as a particle. Whether the relatively electron lucent vesicles should be considered as late-endosomal or early-lysosomal structures is still a matter of debate, since previous reports showed that lysosomal enzymes can be transported to lysosomes via endosomes as also demonstrated for cathepsin D in HEPG2 cells (38).

As we found ultrastructurally similar structures of liver endothelial cells to be involved

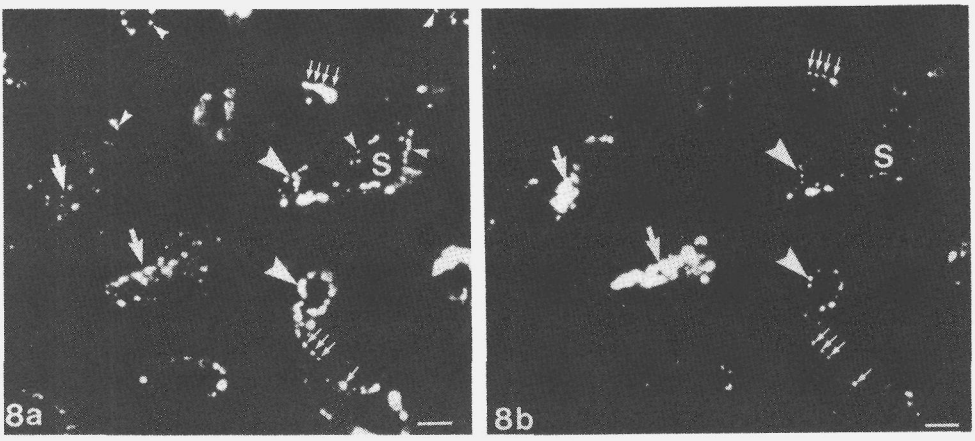

Figure 8. Fluorescence microscopy of rat liver following simultaneous administration of DiI-Ac-LDL (a) and DiO-Ox-LDL (b). Ox-LDL is predominantly associated with Kupffer cells (large arrows) while Ac-LDL is predominantly associated with liver endothelial cells (large arrowheads). Inside the endothelial cells Ox-LDL is always noticed together with Ac-LDL (small arrows), while some structures only contain Ac-LDL (small arrowheads). When DiO-Ac-LDL and DiI-Ox-LDL were applied the reverse was noticed (not shown), indicating that the applied fluorescent dye was responsible for this apparent difference. S = sinusoid. Bars = 20 μm.

in the processing of Ac-LDL and Ox-LDL (10), we evaluated whether actually the same intracellular pathway is utilized by both ligands. Simultaneous administration of DiI-Ac-LDL and DiO-Ox-LDL clearly demonstrates the difference between the cell types involved, showing DiO-fluorescence to be predominantly localized in Kupffer cells and DiI-fluorescence mainly in endothelial cells (Fig. 8), which is in accordance with earlier biochemical data (4). In endothelial cells, DiO, representing Ox-LDL, is always co-localized with DiI, representing Ac-LDL. In addition, single labeled organelles only contained dye representing Ac-LDL. Labeling of Ox-LDL and Ac-LDL with DiI and DiO in the reverse way, showed Ox-LDL and Ac-LDL to be associated with Kupffer and endothelial cells similarly to described above. In the liver endothelial cells, Ox-LDL and Ac-LDL are predominantly co-localized. Single labeled organelles appeared only to contain DiI-Ox-LDL, which is probably related to the relative brightness of the fluorescent probes used, since the above described reverse labeling demonstrated single labeled organelles to contain DiI-Ac-LDL. It is therefore assumed that Ox-LDL and Ac-LDL are processed via the same intracellular pathway by the liver endothelial cells.

In conclusion the scavenger receptor-mediated processing of modified low density lipoproteins by rat liver endothelial cells involves four morphologically distinguishable stages

1) coated vesicles 2) large electron lucent vesicles 3) relatively electron lucent structures representing CURL and 4) electron dense structures, representing a highly effective catabolic route for modified lipoproteins, sustaining the important role of the liver endothelial cells in the protection against circulating atherogenic lipoproteins.

Acknowledgements

The authors would like to thank Johannes van der Boom and Elisabeth Blauw for excellent technical assistance.

References

1. Nagelkerke, J.F., Barto K.P., and van Berkel, Th.J.C. (1983) *J. Biol. Chem.* 258, 12221-12227.
2. Blomhoff, R., Drevon, C.A., Eskild, W., Helgerud, P., Norum, K.R., and Berg T. (1984) *J. Biol. Chem.* 259, 8898-8903.
3. Nagelkerke, J.F., Havekes, L., van Hinsbergh, V.W.M., and van Berkel, Th.J.C. (1984) *Arteriosclerosis* 4, 256-264.
4. Van Berkel, Th.J.C., de Rijke, Y.B., and Kruijt, J.K. (1991) *J. Biol. Chem.* 266, 2282-2289.
5. Gerrity, R.G. (1987) *Am. J. Pathol.* 103, 181-190.
6. Goldstein, J.L., Ho, Y.K., Basu, S.K., and Brown, M.S. (1979) *Proc. Natl. Acad. Sci. USA* 76, 333-337.
7. Henriksen, T., Mahoney, E.M., and Steinberg D. (1981) *Proc. Natl. Acad. Sci. USA* 78, 6499-6503.
8. Parthasarathy, S., Steinbrecher, U.P., Barnett, J., Witztum, J.L., and Steinberg D. (1985) *Proc. Natl. Acad. Sci. USA* 82, 3000-3004.
9. Steinberg, D. (1988) *Atheroscler. Rev.* 18, 1-23.
10. Esbach, S., Pieters, M.N., van der Boom, J., Schouten, D., van der Heyde, M.N., Roholl, P.J.M., Brouwer, A., van Berkel, Th.J.C., and Knook, D.L. (1993) *Hepatology* 18, 537-545.
11. Wisse, E. (1972) *Ultrastruc. Res.* 38, 528-562.
12. Wisse, E. (1977) *in* Kupffer cells and other liver sinusoidal cells (Wisse, E., and Knook, D.L., Eds.), pp. 33-60, Elsevier/Norh Holland Biomedical Press. Amsterdam.
13. Mommaas-Kienhuis, A.M., Nagelkerke, J.F., Vermeer, B.J., Daems, W.Th., and van Berkel Th.J.C. (1985) *Eur. J. Cell Biol.* 38, 42-50.
14. Chan, J., Aoki, C, and Pickel, V.M. (1990) J. Neurosci. Meth. 33, 113-127.
15. Redgrave, T.G., Roberts, D.C.K., and West, C.E. (1975) *Anal. Biochem.* 65, 42-49.
16. Basu, S.K., Goldstein, J.L., Anderson, R.G.W., and Brown, M.S. (1976) *Proc. Natl. Acad. Sci. USA.* 73, 3178-3182.
17. Pitas, R.E., Boyles, J., Mahley, R.W., and Bissell D.M. (1985) *J. Cell Biol.* 100, 103-117.
18. Kleinherenbrink-Stins, M.F., van der Boom, J., Brouwer, A., van Berkel, Th.J.C., and Knook D.L. (1988) *Ultramicroscopy* 24, 439A.
19. Renaud, G., Hamilton, R.L., and Havel, R.J. (1989) *Hepatology* 9, 380-392.
20. Fodor, I., Egyed, A., and Lelkes G. (1986) *Eur. J. Cell. Biol.* 42, 74-78.
21. Van Bezooijen, C.F.A., Grell, T., and Knook, D.L. (1977) *Mech. Age. Dev.* 6, 293-304.
22. Hornick, C.A., Jones, A.L., Renaud, G., Hradek, G., and Havel R. (1984) *Am. J. Physiol.* 246, G187-G194.

23. Handley, D.A., Arbeeny, C.M., Witte, L.D., Goodman, D.S., and Chien, S. (1983) *J. Ultrastruct. Res.* 83, 43-7.
24. Danscher, G. (1981) *Histochemistry* 71, 81-88.
25. Havekes, L.H., Hemmink, J., and de Wit, E. (1981) *Clin. Chem.* 27, 1829-1833.
26. Crowle, A.J. (1961) *in* Immunodiffusion, New York, Academic Press.
27. Kleinherenbrink-Stins, M.F., van der Boom, J., Bakkeren, H.F., Roholl, P.J.M., Brouwer, A., van Berkel, Th.J.C., and Knook, D.L. (1990) *Lab. Invest.* 63, 73-86.
28. Reuser, A.J.J., Kroos, M., Oude Elferink, R.P.J., and Tager, J.M. (1985) *J. Biol. Chem.* 260, 8336-8341.
29. Tokuyasu, K.T. (1980) *Histochem. J.* 12, 381-403.
30. Havekes, L., Mommaas-Kienhuis, A.M., Schouten, D., De Wit, E., Scheffer, M., and Hinsbergh, V.W.M. (1985) Atherosclerosis 56, 81-92.
31. Robenek, H., Schmitz, G., Assmann, G. (1984) *J. Histochem. Cytochem.* 32, 1017-1027.
32. Praaning-Van Dalen, D.P., de Leeuw, A.M., Brouwer, A., de Ruiter, G.H.F., and Knook, D.L. (1982) *in* Sinusoidal liver cells. (Knook, D.L., Wisse, E., Eds.) pp. 271-278, Elsevier Biomedical Press, Amsterdam.
33. De Bruyn, P.P.H., Michelson, S., and Becker, R.P. (1975) *J. Ultrastruct. Res.* 53, 133-151.
34. Praaning-Van Dalen, D.P., de Leeuw, A.M., Brouwer, A., and Knook, D.L. (1987) *Hepatology* 4, 672-679.
35. Stang, E., Kindberg, G.M., Berg, T., and Roos, N. (1990) *Eur. J. Cell Biol.* 52, 67-76.
36. Magnusson, S., and Berg, T. (1989) *Biochem. J.* 257, 651-656.
37. Geuze, H.J., Slot, J.W., Strous, G.J., Lodish, H.F., and Schwartz, A.L. (1983) *Cell* 32, 277-287.
38. Rijnbout, S., Stoorvogel, W., Geuze, H.J., and Strous, G.J. (1992) *J. Biol. Chem.* 267, 15665-15672.

Chapter 5

Visualization of the *In Vivo* Interaction of β-Migrating Very Low Density Lipoproteins with the Remnant Receptor in Rat Liver

Sebastiaan Esbach[1], Johannes van der Boom[1], Moniek N. Pieters[2], Donald Schouten[2], Paul J.M. Roholl[1*], Adriaan Brouwer[1], Dick L. Knook[1] and Theo J.C. van Berkel[2]

[1] TNO Institute of Ageing and Vascular Research, Gaubius Laboratories, Leiden, The Netherlands.

[2] Division of Biopharmaceutics, Center for Bio-Pharmaceutical Sciences, University of Leiden, Sylvius Laboratories, Leiden, The Netherlands.

*present address RIVM, Bilthoven, The Netherlands.

Submitted for publication

Summary

Beta-migrating very low density lipoproteins (β-VLDL) are atherogenic lipoproteins, which accumulate in the plasma of cholesterol-fed animals and patients with type III hyperlipoproteinemia. β-VLDL is predominantly taken up from blood in rats by a lactoferrin inhibitable binding site on liver parenchymal cells, presumably the remnant receptor. In the present study we visualized the *in vivo* interaction of β-VLDL with the parenchymal cells, the possible involvement of endogenous apolipoprotein E (apoE), and the mechanism of inhibition by lactoferrin.

To study the interaction of β-VLDL with the liver, fluorescently labeled rat β-VLDL was injected into untreated rats in the absence or presence of lactoferrin. The localization of lactoferrin and apoE was examined by immuno-histochemical light and electron microscopy. The specificity of inhibition of the remnant receptor by lactoferrin was evaluated by studying its effect in control and in estradiol-treated rats, which show enhanced LDL receptor expression.

β-VLDL shows an avid interaction with parenchymal liver cells of control and estradiol-treated rats, as observed by fluorescence microscopy and by immuno-electron microscopy. Intracellular concentration of fluorescence around the bile canaliculi in the parenchymal cells of control rats was followed by perisinusoidal lipid accumulation. Pre-injection of lactoferrin blocked the interaction of β-VLDL with the parenchymal cells of control liver, but not in estradiol-treated rats. Immuno-localization of lactoferrin and apoE showed that lactoferrin binds to the parenchymal cell membrane without affecting the amount and localization of endogenous apoE.

These data show that the initial binding and subsequent uptake of β-VLDL by rat liver parenchymal cells is independent of endogenous plasma membrane bound apoE, and can be blocked by lactoferrin. Furthermore, since no effect of lactoferrin is noticeable on the LDL receptor-mediated uptake of β-VLDL in estradiol-treated rats it is concluded that lactoferrin and β-VLDL compete for the same binding site, presumably the remnant receptor.

Introduction

Beta-migrating very low density lipoproteins are cholesterol enriched lipoproteins which accumulate in the plasma of cholesterol fed animals and patients with type III hyperlipoproteinemia (1-3). Upon injection into rats, β-VLDL is rapidly cleared from the blood by the liver, and the liver parenchymal cells are predominantly responsible for this uptake (4,5).

The essential component for recognition of lipoprotein remnants by liver cells has previously been shown to be apolipoprotein E (apoE) (6). Two distinct receptors, the LDL

(apo B/E) receptor and the remnant (apoE) receptor, have been described to be able to bind apoE containing lipoproteins like β-VLDL (7-9). In rats, parenchymal cells hardly express active LDL receptors (10,11), and previously obtained biochemical data (9) indicated that an LDL receptor-independent pathway, presumably the remnant receptor, is responsible for the parenchymal cell uptake of β-VLDL in the rat. The *in vivo* interaction of β-VLDL with rat liver parenchymal cells can be blocked by lactoferrin (12). The structural resemblance of the N-terminal domain of lactoferrin with the arginine rich LDL receptor binding sequence of apoE (13) suggests that this sequence is an essential component for liver recognition. Recently it was suggested, that apoE associated with VLDL remnants is not sufficient for an interaction with the liver, but that additional apoE, present on the microvilli of the parenchymal cells is necessary for binding and subsequent endocytosis (14). From these data, it might be speculated that lactoferrin blocks the liver uptake of β-VLDL by replacing the endogenous apoE on the microvilli.

LDL receptor expression in rat liver can be induced by treating rats with pharmacological doses of 17α-ethinyl estradiol (EE), wherewith the amount of LDL receptors on the parenchymal cells is selectively upregulated 17 fold (15,16), without affecting the remnant receptor expression (17). A comparison of the interaction of β-VLDL with livers from estradiol-treated rats vs control rats will allow a direct comparison of the *in vivo* properties of the LDL receptor with those of the remnant receptor.

In the present study we used a visualization approach in order to study the remnant receptor-mediated interaction of β-VLDL with rat liver and the possible role of plasma membrane-bound apoE in the initial binding, while these data were compared with the LDL receptor-mediated interaction by treating rats with estradiol. Furthermore, the mechanism of inhibition of β-VLDL interaction with rat liver by lactoferrin was investigated by visualizing the lactoferrin binding, studying its effect upon the localization of endogenous apoE and analyzing the effect of excess lactoferrin on the binding and uptake of β-VLDL.

Materials and Methods

β-VLDL isolation and labeling

For isolation of β-VLDL, male wistar rats (200-220 g) were maintained on a cholesterol rich chow for 14 days, that included 2% cholesterol, 5% olive oil, and 0.5% cholic acid (Hope Farms, Woerden, The Netherlands). Rats were fasted for 18 h and blood was collected by punction of the abdominal aorta. β-VLDL ($d < 1.006$ g/ml) was isolated from the pooled plasma plus 1 mM EDTA by density gradient centrifugation according to Redgrave et al. (30) as described in Ref. 5. The isolated lipoprotein fraction was routinely checked for its electrophoretic mobility on agarose gel, and appeared as a single band with β-mobility in agreement with previous data (5). β-VLDL was labeled with 1,1' dioctadecyl 3,3,3',3'

tetramethyl indocarbocyanine perchlorate (DiI) (Molecular Probes, Eugene, OR) according to Pitas et al. (31). The density of the DiI and lipoprotein mixture was subsequently raised to 1.21, and the lipoproteins were re-isolated according to the above described procedure.

Animals and perfusion studies

For the visualisation studies on the *in vivo* binding and internalisation of fluorescently labeled β-VLDL, 3-month-old male Wag/Rij rats (200-250 g) were used. When indicated, rats were pretreated subcutaneously with 5 mg/kg of body weight of estradiol dissolved in propylene glycol for 3 successive days as previously described (22). Plasma samples were drawn for determination of cholesterol before and during estradiol-treatment. Low levels of cholesterol (0.15 ± 0.05 mg/ml) were detected after estradiol-treatment in comparison to the values before (0.70 ± 0.08 mg/ml), similar to previously reported (22), and in agreement with previous biochemical and morphological data (15,16,22), which indicated a strong increase in the amount of LDL receptors on the plasma membrane of the liver parenchymal cells.

DiI-β-VLDL (50 μg/ml plasma) was injected into the vena cava inferior or vena jugularis of untreated and estradiol-treated, overnight fasted rats under halothane anaesthesia, and was allowed to circulate for 2, 10, 20 and 45 minutes. Body temperature was kept at 35°C by a lamp. When indicated lactoferrin (Serva, Heidelberg, Germany) was injected 1 minute prior to the lipoproteins, or without subsequent administration of β-VLDL in a concentration of 70 mg/kg bodyweight, similar to previously reported (12). At the described circulation time, rat livers were rinsed shortly with phosphate-buffered saline (1 minute), and subsequently fixed with 4% paraformaldehyde (PF) and 0.1% glutaraldehyde (GA) in phosphate-buffered saline (PBS) by *in situ* perfusion via the portal vein for 10 minutes. Fixed liver tissue was stored in 2% PF in PBS at 4°C.

General histology

Part of the liver, which was used for morphological examination was dissected, and 200 μm sections were postfixed in 1% OsO_4 in 0.15 M sodium cacodylate buffer for 45 minutes, dehydrated in a graded series of ethanol and embedded in epon. Semithin and ultrathin sections were stained or contrasted, respectively with toluidine blue, and uranyl acetate and lead citrate according to standard procedures.

Fluorescence microscopy

Liver tissue that was used for fluorescent examination was following fixation dissected, and 200 μm vibratome slices were embedded in 2.3 M sucrose in PBS, overnight. Small pieces of liver tissue were placed on specimen holders and frozen in liquid nitrogen. Semithin cryosections (1-1.5 μm) were cut using a Reichert FC-4D Ultracut cryomicrotome at a temperature of -100°C. Sections were placed on a glass cover slip, and after being mounted

with glycerol viewed with a Leitz ortholux microscope with a standard set of excitation and emission filters used for TRITC, to localize the DiI-fluorescence.

Immuno-histochemistry

Antibodies. Antiserum against rat apolipoprotein E, raised in goat, was kindly donated by Dr. P. Roheim (Louisiana State University, New Orleans, USA). The antibody was tested for cross-reactivity with other lipoproteins using the double radial immuno-diffusion method as described by Crowle (32). The antibody showed a strong reactivity with rat β-VLDL, and no reactivity with human VLDL, LDL, HDL and lipoprotein deficient serum (not shown). IgG fraction against human lactoferrin, raised in rabbit, was obtained from Sigma (St. Louis, MO, USA). Gold-conjugated antibodies (6 nm) were obtained from Aurion (Wageningen, The Netherlands), and peroxidase-conjugated antibodies from Dakopatts (ITK diagnostics, The Netherlands). Rabbit anti-goat immunoglobulins (RAG) were purchased from Nordic (Tilburg, The Netherlands), and protein A-gold (10 nm) was obtained from Janssen Life Sciences Products (Beerse, Belgium). For the immuno-labeling procedure antisera were diluted in PBS containing 0.1% gelatin, 0.5% BSA and 0.1% Tween 20. The dilutions used were: goat anti-apoE, 1:2000 fold; rabbit anti-lactoferrin, 1:1000; RAG, 1:5000; Goat anti-rabbit IgG gold (6 nm), 1:30; Swine anti-rabbit Peroxidase, 1:50; protein A-gold (10 nm), 1:50. For the washing steps the same medium was used unless otherwise indicated.

Light microscopy. Semithin cryosections were incubated with 0.05 M glycine in PBS pH 7.4, washed, incubated with 10% non-immune goat serum, followed by incubation with the primary antibody, washed, incubated with antibody coupled to HRP, washed, washed again with aqua dest and after administration of the substrate DAB with H_2O_2, the interaction with the enzym resulted in a brown polymerized product of DAB. When the primary antibody was omitted from the procedure and non-immune rabbit serum was used instead, no reaction product of DAB was detectable, demonstrating the reaction product to be specific for the used primary antibodies and no aspecific or endogenous peroxidatic activity to be present.

Electron microscopy. Ultrathin cryosections (0.1 μm) were incubated similar to semithin cryosections. To detect primary antibodies, rabbit anti-goat antibodies, and subsequently colloidal gold-conjugated antibodies were used. Sections were washed, washed again with aqua dest, and stained with uranylacetate and covered with tylose according to Tokuyasu (33). In case of a double-labeling procedure, the first antibody (goat anti-apoE) was detected, following RAG incubation with an antibody coupled to colloidal gold particles (6 nm), washed, incubated with an excess protein A (Pharmacia, Uppsala, Sweden), before incubating with the second primary antibody (rabbit anti-lactoferrin) and final detection with protein A-gold (10 nm), as described by Slot et al. (34). In control sections, non-immune goat or rabbit serum was used instead of the primary antibodies. This provoked a random

distribution of only very few gold particles over the sections.

Ultrathin sections were examined in a Philips EM 410 electron microscope.

Results

In vivo binding and internalization of β-VLDL

Two minutes following the injection of DiI-β-VLDL into untreated rats, fluorescence is concentrated around sinusoids, in the portal region of the liver lobules (Fig. 1a). At 10 and 20 minutes after administration, DiI is present around sinusoids in portal as well as in central areas, and at the latter time, some fluorescence is also noticeable inside parenchymal cells, in the portal regions (Fig. 1b). At 45 minutes after administration, fluorescence is concentrated mainly inside the parenchymal cells in portal as well as in central areas of the liver lobules, while, in the central areas, low amounts of fluorescence are still present around the sinusoids (Fig. 1c). Intracellular fluorescence is localized as bright spots around bile canaliculi. Besides parenchymal cells, Kupffer cells, as recognized by their preferential localization in periportal areas inside the sinusoids, also contain DiI-fluorescence at the indicated time points (Figs. 1a-c).

Histological examination of the morphology of toluidine blue stained sections of the rat livers, shows that β-VLDL administration has a remarkable effect on the lipid content of the parenchymal cells. In comparison to control liver (Fig. 2a), an increase in the number of lipid vacuoles was noticed already at 20, and more clearly at 45 minutes after injection of β-VLDL (Fig. 2b). Ultrastructural examination of the epon-embedded liver tissue showed that the lipid droplets are situated inside the parenchymal cells closely to the sinusoid (Fig. 2c), distinct from the light microscopic pericanalicular concentration of DiI-fluorescence described above. However, around the bile canaliculi more frequently electron dense structures were noticed following β-VLDL administration (Fig. 2c).

Similar experiments performed in estradiol-treated rats show that 2, 20 and 45 minutes after the administration of DiI-β-VLDL, fluorescence is concentrated around sinusoids in portal as well as in central areas of the liver lobules (Fig. 3). Relatively lower amounts of fluorescence are found inside the parenchymal cells in comparison to what was observed in the untreated rats, particularly at 45 minutes after injection of β-VLDL (Fig. 3c). Kupffer cells contained fluorescence at all time points studied (Fig. 3a-c), with no noticeable difference between control livers and livers from estradiol-treated rats.

Histological examination of the estradiol-treated rat livers at the light and electron microscopic level showed neither a perisinusoidal lipid accumulation nor an increase of electron dense structures around bile canaliculi in the parenchymal cells at any time point after β-VLDL administration (not shown).

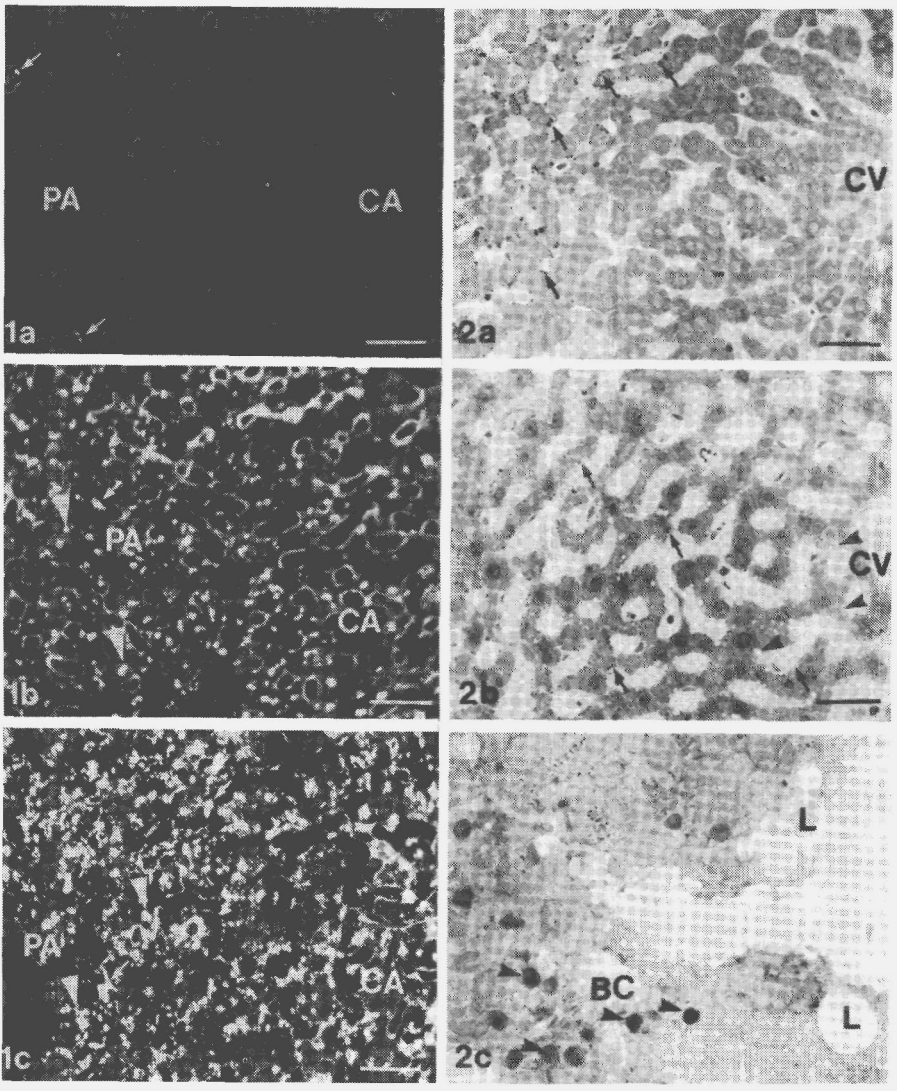

Figure 1. Fluorescence microscopy of rat liver at 2 (a), 20 (b), and 45 (c) minutes after intravenous injection of DiI-β-VLDL. Fluorescence is mainly concentrated around periportal sinusoids 2 minutes after injection of DiI-β-VLDL (a), while at 20 minutes after injection, fluorescence is also present around pericentral sinusoids (b). Concentration of fluorescence inside parenchymal cells is noticed predominantly in periportal regions (arrowheads), at both 20 and 45 minutes after administration of β-VLDL (b,c). Kupffer cells (arrows) also contain DiI-fluorescence (a-c). PA = portal area, CA = central area. Bars = 25 μm.

Figure 2. Micrographs of semi- and ultrathin epon sections of control liver (a) and liver 45 minutes after β-VLDL administration (b,c). Following β-VLDL administration an increase in the number of perisinusoidal lipid vacuoles is noticed (arrows), as is most evident in the central regions of the liver lobules (compare a to b). Some of the lipid vacuoles appear empty in Fig. 2b due to extraction, especially in central areas of the liver (arrowheads). Note the presence of significant numbers of electron dense structures (arrowheads) around the bile canaliculi, and of perisinusoidal lipid droplets (L) in Fig. 2c, some of which are extracted (magnification: 5500x). CV = central vein, BC = bile canaliculus. Bars = 35 μm.

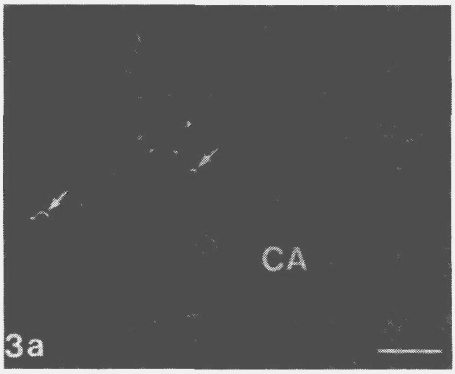

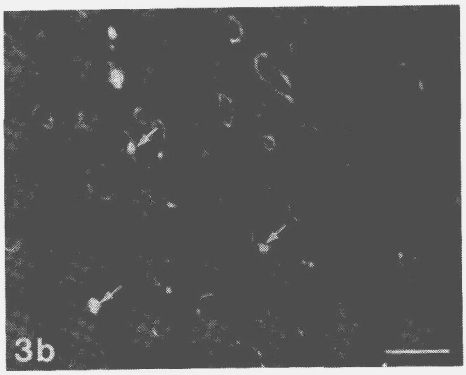

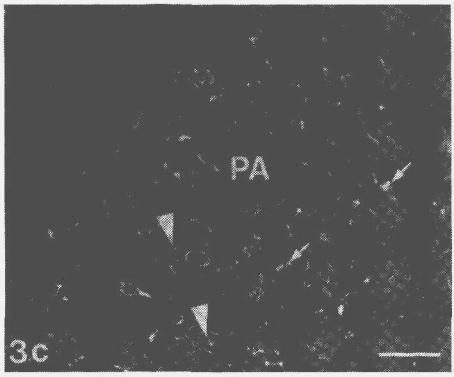

Figure 3. Fluorescence microscopy of liver of estradiol-treated rats at 2 (a), 20 (b), and 45 (c) minutes after DiI-β-VLDL administration. Fluorescence is localized predominantly around the sinusoids, both in portal and in central areas of the liver (a-c). In comparison to untreated rats (Fig. 1c), small amounts of DiI-fluorescence accumulate intracellularly (arrowheads) in the parenchymal cells (c). Kupffer cells contain DiI-fluorescence at all time intervals studied (arrows). PA = portal area, CA = central area. Bars = 25 μm.

Immuno-electron microscopic localization of apolipoprotein E

A prominent localization of endogenous apoE is found at the microvilli of parenchymal cells (Fig. 4a), in agreement with earlier data published by Hamilton et al. (14). In addition, immuno-label is demonstrated intracellularly in Golgi stacks, multi-vesicular bodies (Fig. 4b), and peroxisomes (Fig. 4b, inset) of parenchymal cells, as also described by Hamilton et al. (14).

Injection of β-VLDL in untreated rats provoked a strong increase in the amount of immuno-reactive apoE in the space of Disse, from two minutes after injection upto 45 minutes after injection (Table 1). This increase in apoE immuno-label is less prominent for central regions at the 2 minute time interval, and for portal regions at the 45 minute time interval (Table 1). In addition to immuno-label associated with the microvilli of the parenchymal cells, a strong association with electron lucent roundish particles, with a diameter of 35-60 nm, is found (Fig. 4c). For reason that these structures are found in large amounts only in rats that were injected with β-VLDL, it is reasonable to assume that these structures represent β-VLDL particles containing apoE.

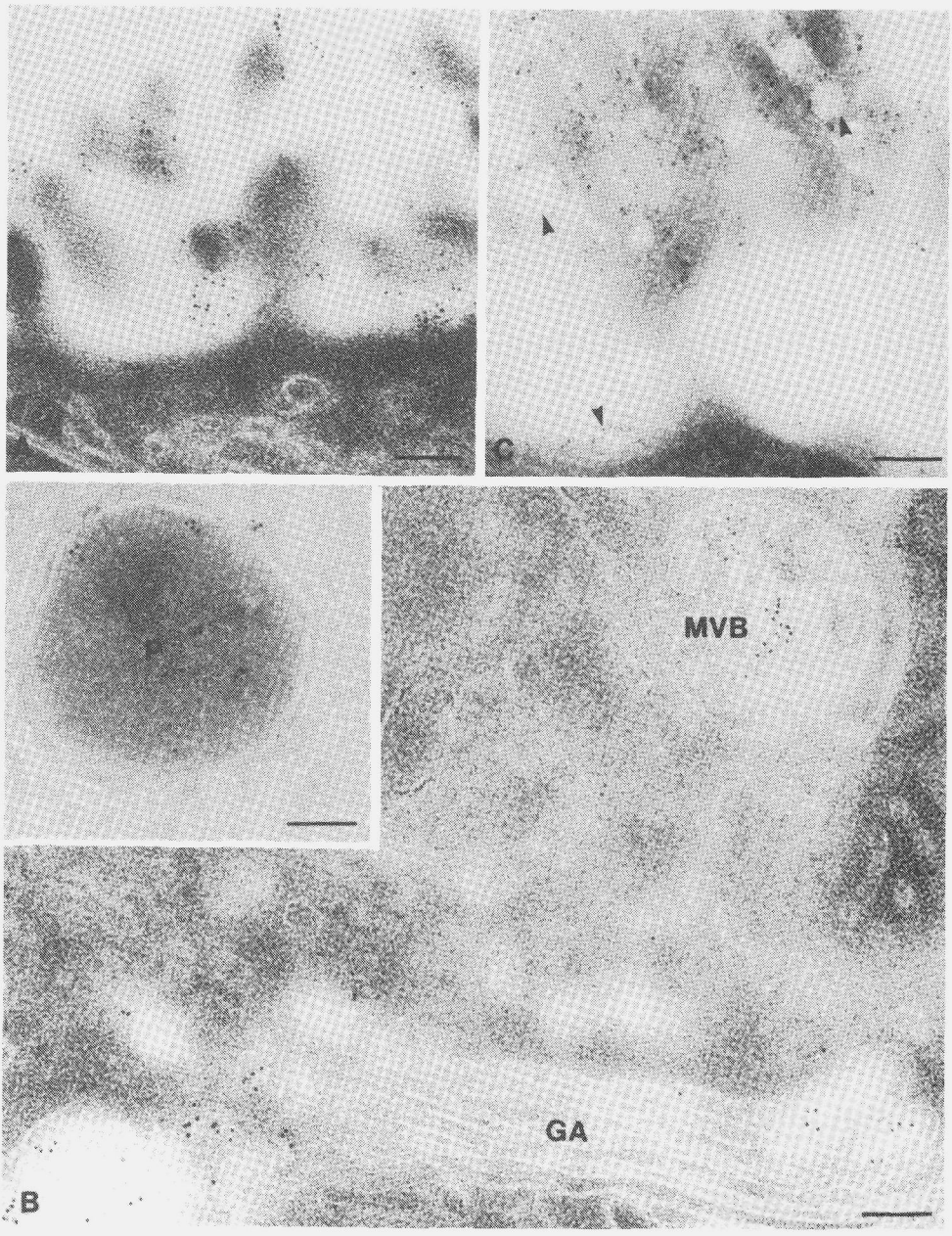

Figure 4. Immuno-labeling with anti-apoE on an ultrathin cryosection of control liver tissue (A,B), and liver tissue 10 minutes after injection of β-VLDL (C). Immuno-gold is associated with microvilli of parenchymal cells (A), with the golgi-apparatus (GA), and multi-vesicular bodies (MVB) (B), and with peroxisomes (P) (B-inset). Following injection of β-VLDL strongly increased amounts of immuno-label, representing apoE, are found on microvilli in the space of Disse, predominantly associated with lipoprotein-like particles (arrowheads) (C). Bars = 0,1 μm.

Table 1. Apolipoprotein E presence in the space of Disse under the experimental conditions indicated.

time after β-VLDL injection	untreated rats — lactoferrin PA	untreated rats — lactoferrin CA	untreated rats + lactoferrin PA/CA	estradiol-treated rats — lactoferrin PA	estradiol-treated rats — lactoferrin CA	estradiol-treated rats + lactoferrin PA/CA
0 min	+	+	+	+	+	+
2 min	+++	+	+	+++	+++	+++
10 min	+++	+++	+	+++	+++	+++
20 min	+++	+++	+	+++	+++	+++
45 min	+	+++	+	+++	+++	+++

Representation of the amount of apoE immuno-label present in the space of Disse, following β-VLDL administration in the absence or presence of lactoferrin, in control and estradiol treated rats. Semi-quantitative evaluation was done on immuno-stained ultrathin cryosections by TEM. + = The amount of immuno-gold as represented by Fig. 4a, showing relatively low amounts of immuno-label associated with microvilli. +++ = The amount of immuno-gold as represented by Fig. 4c, associated with microvilli, but predominantly with β-VLDL particles. PA = portal area, CA = central area.

Estradiol-treatment of rats does not lead to a different localization of immuno-label for endogenous apoE. Notably, the amount of immuno-label present in the space of Disse did not change (Table 1). Following injection of β-VLDL into estradiol-treated animals, a strong increase in the amount of apoE-immuno-label in the space of Disse is noticed (Table 1). Gold label is associated with microvilli and β-VLDL particles, in portal and central areas of the liver lobules, at all time intervals studied (Table 1).

Influence of lactoferrin administration

Immuno-histochemical detection of lactoferrin at the light microscopic level in the liver of untreated and estradiol-treated rats demonstrates that lactoferrin is present around all sinusoids, bound to the parenchymal cells from the 2 minute time point onwards, at least up to 45 minutes after injection of lactoferrin (Fig. 5A). At 45 minutes after injection, small amounts of lactoferrin are localized also intracellularly in parenchymal cells, in portal as well as in central areas, mainly around the bile canaliculi (Fig. 5A). No other liver cell types showed any specific reaction product.

Injection of lactoferrin does not influence the amount and localization of endogenous apoE in the liver, neither in the untreated nor in the estradiol-treated rats. Notably, the amount of apoE present in the space of Disse was unaffected (Fig. 5B-C).

Injection of lactoferrin 1 minute prior to DiI-β-VLDL administration into untreated rats, has a clearcut effect on the amount of fluorescence present in the liver, and a change in relative involvement of the cell types with which β-VLDL becomes associated is particularly

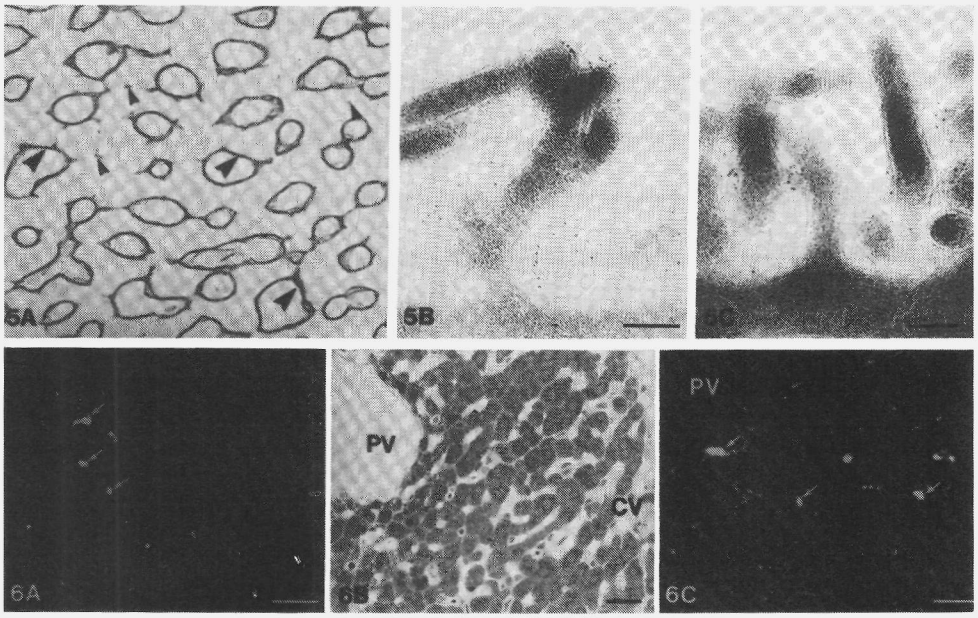

Figure 5. Immuno-histochemical detection of lactoferrin (A) and electron microscopic immuno-detection of endogenous apoE (B,C) in liver of untreated (A,B) and estradiol-treated rats (C), all at 45 minutes after the injection of lactoferrin. Lactoferrin is abundantly present in the space of Disse (large arrowheads), but intracellularly only in low amounts (arrowheads) (A; magnification: 450x). Similar amounts of immuno-label representing immuno-reactive apoE are noticed in the space of Disse in untreated and estradiol-treated rats (B,C), and in liver of rats not injected with lactoferrin (c.f. Fig. 4a). Bars = 0,1 μm.

Figure 6. Fluorescence microscopy and histology of liver tissue of untreated (A,B) and estradiol-treated rats (C), at 20 minutes after injection of DiI-β-VLDL and lactoferrin. No fluorescence is associated with parenchymal cells of untreated rats, while Kupffer cells (arrows) show an avid interaction with DiI-β-VLDL (A, compare to Fig. 1b). No accumulation of lipid in parenchymal cells is noticed in central areas (B). Pre-injection of lactoferrin does not alter the localization of DiI-fluorescence in parenchymal and Kupffer cells (arrows) of estradiol-treated rats (C, compare to Fig. 3b). PV = portal vein, CV = central vein. Bars = 25 μm.

evident. No fluorescence is found to be associated with the parenchymal cells at any of the time points studied up to 45 minutes (Fig. 6A). In contrast, Kupffer cells do contain fluorescence, which even seems to be somewhat increased as compared to the same time points in rats which have not been pre-injected with lactoferrin (Fig. 6A). The histological changes in lipid content (Fig. 6B), and the accumulation of electron dense structures around the bile canaliculi of the parenchymal cells, as described for untreated rats, were prevented by pre-injection of lactoferrin. Lactoferrin administration prior to β-VLDL injection in untreated animals diminished the amount of apoE in the space of Disse to a similar amount

and localization as found in livers of rats not injected with β-VLDL, at all the time intervals studied (Table 1).

In the estradiol treated rats, no alteration in the fluorescent pattern was observed following administration of lactoferrin 1 minute prior to DiI-β-VLDL: fluorescence is mainly concentrated at the sinusoidal surface of the parenchymal cells and also present in Kupffer cells at all time intervals studied (Fig. 6C). Pre-injection of lactoferrin into estradiol-treated rats did not affect the localization of apoE, nor did it affect the amount of apoE immuno-label in the space of Disse compared to estradiol-treated rats, which were injected only with β-VLDL (Table 1).

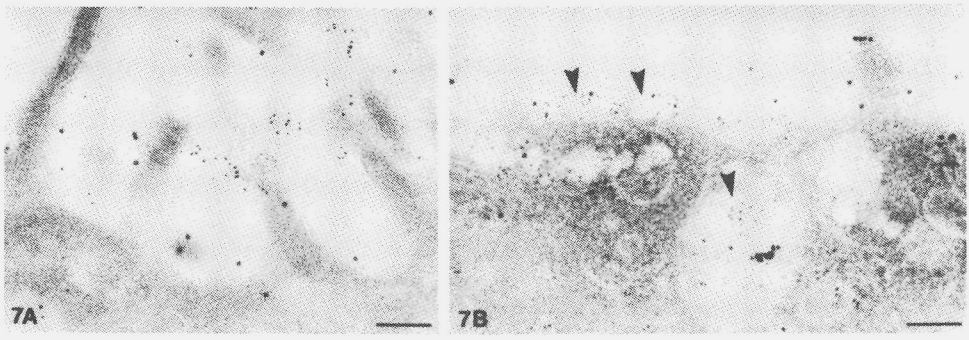

Figure 7. Electron micrographs of ultrathin cryosections of liver tissue of untreated (A) and estradiol-treated rats (B), at 10 minutes following the administration of lactoferrin (A) and of β-VLDL and lactoferrin (B). Double-labeling experiments detecting apoE (6 nm gold) and lactoferrin (10 nm gold) show apoE to be present in the space of Disse associated with microvilli (A,B) and β-VLDL particles (B, arrowheads), while lactoferrin is noticed in the space of Disse along the sinusoidal plasma membrane of the parenchymal cells. No specific relation between the localization of lactoferrin and apoE is noticed, whether β-VLDL was injected (B) or not (A). Bar = 0,1 μm.

Double-labeling experiments, after injection of lactoferrin, showed that lactoferrin and endogenous apoE are present in the space of Disse, randomly distributed along the sinusoidal membrane of the parenchymal cells in untreated (Fig. 7A), as well as in estradiol-treated rats (not shown). The mutual distance of the gold particles representing lactoferrin and those representing apoE does not point to a specific relation between these two labeled components. Detection of lactoferrin and apoE following injection of lactoferrin and β-VLDL, showed in untreated rats a similar random distribution along the sinusoidal membrane of the parenchymal cells of both ligands as described above. In estradiol-treated rats, administration of β-VLDL following lactoferrin injection, provoked a clear increase in the amount of apoE-immuno-label in the space of Disse (Fig. 7B), at all the time points studied similar to the single-labeling results (Table 1). Lactoferrin-immuno-label showed no specific association

with the β-VLDL particles, and was localized randomly along the plasma membrane of the parenchymal cells, without any relation to apoE (Fig. 7B).

Discussion

Fluorescently labeled β-VLDL is used in this study to examine the interaction of β-VLDL with rat liver *in vivo*. The relative proportion of the remnant and the LDL receptor in the interaction of liver with β-VLDL could be modulated by lactoferrin administration and by estradiol-treatment of rats. In untreated rats pre-injection of lactoferrin inhibited specifically the interaction of fluorescently labeled β-VLDL with the liver parenchymal cells and not with the Kupffer cells, in agreement with previously reported biochemical data (12). Immunolocalization of lactoferrin in the space of Disse up to 45 minutes after injection, suggests that the blockade of the interaction of β-VLDL with the parenchymal cells by lactoferrin is caused by its persistent presence at the plasma membrane. Such slow internalization is in agreement with previous biochemical data that showed that lactoferrin is internalized and degraded only slowly by the liver (13). As the interaction of β-VLDL with the parenchymal cells in the estradiol-treated animals could not be blocked by lactoferrin, it can be concluded that lactoferrin acts on a recognition system different from the LDL receptor. These data add to previous biochemical data which suggested β-VLDL to interact in rat liver with an LDL receptor-independent binding site, presumably the remnant receptor (5,9).

When DiI-β-VLDL is used to identify the remnant receptor localization, it appears that the remnant receptor is present in portal as well as in central areas of the liver lobules. This localization is in agreement with previous autoradiography data of Jones et al. (18), who showed that VLDL remnants and chylomicron remnants are evenly distributed over the liver lobules in the space of Disse at 3 minutes after injection. However, the observed differences in the presence of fluorescence in the space of Disse between portal and central areas (Fig. 1), strongly suggest that the remnant receptor preferentially binds and internalizes β-VLDL in portal areas of the liver lobules.

Internalization of DiI-β-VLDL and subsequent pericanalicular accumulation of fluorescence are consistent with other data that showed DiI to be retained within the lysosomes (19). Also, our electron microscopic observations that showed an increase in electron dense vesicles around the bile canaliculi following β-VLDL administration confirm this notion (Fig. 2c). Uptake of β-VLDL was also followed by an accumulation of lipid in the parenchymal cells (Fig. 2). The fact that the fluorescence accumulates at a different site than the lipid may indicate that re-allocation of lipid, i.e. hydrolysis and re-esterification, forms part of the processing route of β-VLDL by parenchymal cells. The lipid accumulation is not a long lasting effect of β-VLDL administration, as can be concluded from a pilot experiment that showed that 24 hours after injection no such accumulation is present

anymore.

Internalization of β-VLDL in estradiol-treated rats appears to happen more slowly than in control animals as no morphological changes (lipid accumulation) were noticed, and the localization of fluorescence did not change as rapidly as in the untreated rats between 2 and 45 minutes after injection (Fig. 3). These differences indicate that, in estradiol-treated rats, β-VLDL binds predominantly to the induced LDL receptor, as was previously suggested also for chylomicron remnants (20). The fact that lactoferrin is not an effective competitor for β-VLDL interaction in the estradiol-treated rats, sustains this notion. Other studies, in which β-VLDL was labeled with iodine, demonstrated that in estradiol-treated rats the protein part of the β-VLDL is cleared from the blood (21), and internalized, as shown by cell fractionation studies, as rapidly as LDL (8). In previous work we observed that DiI-LDL, which was administered to estradiol-treated rats, in similar amounts, on protein base, as β-VLDL, is internalized as rapidly by the parenchymal cells (22) as noticed in the present study for β-VLDL in the untreated rats. Previous autoradiography data showed the same for ^{125}I-VLDL remnants (18), and ^{125}I-β-VLDL (20) in comparison to ^{125}I-LDL. Although β-VLDL and LDL bind mainly to the same receptor in estradiol-treated rats, they are apparently processed differently. Recent reports by Tabas et al. (23,24) also show differences in intracellular processing of LDL and β-VLDL after binding to the LDL receptor on peritoneal macrophages. It has been suggested that particle size and multiple apoE-receptor interactions may influence the intracellular processing (23,24).

ApoE is generally accepted to be of major importance in the receptor-mediated interaction of lipoprotein remnants with the rat liver (6,25,26). Until recently most attention was focused on the apoE which is associated with the particles, particularly its conformation, and its amount relative to apolipoprotein C (27-29). The morphological observation of Hamilton et al. (14) who showed that a major part of endogenous apoE is localized at the microvilli of the parenchymal cells, without being associated with lipoprotein particles, allowed speculations on the role of this microvilli associated apoE. They suggested that apoE binds to hepatic receptors, heparan sulfate, or hepatic lipase, thereby facilitating binding and subsequent endocytosis of VLDL remnants (14). In our study we addressed whether the lactoferrin blockade of remnant receptor mediated lipoprotein uptake would be the consequence of a) replacing apoE on the microvilli, thereby reducing the amount of endogenous apoE at this site or b) binding to, or in close proximity of endogenous apoE, thereby hampering the interaction of β-VLDL with the endogenous apoE. However, since lactoferrin has no effect on the amount and localization of endogenous apoE, and since no indication was obtained for any co-localization of lactoferrin and apoE, it is likely that lactoferrin competes directly with β-VLDL for binding to the remnant receptor. Furthermore, it can be concluded that plasma membrane-bound endogenous apoE is not involved in the initial binding of β-VLDL to rat liver parenchymal cells.

It is concluded that the morphological characterization of the interaction of β-VLDL with

the liver strengthens the biochemical evidence that, in control rats, β-VLDL does bind to a receptor which is distinct from the LDL receptor induced in estradiol-treated rats. Both the initial binding, which is predominantly in portal areas, and the internalization and intracellular processing, indicate that differences exist between the remnant receptor and LDL receptor-mediated interaction. The interaction of lactoferrin with liver parenchymal cells on sites different from the localization of endogenous apoE and without any direct interference with apoE suggests endogenous apoE not to be involved in the initial binding of β-VLDL. The specific ability of lactoferrin to block the binding of β-VLDL in control rats does confirm that a binding site, which is different from the LDL receptor, presumably the remnant receptor is responsible for the initial recognition and subsequent endocytosis of β-VLDL in the rat liver.

References

1. Fredrickson DS, Levy RI, Lindgren FT. A comparison of heritable abnormal lipoprotein patterns as defined by two different techniques. J Clin Invest 1969;47:2446-57.
2. Shore VG, Shore B, Hart RG. Changes in apolipoproteins and properties of rabbit very low density lipoproteins on induction of cholesteremia. Biochemistry 1974;13:1579-85.
3. Mahley RW. Dietary-fat, cholesterol, and accelerated atherosclerosis. Atheroscler Rev 1979;5:1-34.
4. Fainaru M, Funke H, Boyles JK, Ludwig EH, Innerarity TL, Mahley RW. Metabolism of canine β-very low density lipoproteins in normal and cholesterol-fed dogs. Arteriosclerosis 1988;8:130-39.
5. Harkes L, Duijne A, Berkel ThJC. Interaction of β-very low density lipoproteins with rat liver cells. Eur J Biochem 1989;180:241-48.
6. Arbeeny CA, Rifici VA, Handley DA, Eder HA. Determinants of the uptake of very low density lipoprotein remnants by the perfused rat liver. Metabolism 1987;36:1106-13.
7. Mahley RW, Hui DY, Innerarity TL, Weisgraber KH. Two independent lipoprotein receptors on hepatic membranes of dog, swine and man: apo-B,E- and apo-E receptors. J Clin Invest 1981; 68:1197-1206.
8. Jaeckle S, Brady SE, Havel RJ. Membrane binding sites for plasma lipoproteins on endosomes from rat liver. Proc Natl Acad Sci USA 1989;86:1880-84.
9. De Water R, Kamps JAAM, Van Dijk MCM, Hessels EMAJ, Kuiper J, Kruijt JK, Van Berkel ThJC. Characterization of the low density lipoprotein independent interaction of β-migrating very low density lipoproteins with rat and human parenchymal liver cells in vitro. Biochem J 1992;281:41-48.
10. Harkes L, Van Berkel ThJC. Quantitative role of parenchymal cells and non-parenchymal liver cells in the uptake of [14C] sucrose labelled low density lipoproteins in vivo. Biochem J 1984;224:21-27.
11. Nagelkerke JF, Bakkeren HF, Kuipers F, Vonk RJ, Van Berkel ThJC. Hepatic processing of the cholesteryl ester from low density lipoproteins in the rat. J Biol Chem 1986;261:8909-13.
12. Van Dijk MCM, Ziere GJ, Boers W, Linthorst C, Bijsterbosch MK, Van Berkel ThJC. Recognition of chylomicron remnants and β-VLDL by the remnant receptor of parenchymal liver cells is distinct from the α2-macroglobulin recognition site. Biochem J 1991;279:863-70.
13. Ziere GJ, Van Dijk MCM, Bijsterbosch MK, Van Berkel ThJC. Lactoferrin uptake by the rat liver: characterization of the recognition site and effect of selective modification of arginine residues. J Biol Chem 1992;267:11229-35.
14. Hamilton RL, Wong JS, Guo LSS, Krisans S, Havel RJ. Apolipoprotein E localization in rat hepatocytes by immuno-gold labeling of cryothin sections. J Lipid Res 1990;31:1589-1603.

15. Kovanen PT, Brown MS, Goldstein JL. Increased binding of low density lipoprotein to liver membranes from rats treated with 17α-ethinyl estradiol. J Biol Chem 1979;254:1136.
16. Harkes L, Berkel ThJC. Cellular localization of the receptor-dependent and receptor-independent uptake of human LDL in the liver of normal and 17α-ethinyl estradiol-treated rats. FEBS letters 1983;154:75-80.
17. Cooper AD, Nutik R, Chen J. Characterization of the estrogen-induced lipoprotein receptor of rat liver. J Lipid Res 1987;28:59-68.
18. Jones AL, Hradek GT, Hornick C, Renaud G, Windler E, Havel RJ. Uptake and processing of remnants of chylomicrons and very low density lipoproteins by rat liver. J lipid Res 1985;25:1151-58.
19. Pitas RE, Innerarity TL, Mahley RW. Foam cells in explants of atherosclerotic rabbit aortas have receptors for β-VLDL and modified low density lipoproteins. Arteriosclerosis 1983;3:2-12.
20. Jäckle S, Runquist E, Brady SE, Hamilton RL, Havel RJ. Isolation and characterization of three endosomal fractions from the liver of normal rats after lipoprotein loading. J Lipid Res 1991;32:485-492.
21. Jäckle S, Rinninger F, Greeve J, Greten H, Windler E. Regulation of the hepatic removal of chylomicron remnants and β-very low density lipoproteins in the rat. J Lipid Res 1992;33:419-29.
22. Kleinherenbrink-Stins MF, Van der Boom J, Schouten D, Roholl PJM, Van der Heyde MN, Brouwer A, Van Berkel ThJC, Knook DL. Hepatology Visualization of the interaction of native and modified lipoproteins with parenchymal, endothelial and Kupffer cells from human liver. 1991;14:79-90.
23. Tabas I, Lim S, Xu X, Maxfield FR. Endocytosed β-VLDL and LDL are delivered to different intracellular vesicles in mouse peritoneal macrophages. J Cell Biol 1990;111:929-40.
24. Tabas I, Myers JN, Innerarity TL, Xu X, Arnold K, Boyles J, Maxfield FR. The influence of particle size and multiple apoprotein E-receptor interactions on the endocytotic targeting of β-VLDL in mouse peritoneal macrophages. J Cell Biol 1991;115:1547-60.
25. Windler E, Chao Y, Havel RJ. Determinants of hepatic uptake of triglyceride-rich lipoproteins and their remnants in the rat. J Biol Chem 1980;255:5475-80.
26. Cooper AD, Erickson SK, Nutik R, Shrewsbury MA. Characterization of chylomicron remnant binding to rat liver membranes. J Lipid Res 1982;23:42-52.
27. Windler E, Havel RJ. Inhibitory effects of C apolipoproteins from rats and humans on the uptake of triglyceride-rich lipoproteins and their remnants by the perfused rat liver. J Lipid Res 1985;26:556-65.
28. Kowal RC, Herz J, Weisgraber KH, Mahley RW, Brown MS, Goldstein JL. Opposing effects of apolipoproteins E and C on lipoprotein binding to low density lipoprotein receptor-related protein. J Biol Chem 1990;265:10771-79.
29. Weisgraber KH, Mahley RW, Kowal RC, Herz J, Goldstein JL, Brown MS. Apolipoprotein C-I modulates the interaction of apolipoprotein E with β-VLDL and inhibits binding of β-VLDL to low density lipoprotein receptor-related protein. J Biol Chem 1990;265:22453-59.
30. Redgrave TG, Roberts DCK, West CE. Separation of plasma lipoproteins by density gradient ultracentrifugation. Anal Biochem 1975;65:42-49.
31. Pitas RE, Boyles J, Mahley RW, Bissell DM. Uptake of chemically modified low density lipoproteins in vivo is mediated by specific endothelial cells. J Cell Biol 1985;100:103-17.
32. Crowle AJ. In: Immuno-diffusion, New York, Academic Press, 1961
33. Tokuyasu KT. Immuno-cytochemistry on ultrathin frozen sections. J Histochemistry 1980;12:381-86.
34. Slot JW, Geuze HJ, Freeman BA, Crapo JD. Intracellular localization of the copper-zinc and manganese superoxide dismutases in rat liver parenchymal cells. Lab Invest 1986;55:363.

Chapter 6

Visualization of the Interaction of β-Migrating Very Low Density Lipoproteins with Human Liver Cells: Involvement of Remnant- and LDL Receptors

Sebastiaan Esbach[1], Anne Bosma[2], Adriaan Brouwer[1], Theo J.C. van Berkel[3] and Dick L.Knook[1]

[1] TNO Institute of Ageing and Vascular Research, Gaubius Laboratories, Leiden, The Netherlands.

[2] Department of Pathology, Academic Medical Center, University of Amsterdam, Amsterdam, The Netherlands.

[3] Division of Biopharmaceutics, Center for Bio-Pharmaceutical Sciences, University of Leiden, Sylvius Laboratories, Leiden, The Netherlands.

Submitted for publication

Summary

The interaction of β-VLDL with human liver cells was visualized in *ex situ* perfused liver tissue by fluorescence microscopy and immuno-histochemistry. The participation of remnant and LDL receptors in the binding of β-VLDL was examined by competition experiments using excess lactoferrin, a specific inhibitor of the remnant receptor, and high concentrations of LDL, respectively.

During perfusion, β-VLDL becomes predominantly associated with parenchymal cells and to a lower extent with Kupffer cells. Simultaneous addition of lactoferrin and LDL to the perfusion medium resulted in a strong inhibition of the association of β-VLDL with parenchymal cells, in contrast to the addition of lactoferrin or LDL alone, suggesting that both the LDL and remnant receptor must be blocked for an effective inhibition of the β-VLDL association with the human liver parenchymal cells. Immuno-staining for LDL receptors showed that parenchymal cells do express LDL receptors, although the amount of immuno-staining varied considerably between the different donors. Immuno-localization of the administered lactoferrin demonstrated that this ligand bound predominantly to the parenchymal cells, indicating a cell-specific binding site.

These results demonstrate that in the human situation β-VLDL is able to interact with human liver parenchymal cells by binding to LDL and remnant receptors. The fluctuation in LDL receptor expression on the parenchymal cells and the noticed competition with binding of β-VLDL to this receptor by physiological concentrations of LDL, suggests that remnant receptor activity in human liver is very important for the uptake of circulating β-VLDL, especially under high LDL conditions.

Introduction

Beta-migrating very low density lipoproteins (β-VLDL) are cholesterol enriched lipoproteins which accumulate in the plasma of cholesterol fed animals and patients with type III hyperlipoproteinemia (1,2). Upon injection into rats, β-VLDL is rapidly cleared from the blood by the liver, mainly by the action of the liver parenchymal cells, and to some extent by Kupffer cells (3).

Two distinct receptors, the low density lipoprotein (LDL) receptor and the remnant receptor, both recognizing apolipoprotein E (apoE), are able to bind β-VLDL (4,5). In rat, the expression of active LDL receptors on the liver parenchymal cells is low (6), and, *in vitro* data indicate that an excess of LDL is not able to block the interaction of β-VLDL with the parenchymal cells (3). It is therefore concluded that the uptake of β-VLDL in rats is predominantly mediated by the remnant receptor.

To identify remnant receptor-mediated processes, lactoferrin has been utilized (7).

Lactoferrin is a glycoprotein with a similar amino acid sequence as the cellular recognition site of apoE (8). Lactoferrin competes with β-VLDL and chylomicron remnants for the binding site on rat liver parenchymal cells (7), while lactoferrin has recently been demonstrated to block the interaction of apoE enriched β-VLDL with the LDL receptor-related protein (LRP)/α_2-macroglobulin receptor on nitrocellulose blot (9). LRP is abundantly present in the liver and has been suggested to function as remnant receptor (10). Since the liver cell interaction of β-VLDL in estradiol-treated rats, which show a cell specific up-regulation of LDL receptors on the liver parenchymal cells, was not affected by lactoferrin, the inhibitory effect of lactoferrin is indicated to be receptor-specific (7). This is confirmed by findings of Huettinger et al. (11) who demonstrated that lactoferrin was not able to inhibit the interaction of chylomicron remnants with human skin fibroblasts, described to possess functional remnant- as well as LDL receptors. In a recent study (12) we showed, by a morphological approach, that in rat liver lactoferrin binds to the plasma membrane of the parenchymal cells, thereby specifically blocking the interaction of β-VLDL with the parenchymal cells, while the β-VLDL interaction with the Kupffer cells was not affected.

In human liver both LDL- and remnant receptor activity, are expected to be expressed on parenchymal cells (13,14). The amount of LDL receptors was demonstrated to vary highly between individuals, probably by differences in genetic background, hormone status and lipid content of the diet (13). The presence of remnant receptor activity in human liver was indicated by the unchanged capacity to clear chylomicron remnants in patients with familial hypercholesterolemia, a disease which is characterized by the absence of LDL receptor activity and high LDL blood levels (14).

In the present study we used a visualization approach in order to study the *ex situ* interaction of β-VLDL with human liver cells. The involvement of LDL receptors in the binding of β-VLDL was examined by analyzing the effect of an excess of LDL, while the potential role of the remnant receptor was searched for by analysis of an additional effect of lactoferrin.

Materials and Methods

Materials

Human serum albumin (HSA) was purchased from Sigma (St. Louis, MO, USA). Gelatin and glycine were obtained from Merck (Darmstadt, Germany). Dulbecco's DMEM was obtained from Flow Laboratories (Irvine, UK) and 1,1' dioctadecyl 3,3,3',3' tetramethyl indocarbocyanine perchlorate (DiI) was obtained from Molecular Probes (Eugene, OR).

Lipoprotein isolation and labeling

For isolation of β-VLDL, male wistar rats (200-220 g) were maintained on a cholesterol rich chow for 14 days, that included 2% cholesterol, 5% olive oil, and 0.5% cholic acid (Hope

Farms, Woerden, The Netherlands). β-VLDL (d < 1.006 g/ml) was isolated from the pooled plasma by density gradient centrifugation as described in detail in Ref. 3. The isolated lipoprotein fraction was routinely checked, and appeared as a single band with β-mobility on agarose gel. β-VLDL was labeled with DiI (Molecular Probes, Eugene, OR) as described in detail in ref. 12. LDL (density between 1.024 and 1.055 g/ml) was isolated from human plasma plus 1mM EDTA by density gradient centrifugation, and, before use, dialysed against phosphate-buffered saline (PBS) containing 10 μM EDTA (13).

Human tissue processing

Human liver tissue (n = 5, 3 female, 2 male, age between 46 and 72) was obtained from patients undergoing partial hepatic resection for liver tumors (Academic Medical Centre and Anthonie van Leeuwenhoek Hospital, Amsterdam, The Netherlands) under protocol of the Medical Ethical Commission. Tissue blocks were used for perfusion experiments within four hours after resection; during this period liver tissue was preserved at 4°C. Fluorescently labeled β-VLDL (10 μg/ml DMEM containing 1% HSA) was perfused (10 ml/min) through the pieces of liver via a portal vein for 10 minutes at 37°C, in the absence or presence of 400 μg/ml lactoferrin and/or of 180 μg/ml LDL. The liver pieces were shortly rinsed by perfusion with PBS and fixed with 4% paraformaldehyde (PF) and 0,1% glutaraldehyde (GA) in PBS for 12 minutes. Control tissue was rinsed with only PBS and subsequently fixed according to the above procedure. After fixation liver tissue was stored in 2% PF in PBS at 4°C.

Liver tissue, which was used for morphological examination was dissected, and postfixed in OsO_4, dehydrated in a graded series of ethanol and embedded in epon according to standard procedures. Semithin sections were stained with toluidine blue (Merck, Darmstadt, Germany) and examined by a Zeiss light microscope. Ultrathin sections were contrasted with uranyl acetate and lead citrate, and examined in a Philips EM 410 electron microscope.

Liver tissue that was used for fluorescence microscopy was embedded in 2.3 M sucrose in PBS, overnight. Semithin cryosections (1-1.5 μm) were cut using a Reichert FC-4D Ultracut cryomicrotome, placed on glass cover slips, and after being mounted with glycerol viewed with a Leitz ortholux microscope (Leica, Rijswijk, The Netherlands) with a standard set of excitation and emission filters used for TRITC, to localize the DiI-fluorescence.

Immuno-histochemistry

Antiserum against rat apolipoprotein E, raised in goat, was kindly donated by Dr. P. Roheim (Louisiana State University, New Orleans, USA). A strong reactivity of the antibody with rat β-VLDL was noticed by double radial immuno-diffusion, while no reactivity with human VLDL, LDL, HDL and lipoprotein deficient serum was present (not shown). The IgG fraction of an antiserum against human lactoferrin, raised in rabbit, was obtained from Sigma (St. Louis, MO, USA). Chicken antibodies against the LDL receptor were kindly donated

by Dr. P. Kroon (Merck Institute NJ, USA). Specificity of the chicken antibody has been described by Kleinherenbrink-Stins et al. (13).

Cryosections (1-1.5 μm), or cryostatsections (6 μm) of unfixed liquid N_2 frozen tissue, were incubated according to routine immuno-histochemical procedures as described in more detail in refs. 12 and 13 to localize respectively apoE, lactoferrin and the LDL receptor. Antibodies conjugated to peroxidase or alkaline phosphatase, purchased from Dakopatts (ITK diagnostics, The Netherlands), were used in combination with respectively diaminobenzidine (Sigma, St. Louis, MO, USA) and Fast red (Merck, Darmstadt, Germany) for immuno-staining. In control experiments the primary antibody was omitted from the procedure and non-immune serum was used instead.

Results

Morphology

To study the tissue preservation of the human livers, plastic embedded tissue was examined by light and electron microscopy. As demonstrated in Fig. 1a parenchymal, Kupffer and endothelial cells were clearly recognizable at the light microscopical level. Some parenchymal cells only stained faintly with toluidine blue due to loss of material, indicating severe cell damage. Electron microscopic evaluation of the liver tissue demonstrated that cell-cell contacts of parenchymal cells and organelles like nuclei, RER and lysosomes were generally well preserved (Fig. 1b). No changes in cell morphology or histology were noticed after perfusion of the liver tissue blocks with β-VLDL, LDL or lactoferrin.

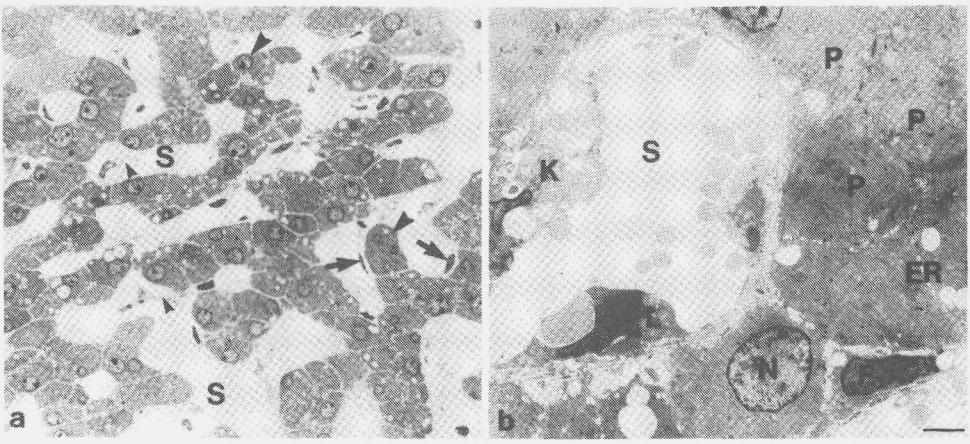

Figure 1. Micrographs of semithin (a) and ultrathin (b) sections of epon embedded human liver tissue. (a) Parenchymal (large arrowhead), Kupffer (small arrowhead) and endothelial cells (arrow) are easily recognizable. (b) Ultrastructural examination shows that the tissue is well preserved as evidenced by cell-cell contacts between the parenchymal celis (P) and by the appearance of nuclei (N), rough endoplasmatic reticulum (ER) and lysosomes (L). K = Kupffer cell, F = fat-storing cell, S = sinusoid. bars = 4 μm.

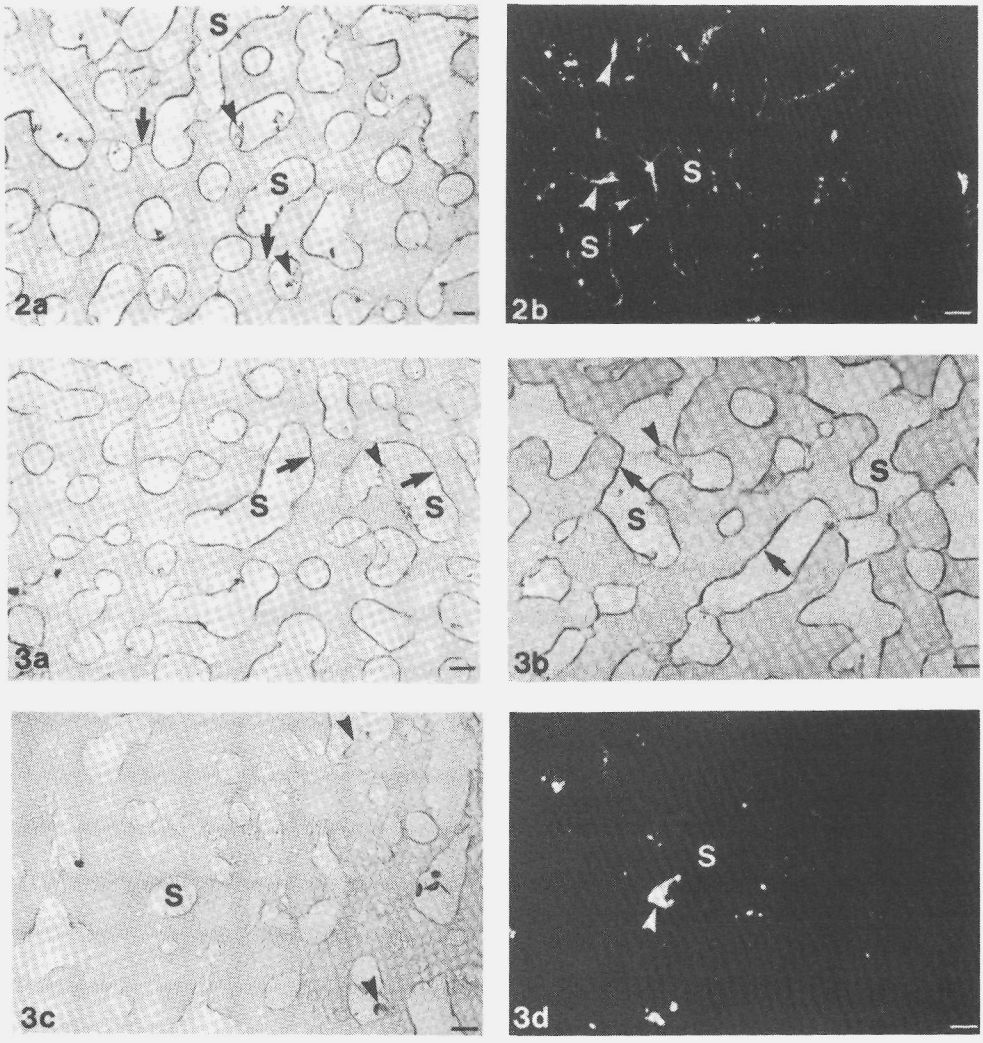

Figure 2. Immuno-labeling with antibodies against apoE (a) and fluorescence microscopy (b) of semithin cryosections after DiI-β-VLDL perfusion. Immuno-label and fluorescence are present around sinusoids (S) and in recesses between parenchymal cells (arrows). Some association of immuno-label and fluorescence is noticed with Kupffer cells (large arrowheads). Some autofluorescence is evident in parenchymal cells (small arrowheads) bars = 10 μm.

Figure 3. Immuno-labeling with antibodies against apoE (a,b,c) and fluorescence microscopy (d) of semithin cryosections after DiI-β-VLDL perfusion in the presence of respectively excess lactoferrin (a), LDL (b), or lactoferrin and LDL (c,d). Addition of LDL or lactoferrin to the perfusion medium does not affect the perisinusoidal presence (arrows) of β-VLDL (a,b) in comparison to Fig. 2, while simultaneous addition shows a marked decrease of the parenchymal cell interaction of β-VLDL, while the interaction with Kupffer cells (arrowheads) is not affected or even slightly increased (c,d). S = sinusoid. bars = 10 μm.

Cellular distribution of β-VLDL

Localization of DiI-labeled β-VLDL by immuno-histochemistry, or by fluorescence microscopy showed a similar cell distribution and localization of β-VLDL (Fig. 2). β-VLDL was present around sinusoids of portal and central areas of the liver lobules and in recesses between adjacent parenchymal cells. Some immuno-staining and fluorescence was associated with Kupffer cells (Fig. 2). No immuno-staining of endothelial cells was evident. No staining of liver tissue was noticed following immuno-staining of control tissue (not perfused with β-VLDL), or after control incubation with non-immune serum. Some autofluorescence inside parenchymal cells, representing lipid, was noticed by fluorescence microscopy in accordance to previous data (13).

Nature of recognition of β-VLDL

Localization of β-VLDL by immuno-histochemistry or by fluorescence microscopy after perfusion in the presence of excess lactoferrin (Fig. 3a) or LDL (Fig. 3b) showed no significant differences in the amount or cellular localization of β-VLDL, in comparison to livers only perfused with β-VLDL (Fig. 2). Immuno-label and fluorescence (not shown) were predominantly localized perisinusoidally, in recesses between parenchymal cells and to some extend associated with Kupffer cells. However, if both lactoferrin and LDL were present in the perfusion medium, the amount of β-VLDL associated with the parenchymal cells was strongly diminished as evidenced in Figs. 3c and 3d, while the Kupffer cell interaction seemed comparable or even slightly increased in comparison to liver tissue only perfused with β-VLDL.

Immuno-localization of lactoferrin after perfusion, demonstrated a clear perisinusoidal localization (Fig. 4). Immuno-staining present between adjacent parenchymal cells indicates that lactoferrin binds to the parenchymal cells. Occasionally,individual parenchymal cells were diffusely stained, indicating that the permeability of the cell had changed, probably due to severe cell damage. Small amounts of immuno-label were associated with Kupffer and endothelial liver cells. Liver tissue perfused only with β-VLDL did not show any immuno-staining for lactoferrin.

Immuno-localization of the LDL receptor in the different donor livers demonstrated that both Kupffer and parenchymal cells express LDL receptors. In accordance to previous data (13) the amount of immuno-label associated with the parenchymal cells fluctuated between the individual livers, although staining at the plasma membrane was always present (Fig. 5).

Discussion

β-VLDL is shown in the present study to interact with parenchymal and Kupffer cells of the human liver, very similarly as previously described for rat liver (12). In rat, parenchymal

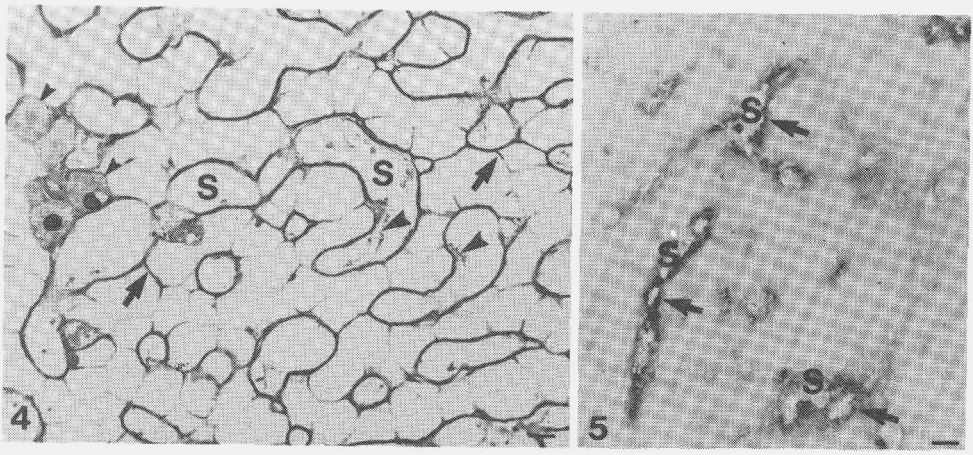

Figure 4. Immuno-localization of lactoferrin after perfusion on semithin cryosection. Lactoferrin is present around sinusoids and between adjacent parenchymal cells (arrows). Occasionally parenchymal cells were diffusely stained due to severe cell damage (small arrowheads). Note the small amount of lactoferrin associated with Kupffer cells (large arrowheads). S = sinusoid. bars = 10 μm.

Figure 5. Immuno-labeling with antibodies against the LDL receptor of a cryostat (6 μm) section. LDL receptors are noticed perisinusoidally (arrows). S = sinusoid. bars = 5 μm.

cells are responsible for about 95% of the total liver uptake of β-VLDL, while Kupffer cells contribute for about 4% to the liver uptake (3,7). Even this relative low contribution allows the Kupffer cell interaction in the rat to be visualized, since the Kupffer cells only represent 2,1% of the total liver protein mass leading to a 2 fold higher specific activity than for parenchymal cells (92,5% of liver protein). Based upon the similar amount of fluorescence and immuno-label, noticed in Kupffer vs. parenchymal cells for human liver and rat liver (12), it is conceivable that also in human liver, parenchymal cells will internalize the majority of circulating β-VLDL, while Kupffer cells only contribute to a minor extend to the liver uptake.

In principle both the tentative remnant receptor and LDL receptor are able to bind β-VLDL (4,5). In contrast to rat liver (7,12), it is found that lactoferrin does not block the β-VLDL association to parenchymal cells. Also an excess of LDL, in order to block the LDL receptor, did not affect the interaction of β-VLDL with parenchymal cells. Since simultaneous administration of lactoferrin and an excess of LDL prevented the binding of β-VLDL to the parenchymal cells, it is conceivable that both the LDL receptor and a second receptor inhibitable by lactoferrin (the remnant receptor) are involved in β-VLDL binding. Lactoferrin bound predominantly to the plasma membrane of the parenchymal cells in the

human livers indicating that indeed a specific recognition site on human parenchymal cells was present for this ligand, a similar finding as in rats. In estradiol-treated rats, which show enhanced expression of LDL receptors on parenchymal cells, lactoferrin is not able to inhibit the β-VLDL interaction with parenchymal cells (12), as the effect of lactoferrin is specific for the remnant receptor (7,11). These findings are in agreement with the data with human livers, because parenchymal cells always stained for LDL receptors.

Although in rat preferential binding of β-VLDL to LDL receptors was noticed (12,15), the physiological relevance of the LDL receptor in the uptake of β-VLDL in human liver is not certain, since recent data demonstrated that *in vitro* remnant receptor-mediated uptake of β-VLDL by human parenchymal cells leads to a complete down regulation of LDL receptor expression (16). The high fluctuation in the amount of LDL receptors and the inhibition of the interaction of β-VLDL with parenchymal cells by physiological concentrations of LDL further indicates that the remnant receptor activity in human liver, as evident from our findings, is important to protect the body against circulating β-VLDL particles, especially under conditions that LDL receptors are down-regulated or possibly blocked by an excess of circulating LDL.

Acknowledgements

We thank Johannes van der Boom and Elisabeth Blauw for excellent technical assistance.

References

1. Fredrickson DS, Levy RI, Lindgren FT. A comparison of heritable abnormal lipoprotein patterns as defined by two different techniques. J Clin Invest 1969;47:2446-57.
2. Shore VG, Shore B, Hart RG. Changes in apolipoproteins and properties of rabbit very low density lipoproteins on induction of cholesteremia. Biochemistry 1974;13:1579-85.
3. Harkes L, Duijne A, Berkel ThJC. Interaction of β-very low density lipoproteins with rat liver cells. Eur J Biochem 1989;180:241-48.
4. Mahley RW, Hui DY, Innerarity TL, Weisgraber KH. Two independent lipoprotein receptors on hepatic membranes of dog, swine and man: apo-B,E- and apo-E receptors. J Clin Invest 1981; 68:1197-1206.
5. De Water R, Kamps JAAM, Van Dijk MCM, Hessels EMAJ, Kuiper J, Kruijt JK, Van Berkel ThJC. Characterization of the LDL-independent interaction of β-migrating VLDL with rat and human parenchymal liver cells in vitro. Biochem J 1992;281:41-48.
6. Harkes L, Van Berkel ThJC. Quantitative role of parenchymal cells and non-parenchymal liver cells in the uptake of [14C] sucrose labelled low density lipoproteins in vivo. Biochem J 1984;224:21-27.
7. Van Dijk MCM, Ziere GJ, Boers W, Linthorst C, Bijsterbosch MK, Van Berkel ThJC. Recognition of chylomicron remnants and β-VLDL by the remnant receptor of parenchymal liver cells is distinct from the α2-macroglobulin recognition site. Biochem J 1991;279:863-70.

8. Ziere GJ, Van Dijk MCM, Bijsterbosch MK, Van Berkel ThJC. Lactoferrin uptake by the rat liver: characterization of the recognition site and effect of selective modification of arginine residues. J Biol Chem 1992;267:11229-35.
9. Willnow TE, Goldstein JL, Orth K, Brown MS, Herz J. LRP and gp330 bind similar ligands, including PAI complexes and lactoferrin, an inhibitor of chylomicron remnant clearance. J Biol Chem 1992;267:26172-180.
10. Herz J, Hamann U, Rogne S, Myklebost O, Gausepohl H, Stanley KK. EMBO J 1988;224:41-48.
11. Huettinger M, Retzek H, Hermann M, Goldenberg H. Lactoferrin specifically inhibits endocytosis of chylomicron remnants but not α2-macroglobulin. J Biol Chem 1992;267:18551-57.
12. Esbach S, Van der Boom J, MN Pieters, Schouten D, Roholl PJM, Brouwer A, Knook DL, Van Berkel ThJC. Visualization of the in vivo interaction of β-VLDL with the remnant receptor of rat liver. submitted.
13. Kleinherenbrink-Stins MF, Van der Boom J, Schouten D, Roholl PJM, Van der Heyde MN, Brouwer A, Van Berkel ThJC, Knook DL. Visualization of the interaction of native and modified lipoproteins with parenchymal, endothelial and Kupffer cells from human liver. Hepatology 1991;14:79-90.
14. Eriksson M, Angelin B, Henriksson P, Ericsson S, Vitols S, Berglund L. Metabolism of lipoprotein remnants in humans. Arteriosclerosis and thrombosis 1991;11:827-37.
15. Jackle S, Runquist E, Brady SE, Hamilton RL, Havel RJ. Isolation and characterization of three endosomal fractions from the liver of normal rats after lipoprotein loading. J Lipid Res 1991;32:485-92.
16. Kamps JAAM, Kuiper J, Kruijt JK, Van Berkel ThJC. Complete down-regulation of LDL receptor activity in human liver parenchymal cells by β-VLDL. FEBS Lett 1991;287:34-38.

Chapter 7

The Fate of Recombinant Rat Bile Salt-Stimulated Cholesterol Ester Hydrolase *In Vivo*

Donald Schouten[1], Sebastiaan Esbach[2], Moniek N. Pieters[1], David Y. Hui[3], Adriaan Brouwer[2], Dick L. Knook[2] and Theo J.C. van Berkel[1]

[1] Division of Biopharmaceutics, Center for Bio-Pharmaceutical Sciences, University of Leiden, Leiden, The Netherlands.

[2] Department of Pathology and Laboratory Medicine, University of Cincinnati College of Medicine, Cincinnati, Ohio USA.

[3] TNO Institute of Ageing and Vascular Research, Gaubius Laboratories, Leiden, The Netherlands.

Submitted for publication

Summary

Intravenously injected rat pancreas bile salt-stimulated cholesterol esterase, serving as a model for the secreted enzyme either from the liver or the pancreas, is associated in rat serum with the high density lipoproteins. The enzyme is rapidly taken up by the liver and after ten minutes a maximal uptake of 46.8 ± 2.5% is observed. Besides the liver bones adsorbed a considerable amount of activity (20.3 ± 1.9% at 10 min and 31.4 ± 2.3% at 30 min). No clear function for the presence of the enzyme associated with bones was found. In the liver, the enzyme is subsequently degraded to trichloroacetic acid soluble activity. No significant activity is found in the bile (6% in 72 hours). The Kupffer cells are found to be the most active liver cells in the uptake of the esterase (77.4 ± 0.9 of the liver associated activity). *In vivo* morphological studies using antibodies specific for the enzyme show that the endogenous enzyme is strongly present on Kupffer cells, mainly localized at the plasma membrane. Besides on Kupffer cells, in parenchymal cells, light microscopical studies show that the enzyme is present in the cytosolic fraction.

We conclude that the bile salt-stimulated cholesterol esterase in rat serum is associated with the high density lipoproteins and that the liver is the major site of uptake of circulating enzyme. Kupffer cells and parenchymal cells play an important role in the metabolism of the bile salt-stimulated cholesterol esterase. Light microscopical studies show that, the esterase in Kupffer cells is mainly localized at the membrane compartment while the esterase in parenchymal cells is mainly localized in the cytosolic compartment. The Kupffer cells are the major site of uptake and catabolism of circulating bile salt-stimulated cholesterol esterase *in vivo*.

Introduction

Excess of intracellular cholesterol can be esterified by the enzyme acylcoenzym A:cholesterol acyl transferase and stored at the site of esterification, the membrane of the endoplasmic reticulum, or in the cytoplasm as lipid droplets (1). Inside the liver cholesteryl esters can be utilized for lipoprotein biosynthesis or converted to free cholesterol by a cholesteryl ester hydrolase which may be coupled to conversion to bile acids. A neutral cholesterol esterase, located in the endoplasmic reticulum (2), is thereby essential. In addition to a neutral cholesterol esterase, localized in the endoplasmic reticulum, another neutral cholesterol esterase, localized in the cytosol is described (3). This cholesterol esterase requires millimolar concentrations of cholate or taurocholate for activity. The function of this bile salt-stimulated cholesterol esterase in the rat liver, which is identical to the rat bile salt-dependent cholesterol esterase as found in the pancreas (4,5), is unknown. The enzyme activity appears to be highly variable among homogenates from the livers of individual rats

and it was first proposed that the enzyme found in the liver might be due to pancreatic enzyme that had been taken up by the liver (4). Recent studies indicate the presence of mRNA corresponding to the cDNA for rat pancreatic enzyme in liver (6). Furthermore, liver mRNA could be translated in bile salt-stimulated cholesterol esterase activity in Xenopus oocytes (7). Synthesis of this enzyme maybe coupled to a secretory pathway as Winkler and Harrison (8) found that the liver hepatoma cell line HEPG2 did secrete the esterase. In addition, they showed that the enzyme is also released from rat liver in a perfusion system.

The fate of the enzyme, either secreted from liver or the pancreas, is unknown and its possible role accelerating either selective cholesteryl ester delivery from HDL, or HDL cholesteryl ester hydrolysis is an important option. In the present study we describe the localization of endogenous cholesterol esterase and the possible association of the recombinant bile-salt stimulated cholesterol esterase with lipoproteins and its subsequent fate in the body.

Materials and Methods

Materials

Nycodenz was obtained from Nycomed, Oslo, Norway. Collagenase type I and bovine serum albumin (BSA; fraction V) were purchased from Sigma, St. Louis, U.S.A. $Na^{125}I$ (carrier free) in NaOH was purchased from Amersham International, Amersham, Bucks, U.K. Pronase was obtained from Boehringer Mannheim, Germany. All other chemicals were analytical grade.

Throughout this study 12-week old male Wistar rats were used.

Methods, enzyme preparation

Recombinant rat pancreatic cholesterol esterase was prepared as described by Kissel et al. (6). Iodination of the cholesterol esterase was performed using the iodogen method (9), the lyophilized enzyme was taken up in a 10 mM Tris/HCl buffer, pH 8.3 and incubated for 15 min. at room temperature with ^{125}I (carrier free) in NaOH. The preparation was extensively dialysed against phosphate-buffered saline, tested for esterase activity and stored at -20°C. Because it is known that the enzyme is unstable (8,10), we checked its integrity before every experiment. Only enzyme preparations with less than 3% of the radioactivity present as trichloroacetic soluble were applied.

Determination of the association of the bile salt stimulated cholesterol esterase with serum lipoproteins in vitro

The radiolabeled esterase was incubated for 5 min. at 37°C with either rat serum, human serum, LDL, HDL, albumin or phosphate-buffered saline and subjected to agarose

electrophoresis according to the method of Demacker (11), using HDL and LDL as standards. The agarose plate was dried by a stream of hot air and subjected to autoradiography.

In vivo serum clearance and liver association

Male Wistar rats (approximately 250 gram) were anaesthetized by intraperitoneal injection of approximately 30 mg of sodium pentobarbital. The abdomen was opened and 100 μg of radiolabeled ligand was injected into the inferior vena cava at the level of the renal veins. Blood sampling and excising of liver lobules were performed at the indicated times as described before (12).

Determination of association to liver cells

Rats were anaesthetized and injected with the radiolabeled ligand. At the indicated times after injection, parenchymal, endothelial and Kupffer cells were separated by collagenase perfusion (collagenase type I), followed by differential centrifugation and counterflow centrifugal elutriation at 4°C as described in detail elsewhere (13). The contributions of the different liver cell types to the total hepatic uptake of the injected ligands were calculated with the assumption that parenchymal, endothelial and Kupffer cells account for 92.5, 3.3 and 2.5% of the total liver protein mass, respectively (14).

Tissue distribution

Rats were anaesthetized and injected with the radiolabeled ligand. After 10 or 30 minutes rats were sacrificed and the individual tissues were weighed and counted for radioactivity and corrected for the contribution of blood to the total counts as described earlier (14).

Preparation of cholesterol esterase antibodies

Purified porcine cholesterol esterase (250 μg), was injected, subcutaneously, into a New Zealand White rabbit at two-weeks intervals, as described by Camulli et al. (5). Blood was collected from the ear vein and the IgG fraction was isolated from the blood serum by affinity chromatography on a protein A-agarose column and stored at -70°C until use. Serum and IgG-fractions were tested against the porcine cholesterol esterase, crude rat liver material and rat serum in double-radial immuno-diffusion experiments and immuno-blotting experiments. These experiments showed no cross-reactivity with other proteins.

Light microscopical studies

Rat liver was perfused for 10 minutes with 4% PBS buffered paraformaldehyde at room temperature and stored in the same solution. Fixed liver tissue samples were immersed with 2.3. M sucrose, frozen in liquid nitrogen. Semithin cryosections (1 μM) were cut on a Reichert FC 4 cryomicrotome. Sections were immuno-labeled, mounted with entellan and

viewed on a Zeiss light microscope as described before (15).

Immuno-labeling procedure

The antibodies were diluted in PBS containing 0.1% gelatin, 0.5% BSA and 0.1% Tween 20. Mouse anti-rabbit IgG was labeled with the indirect alkaline phosphatase-anti-alkaline phosphatase (APAAP) method as described by Cordell et al. (16). In short, samples were incubated with the first antibody, rabbit anti bile salt-stimulated cholesterol esterase (dilution 1:100), rinsed, incubated with mouse anti-rabbit IgG (dilution 1:150), rinsed, incubated with rabbit anti-mouse IgG (dilution 1:150), rinsed and incubated with the APAAP complex (dilution 1:100) and developed in 1mM Naphthol A.S.M.X. phosphate in 0.1 M TRIS, pH 8.2. Endogenous alkaline phosphatase activity was inhibited by including 1 mM Levamisole in the developer solution. Control incubations in which the primary antibody was omitted and non-immune rabbit serum was used instead, demonstrated that no reaction product was present.

Bile sampling

Bile was collected from unrestrained rats as reported previously (17). Rats received tap water and standard chow *ad libitum*. Rats were equipped with permanent catheters in the bile duct, the duodenum and the heart. In order to maintain an intact enterohepatic circulation, the bile duct and duodenum catheters were connected immediately after surgery. Rats were allowed to recover for 1 week. Iodinated bile salt-stimulated cholesterol esterase was introduced via the heart catheter. The bile duct catheter was then connected to a fraction collector and bile was collected for 72 h. Bile samples were counted for radioactivity.

Protein determination

Protein was determined according to Lowry et al. (18) with BSA as standard.

Results

Determination of the association of the bile salt-stimulated cholesterol esterase with serum lipoproteins in vitro

The interaction of the bile salt-stimulated cholesterol esterase with serum fractions was investigated by incubating the radiolabeled esterase for 5 min. at 37°C with either rat serum, human serum, LDL, HDL or phosphate-buffered saline, followed by agarose electrophoresis.

Figure 1 shows that upon incubation with rat serum, the enzyme becomes mainly associated with the HDL-fraction. Since in rats the predominant lipoprotein is HDL, we used also human serum to study the enzymes preference for particular lipoproteins (Fig. 1). Upon incubation with human serum the enzyme associate with the larger lipoproteins and not with

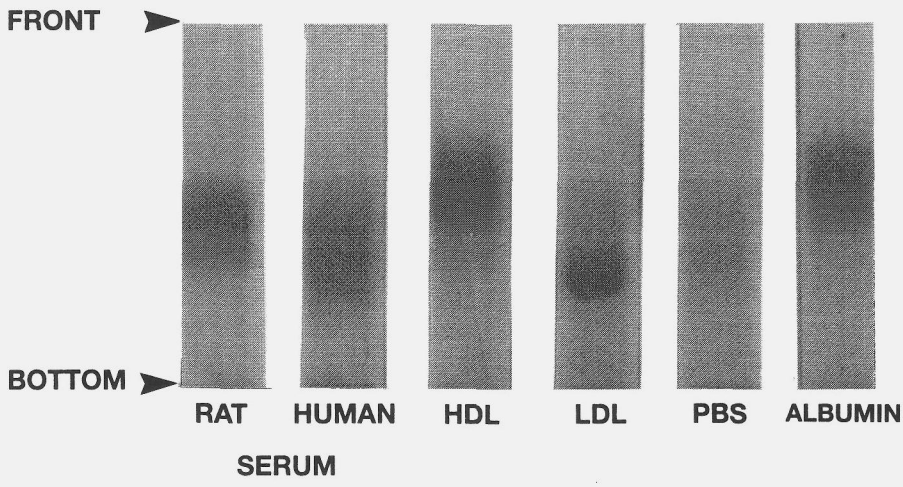

Figure 1. The interaction of the bile salt-stimulated cholesterol esterase with serum fractions. The cholesterol esterase was incubated for 5 min. at 37°C with either rat serum, human serum, LDL, HDL, albumin or phosphate-buffered saline and subjected to agarose electrophoresis and autoradiography.

serum albumin. When both LDL and HDL are present, the enzym is mainly attached to the LDL-fraction. The esterase alone (PBS) did not migrate into the agarose gel. The cholesterol esterase appears however to be loosely bound to the lipoproteins, because upon isolation of the lipoprotein fractions by ultracentrifugation, the enzym is solely found in the lipoprotein-deficient fraction (not shown).

Serum decay and liver uptake

Upon injection of the bile salt-stimulated cholesterol esterase in the rat, the enzym is very rapidly cleared from the circulation (Fig. 2). Five minutes after injection only 35 $\pm$ 1.6% of the activity is still present in the serum. The liver uptake is also very rapid and at ten minutes a maximal uptake of 46.8 $\pm$ 2.5% of the injected dose was observed, after which the trichloroacetic acid (TCA) precipitable radioactivity disappeared gradually. At 45 minutes still 15% of the precipitable radioactivity was present in the liver. The inset shows that the disappearance of the trichloroacetic acid precipitable radioactivity is accompanied by an increase in TCA-soluble radioactivity, indicative for degradation of the enzyme.

Intrahepatic cellular distribution of the bile salt-stimulated cholesterol esterase in the liver

In order to identify the cell type(s) responsible for uptake in the liver, rats were injected with the radiolabeled enzym, and parenchymal, Kupffer and endothelial cells were isolated from the at liver ten minutes after injection. The cell isolation procedure was performed at a low

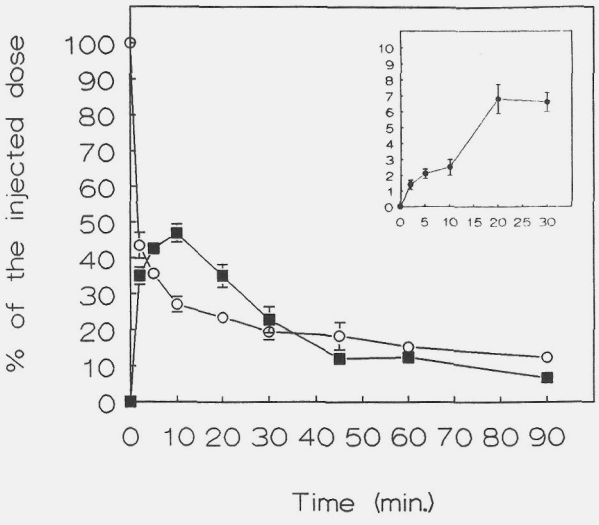

Figure 2. Serum decay and liver uptake of iodinated bile salt-stimulated cholesterol esterase. Rats were injected with radiolabeled bile salt-stimulated cholesterol esterase, at a dose of 40 μg protein/kg body weight. At the indicated times, radioactivity in serum (○) and liver (■) were determined. The radioactivity in the liver was corrected for the activity present in blood. The inset shows the amount of TCA-soluble radioactivity recovered in the liver. Values are means ± standard errors of three rats.

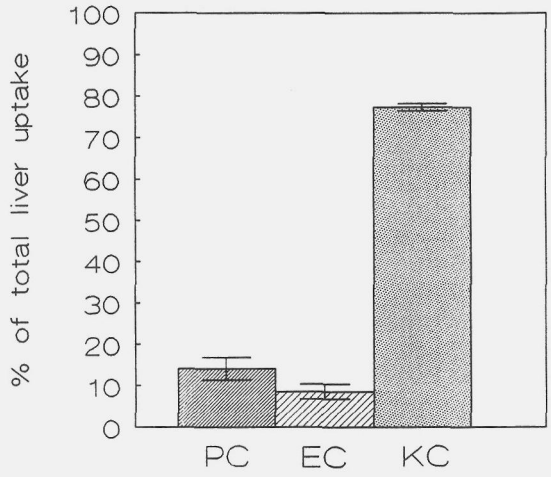

Figure 3. Distribution of radiolabeled bile salt-stimulated cholesterol esterase between parenchymal, endothelial and Kupffer cells from rat liver. Rats were injected with ^{125}I-bile salt-stimulated cholesterol esterase at a dose of 40 μg/kg body weight. Ten minutes after injection, parenchymal, endothelial and Kupffer cells were isolated, and the association of radioactivity to each cell type was determined. The association is expressed as percentage of the total liver uptake. Values are means ± standard errors of three rats.

temperature in order to prevent degradation of the ligand. The results as shown in Fig. 3 indicate that the Kupffer cells were mainly responsible for the liver uptake of the esterase. Taking into account the relative contribution of each cell type to the total liver, it can be calculated that 77.4 ± 0.9 of the liver associated esterase can be ascribed to Kupffer cells. The remaining 22.6% is found in the parenchymal cells (14.1 ± 2.8%) and the endothelial cells (8.6 ± 1.9%).

To investigate whether the labeled bile salt-stimulated cholesterol esterase was released during the initial 8' perfusion, we collected the perfusate in 3 ml fractions. During the perfusion only 1.5% of the injected radiolabel could be recovered in the perfusate.

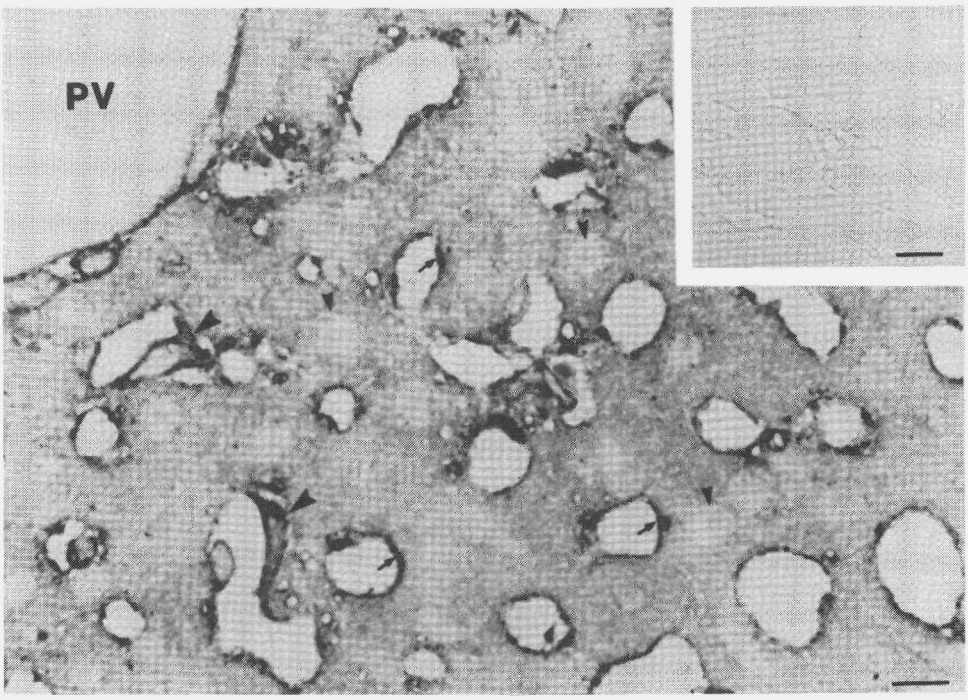

Figure 4. Visualization of bile salt-stimulated cholesterol esterase. Cryosections of livers from rats were labeled with antibodies raised against porcine bile salt-stimulated cholesterol esterase and visualized using the indirect alkaline phosphatase-anti-alkaline phosphatase (APAAP) method as described by Cordell et al. (15). Kupffer cells are indicated with the large arrowheads. Perisinusoidal immuno-staining is indicated with arrows. The nuclei of parenchymal cells are indicated with small arrowheads. PV: portal vein. The inset shows a control incubations in which the primary antibody was omitted and non-immune rabbit serum was used instead.

In vivo visualization of bile salt-stimulated cholesterol esterase

To establish the cellular and intracellular localization of the endogenous bile salt-stimulated cholesterol esterase, we used antibodies specific for porcine bile salt-stimulated cholesterol esterase in combination with an indirect immuno-staining technique. As represented in Fig. 4, immuno-staining of the bile salt-stimulated cholesterol esterase is strongly positive with Kupffer cells (large arrows), mainly at the plasma membrane.

Immuno-staining is also found perisinusoidal, although at a variable amount in different rat livers (n = 11). Since the perisinusoidal staining is only noticed nearby the sinusoidal

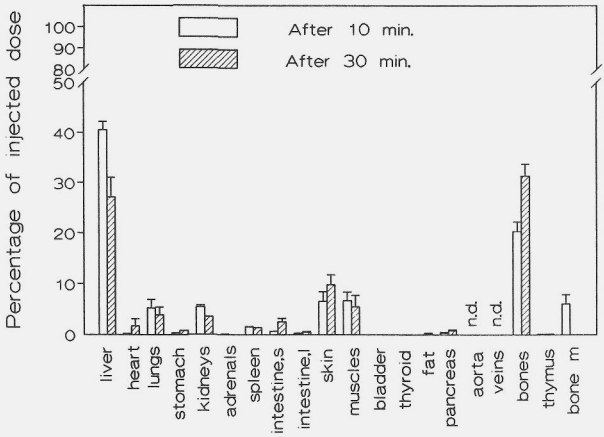

Figure 5. Tissue distribution of intravenously injected radiolabeled bile salt-stimulated cholesterol esterase in rats. Rats were injected with ^{125}I-bile salt-stimulated cholesterol esterase at a dose of 40 μg/kg body weight. Ten and thirty minutes after injection radioactivity in the indicated tissues and organs were determined. All values have been corrected for the presence of serum in the tissues. The results are expressed as percentage of the recovered dose (respectively 105.2 $\pm$ 5.5% and 103.9 $\pm$ 4.1%). Values are means $\pm$ standard errors of three rats.

lumen, and never between adjacent parenchymal cells, it is likely that the staining is due to the presence of the bile salt-stimulated cholesterol esterase on the liver endothelial cells.

Although immuno-staining for the enzym in the parenchymal cells was also variable between the livers studied, a significant amount was always found diffusely localized over the cytosol of the parenchymal cells with exclusion of the nuclei. The inset in Fig. 4 shows a control incubation in which the primary antibody was omitted and non-immune rabbit serum was used instead. It is shown that no reaction product was present.

Tissue distribution of the bile salt-stimulated esterase in the rat in vivo

In addition to the liver also other organs may contribute to the serum uptake of the enzyme. To investigate quantitatively the uptake by other organs and tissues, the distribution of labeled bile salt-stimulated cholesterol esterase over a large number of tissues was determined at 10 and 30 min after injection. Figure 5 shows that besides the liver, a considerable amount of activity (20.3 $\pm$ 1.9% at 10 min and 31.4 $\pm$ 2.3% at 30 min after injection of the ligand) becomes associated with bones. Lungs, kidney, skin and muscles were responsible for the remainder. The recovery was at 10 min was 105.2 $\pm$ 5.5% and at 30 min 103.9 $\pm$ 4.1% of the injected dose.

The association to the bones was not specific to any site in the body as the radioactivity of bones recovered from various parts of the rat (18.8 $\pm$ 2.2%) showed no significant deviation from the value given above (20.3 $\pm$ 1.9%).

Transport of iodinated bile salt-stimulated esterase to the bile

In order to investigate the possible transport of bile salt-dependent cholesterol esterase into the bile, rats were equipped with permanent catheters in the bile duct, duodenum and heart. The secretion of biliary radioactivity expressed as percentage of the injected dose/10 min is

low and radioactivity is mainly present in the form of trichloroacetic acid soluble activity (see inset Fig. 6). In the first hour after administration 1.34% of the injected activity was found in the bile. As shown in Fig. 6, in which the secretion is expressed as percentage of the injected dose/hour, after the first hour the secretion of activity in the bile decreased and 72 hours after injection only 6% of the injected dose was recovered in the bile.

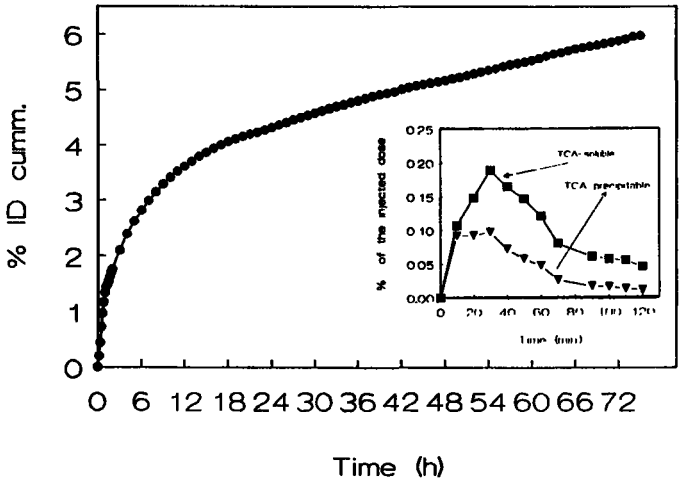

Figure 6. Biliary accumulation of ^{125}I-bile salt-stimulated cholesterol esterase activity during 72 hours after injection. ^{125}I-bile salt-stimulated cholesterol esterase was injected into rats equipped with permanent heart and bile catheters. Bile was collected for 72 hours, the first 2 hours in 10 min fractions, thereafter in 1 hour fractions and counted for radioactivity. The inset shows the trichloroacetic acid soluble- (■), and the trichloroacetic acid precipitable radioactivity (▼).

Discussion

To investigate the fate of the bile salt-stimulated cholesterol esterase released from the pancreas or the liver in the bloodstream, we followed its fate after intravenous injection into the rat. In serum, enzym is associated with lipoproteins which can be explained by its lipid interfacial binding site (6,10). In rat serum, the esterase is mainly associated with the high density lipoprotein, the predominant lipoprotein in this species. However, if other lipoproteins are present, like the low density lipoprotein, the enzyme prefers this lipoprotein. This phenomenon is probably due to the surface composition of the lipoproteins (3,19,20). After isolation of lipoproteins with ultracentrifugation techniques (21), the esterase was found in the lipoprotein depleted fraction, indicating that it is only loosely bound to lipoprotein (not shown).

Upon injection of the bile salt-stimulated cholesterol esterase in the rat, irrespective of its association to lipoproteins, the enzyme is very rapidly cleared from the circulation which is mainly explained by an avid interaction with the liver. At ten minutes after injection a maximal liver uptake is observed, after which the liver-associated trichloroacetic acid (TCA) precipitable radioactivity disappeared gradually. The disappearance of the trichloroacetic acid

precipitable radioactivity from the liver can be explained by degradation of the ligand to TCA-soluble radioactivity. A preincubation of the esterase with HDL prior to injection in the rat had no effect on the serum decay and liver uptake (not shown) indicating that association with the liver involves a site with higher affinity than the adsorption of the esterase to the high density lipoprotein. The Kupffer cells were found to be the most active liver cells in the uptake of the esterase. Using a low temperature isolation procedure in order to prevent degradation of the ligand, we found that 77.4 $\pm$ 0.9% of the associated esterase is attached to the Kupffer cells.

The cellular localization of endogenous bile salt-stimulated cholesterol esterase in the liver, was studied by using a morphological approach, in cryosections of the livers of eleven individual rats. In all rat livers a strong immuno-staining is seen to be associated with Kupffer cells, mainly localized at the plasma membrane. We also found a variable perisinusoidal staining. Since the perisinusoidal staining is only noticed nearby the sinusoidal lumen, and never between adjacent parenchymal cells, it can be suggested that the variable staining is due to the variable presence of the enzym on the liver endothelial cells. The immuno-staining as found in parenchymal cells was also variable between the livers of individual rats. The localization in the parenchymal cells, is probably the cytosolic fraction of the cell, since immuno-label was diffusely localized over the cytosol of the parenchymal cells with exclusion of the nuclei. This localization of the enzyme would be in agreement with the assumption that the bile salt-dependent cholesterol esterase is synthesized and secreted from the liver parenchymal cell. Because Winkler et al. (8) showed that esterase activity is released from the liver in a perfusion model, we investigated whether the radio-labeled bile salt-stimulated cholesterol esterase which became associated to the liver could be subsequently released during perfusion. Only 1.5% of the injected dose could be recovered in the perfusate. This indicates that the esterase activity which is released by the liver (Winkler et al.) may indeed originate from synthesis by the parenchymal cells, rather then from esterase reversibly attached to the Kupffer cells. Furthermore, these data suggests that the rate of synthesis and subsequent release of the esterase from rat liver cells may be even greater than found by Winkler et al. since part of the secreted esterase maybe trapped (and degraded) by Kupffer cells, especially if the esterase is released in the periportal area of the liver.

To obtain a complete view of the sites of uptake of the injected esterase, we investigated the uptake of the bile salt-stimulated cholesterol esterase by other rat organs and tissues and the possible secretion into the bile. We found that besides the liver, bones, a negatively charged matrix, took up a considerable amount of activity (20.3 $\pm$ 1.9% at 10 min and 31.4 $\pm$ 2.3% at 30 min after injection of the ligand). The uptake by bones was defined by taking into account the contribution of the radioactivity from bones recovered from various parts of the rat ($n = 5$). It is possible that this high uptake is due to the positive charge of the domain at amino acid residues 61-66 of the enzym which fits the charge distribution of the

consensus heparin-binding domain (6,10). The negatively charged proteoglycans present in bone may account for this adsorption. The function of the bile salt-stimulated cholesterol esterase adsorbed by bones is not clear but might give a new insight in the significance of the release of the enzym by the liver. Lungs, kidney, and muscles were responsible for most of the remaining activity. Only 6% of the injected radioactivity was recovered in the bile after 72 hours, mainly in the form of trichloroacetic acid soluble activity.

The data presented in this paper provide further evidence for the dual involvement of the liver in the metabolism of the bile salt-stimulated cholesterol esterase. Kupffer cells are the major site of uptake and catabolism of circulating bile salt-stimulated cholesterol esterase *in vivo* while the presence of the enzym in the cytosolic compartment of the parenchymal cells may represent newly synthesized enzym.

References

1. Hasimoto, S., and Fogelman, A.M. (1980) *J. Biol. Chem.* 255:8678-8684.
2. Fernandez, C.J., Lacort, M., Gandarias, J.M., and Ochoa, B.(1987) *Biochim. Biophys. Res. Comm.* 146:1212-1217.
3. Rudd, E.A., and Brockman, H.L. (1984) in:Lipases. eds Borgstrom, B. and Brockman, H.L.pp. 185-204.
4. Harrison, E.H. (1988) *Biochim. Biophys. Acta* 963:28-34.
5. Camulli, E.D., Linke, M.J., Brockman, H.L., and Hui, D.Y. (1989) *Biochim. Biophys. Acta* 1005:177-182.
6. Kissel, J.A., Fontaine, R.N., Turck, C.W., Brockman, H.L., and Hui, D.Y. (1989) *Biochim. Biophys. Acta* 1006:227-236.
7. Zolfaghari, R., Harrison, E.H., Ross, A.C., and Fisher, E.A. (1989) *Proc. Natl. Acad. Sci. U.S.A.* 86:6913-6916.
8. Winkler, K.E., Harrison, E.H., Marsh, J.B., Glick, J.M., and Ross, A.C. (1992) *Biochim. Biophys. Acta* 1126:151-158.
9. Fraker, P.J. and Speck, J.C. (1978) *Biochim. Biophys. Res. Commun.* 80:849-857.
10. Fontaine, R.N., Carter, C.P., and Hui, D.Y. (1991) *Biochemistry* 30:7008-7014.
11. Demacker, P.N.M.(1978) *Hyperlipoproteinemia-a study on diagnostic methods* [dissertation]. Nijmegen: The Netherlands, University of Nijmegen.
12. Van Berkel, Th.J.C., Kruijt, J.K., and Kempen, H.J.M. (1985) *J. Biol. Chem.* 260:12203-12207.
13. Van Berkel, Th.J.C., Dekker, C.J., Kruijt, J.K., and van Eijk, H.G. (1987) *Biochem. J.* 243:715-722.
14. Nagelkerke, J.F., Barto, K.P., and van Berkel, Th.J.C. (1983) *J. Biol. Chem.* 258:12221-12227.
15. Kleinherenbrink-Stins, M.F., van der Boom, J., Bakkeren, H.F., Roholl, P.J.M., Brouwer, A., van Berkel, Th.J.C., and Knook, D.L. (1989) *Lab.Invest.* 63:73-86.
16. Cordell, J.L., Falini, B., Erber, W.N., Gosh, A.K., Abdulaziz, Z., MacDonald, S., Pulford, K.A.F., Stein, H., and Mason, D.Y. (1984) *J. Hist. Cyt.* 32:219-229.
17. Kuipers, F., Havinga, R., Bosschieter, H., Toorop, G.P., Hindriks, F.R., and Vonk, R.J. (1985) *Gastroenterology* 88:403-411.
18. Lowry, O.H., Rosebrough, N.J.,Farr, A.L., and Randall, R.J.k *J. Biol. Chem.* 193:265-275 (1951).
19. Bath, S.G., and Brockman, H.L. (1982) *Biochemistry* 21:1547-1552.
20. Lombardo, D., and Guy, O. (1981)*Biochim. Biophys. Acta.* 659:401-410.
21. Redgrave, T.G., Roberts, D.C.K., and West, C.E. *Anal. Biochem.* 65:42-49 (1975).

Chapter 8

General Discussion and Conclusions

The experimental results presented in this thesis will be discussed with the emphasis on respectively, the visualization techniques that were used, the uptake and processing of modified LDL and β-VLDL by the liver, and the role of HDL in reverse cholesterol transport and the involvement of cholesteryl ester hydrolase in the selective uptake of cholesteryl esters from HDL by the liver.

8.1 Visualization techniques

The microscopical techniques which were used in this thesis can be divided into three categories;

1) standard plastic embedding and staining techniques for an adequate morphological description of the liver tissue,
2) a specific staining technique to study the internalization mechanisms of the various liver cell types, and
3) techniques for visualization of the lipoproteins.

Standard plastic, embedded and stained liver tissue was taken to study tissue preservation using light and electron microscopy. Human liver needed special attention because of the long period (up to 4 hours) between the moment of resection and the experimental use of the tissue (chapters 2 and 6). Severely damaged tissue, as evidenced by the loss of organization of the liver, or by the loss of integrity of the parenchymal cells, was excluded from the analysis. Examination of the plastic embedded human tissue also allowed the detection of minor abnormalities, like the widening of the space of Disse and the presence of blebs in the sinusoids.

Furthermore, evaluation of the plastic embedded tissue contributed to the understanding of the lipoprotein processing in the liver. At the light microscopical level, a significant increase in the amount of lipid vacuoles was noticed in rat liver parenchymal cells following β-VLDL administration (chapter 5). This increase is in agreement with biochemical data which demonstrated the predominant role of this cell type in the uptake of β-VLDL (1). At

the electron microscopical level, besides an increase in the amount of extra-lysosomal lipid vacuoles, a concomitant increase in lysosomal structures was noticed in the parenchymal cells. The increase in the amount of lysosomal structures in the parenchymal cells is in accordance with previous biochemical data which demonstrated that β-VLDL is processed by parenchymal cells via a route which involves the lysosomes (1). The morphological changes in the liver after β-VLDL administration, therefore, not only confirmed which cell type is involved in the uptake of this lipoprotein, but also indicated that re-allocation of lipid, i.e. hydrolysis and re-esterification, forms part of the processing route of β-VLDL by the parenchymal cells.

A special staining technique was used to study the internalization mechanisms of the various liver cells. *En bloc* staining of liver tissue with ruthenium red leads to a selective contrasting of plasma membranes which are in direct contact with the extracellular space. Internalization mechanisms are therefore more easily definable. Endothelial liver cells can internalize compounds via 1) coated vesicle formation, and 2) by so-called macropinocytosis which is characterized by internalization of large areas of plasma membrane, leading to the formation of macropinocytotic vesicles (2). Ruthenium red staining of endothelial cells demonstrated that coated pits and coated vesicles which, in cross-sections, appeared completely surrounded by cytoplasm, were in contact with the extracellular space (chapter 4). This latter finding is in accordance with previous data of Pastan and Willingham (3), who demonstrated that coated vesicles can be connected to the extracellular space by long necks ranging in size up to 1 μm. Since no engulfment of large areas of plasma membrane was noticed and macropinocytotic vesicles were never stained by ruthenium red, macropinocytotic vesicles probably arise from a different mechanism as will be discussed in 8.2.

Kupffer cells contain 4 different structures involved in internalization 1) coated vesicles 2) worm-like structures, 3) pinocytotic vesicles with a fuzzy coat at the inside of the membrane and 4) pseudopodia involved in phagocytosis (2). Ruthenium red staining of Kupffer cells showed that besides plasma membrane extensions, coated pits and coated vesicles, tubular structures and vacuoles at the periphery of the cell body were contrasted. The connections noticed between the tubular structures and the vacuoles, both stained with ruthenium red, and the number of stained structures in the cell periphery indicated that these structures should not be considered separately, but rather as a specialized area of the Kupffer cell. The results of chapter 2 demonstrate that these complex membrane foldings of the Kupffer cells are involved in the internalization of oxidized LDL.

To allow the actual detection of lipoproteins, apoB and apoE were visualized by immunohistochemistry on semithin and ultrathin cryosections. Light microscopical localization of the apolipoproteins indicated the cell types involved in the lipoprotein uptake. Localization of the lipoproteins by electron microscopy at subsequent time points after administration demonstrated which structures were involved in the actual uptake, like coated vesicles, and in processing, like endosomes and lysosomes.

Application of this technique also indicated whether lipoproteins were degraded and how fast, based on the concomitant loss of the antigenicity of the protein part of the lipoproteins. For example, pre-injection of chloroquine, an inhibitor of lysosomal degradation, led at 30 minutes after injection of Ac-LDL to a clear increase in the amount of apoB immuno-staining in the liver endothelial cells (chapter 4). This suggests lysosomal processing, in accordance with biochemical data obtained with isolated cells in suspension, which demonstrated a high capacity for lysosomal degradation of Ac-LDL (4).

Immuno-histochemistry offered additional advantages by the use of species-specific antibodies and the use of antibodies conjugated with gold particles of different sizes. Interference of immuno-reactive endogenous apolipoproteins with the interpretation of the uptake and processing of administered lipoproteins could be prevented by the use of species-specific antibodies and lipoprotein donors and acceptors of different species (chapters 2 and 6). In chapter 5 antibodies coupled to gold particles of 6 and 10 nm were used in a double-labeling procedure to examine whether administered lactoferrin and endogenous apoE were localized in close proximity to each other.

An additional advantage of cryomicrotomy is the actual visibility of the lipoprotein particles at the electron microscopical level due to the negative staining procedure used. Localization of the negatively stained particles at subsequent time points after injection indicated their intracellular processing route. In agreement with the lysosomal degradation of Ac-LDL (4), Ac-LDL particles, as recognized by their size and characteristic roundish appearance, were observed in several intracellular organelles (as discussed in 8.2), but not in lysosomes (chapter 4).

A clear localization of apoB and apoE was demonstrated following immuno-histochemical detection on semi and ultrathin cryosections (chapters 2, 4-6). Besides apolipoproteins this technique allows the localization of other proteins like the LDL receptor (chapter 6), cholesteryl ester hydrolase (chapter 7) and lactoferrin (chapters 5 and 6). A satisfactory preservation of the antigenicity was obtained in combination with a satisfactory ultrastructure.

We also applied a pre-embedding labeling method in which lipoproteins were conjugated with gold particles before they were injected into rats. This approach allows an electron microscopical localization of the ligand as described in numerous studies. However, increasing evidence indicates that the use of colloidal gold can interfere with both receptor recognition and intracellular processing of lipoproteins (5-7). The increase in size and the negative charge added to the conjugate may influence the behaviour of the ligand. To circumvent this problem ultra small gold particles (1 nm) were conjugated with Ac-LDL in a ratio of 1 gold particle per Ac-LDL particle. This conjugate was compared with "native" Ac-LDL with respect to cell recognition by *in vitro* competition experiments and with respect to intracellular processing by ultrastructural visualization of the intracellular handling *in vivo* (chapter 4). Since, the *in vivo* cell distribution and intracellular processing as well as *in vitro* competition studies showed no differences between Ac-LDL and Ac-LDL conjugated with

1 nm gold particles it is indicated that conjugation with gold particles does not add an additional modification to Ac-LDL. In comparison to cryomicrotomy this pre-embedding labeling technique allowed a more vigorous fixation and embedding of the tissue without loss of detectability of the ligand. The ultrastructural preservation allowed the visualization of tubular structures in liver endothelial cells which were hardly recognizable in cryosections (chapter 4). Whether pre-conjugation of ultra small gold particles is also applicable for the visualization of other lipoprotein subclasses requires further study.

Pre-conjugation of the fluorescent probe DiI to lipoproteins was reported to allow an adequate light microscopical localization, without interfering with receptor recognition (8). Since the dye is non-degradable and accumulates in the lysosomal compartment not only a qualitative description of the cell types involved in the uptake, but also a semi-quantitative assessment is possible. Examination of the fate of DiI-labeled Ox-LDL showed that Ox-LDL was predominantly associated with Kupffer cells and to a lesser extent with endothelial cells (chapter 2). The results in chapter 4 demonstrated that the relative involvement of Kupffer and endothelial cells in the uptake of Ox-LDL and Ac-LDL, which is predominantly taken up by the liver endothelial cells, is even more pronounced after simultaneous injection of Ox-LDL and Ac-LDL labeled with different fluorochromes. Localization of the different fluorescent probes in endothelial cells allowed speculation about the intracellular pathways of each ligand.

Furthermore, incorporation of DiI into β-VLDL enabled an estimation of the cellular distribution of remnant receptor activity on basis of the localization of fluorescence. The time dependency of label in periportal and pericentral areas of the liver lobules clearly contrasted with the simultaneous appearance of label in periportal and pericentral areas in rats which were treated with estradiol. Estradiol-treatment selectively upregulates LDL receptors, which are also capable of interacting with β-VLDL, leading to the conclusion that a zonal difference in the activity of the remnant receptor exists.

8.2 Uptake and processing of modified LDL

Modification of LDL causes an important change in the metabolic fate of the particle. Modification leads to enhanced uptake by macrophages via a scavenger receptor, resulting in a foamy appearance of the macrophages as also observed in early atherosclerotic lesions (9). Various modifications of LDL were described including acetylation, malondialdehyde treatment, and oxidation. Although the physiological relevance of Ac-LDL has always been disputed, Ac-LDL is a useful ligand to study scavenger receptor-mediated processes. Several lines of evidence now indicate that oxidation is the (patho)physiologically relevant modification of LDL. Oxidized LDL is localized in and can be extracted from atherosclerotic lesions of rabbits and man (10). Furthermore, probucol, an antioxidant, can prevent the

progression of atherosclerosis in rabbits by limiting the oxidative modification of LDL (11).

Comparison of the *in vivo* fate of Ac-LDL and Ox-LDL in the rat showed that both were rapidly cleared from the blood by the liver (12). However, isolation of the various liver cell types demonstrated that Ox-LDL was predominantly taken up by Kupffer cells, while Ac-LDL was predominantly taken up by the endothelial cells. *In vitro* competition experiments with purified liver cells demonstrated that two receptors are able to bind oxidized LDL. One receptor which recognizes both Ox-LDL and Ac-LDL is mainly expressed on liver endothelial cells. A second scavenger receptor, which recognizes Ox-LDL only, is mainly expressed on Kupffer cells. The accumulation of oxidized LDL in tissue macrophages may result from aggregation of the particles and subsequent phagocytosis (13, 14). Scavenger receptor-mediated phagocytosis of aggregated Ox-LDL might also explain the involvement of the liver macrophages, the Kupffer cells, in the uptake of this ligand.

In chapter 2 it is demonstrated that fluorescent labeled Ox-LDL becomes predominantly associated with Kupffer cells while some fluorescence was also associated with endothelial cells in accordance to the biochemical cell distribution observed with ^{125}I-Ox-LDL (12). Immuno-localization of Ox-LDL at 15 seconds after injection, showed that some label was present inside coated vesicles. However, the major part was associated with lamellipodia and the sponge-like areas in the cell periphery of the Kupffer cells previously mentioned (8.1). At later points in time, a shift of immuno-label was noticed, from the cell periphery into the cell body. It appears that bound ligand was transported into the cell body by movements of lamellipodia. This internalization mechanism is clearly different from phagocytosis. Morphological examination of standard embedded and stained liver tissue showed that plasma membrane extensions and vacuoles in the cell periphery were in continuity with worm-like structures. We therefore propose that the internalization mechanism involved in the uptake of Ox-LDL arises from worm-like structures, in agreement with previous suggestions that worm-like structures represent a pool of spare-membrane (2). Following internalization, immuno-label representing Ox-LDL was subsequently demonstrated in endosomal and lysosomal structures in accordance to the previously demonstrated lysosomal directed pathway of Ox-LDL in Kupffer cells in suspension (12).

Immuno-localization of Ox-LDL in endothelial cells at 15 seconds after injection showed that Ox-LDL was primarily present in coated pits. The subsequent appearance of immuno-label in macropinocytotic vesicles suggested that the macropinocytotic structures arise by fusion from internalized coated vesicles and not by direct invagination of the plasma membrane. At later points in time immuno-label appeared dispersed over endosomal structures which were often connected to tubular structures devoid of immuno-label. Studies by Geuze et al. (15) demonstrated that in liver parenchymal cells, morphologically similar endosomal structures were present in which uncoupling of receptor and ligand, and subsequent sorting occurred. The tubular structures are suggested as being involved in the recycling of the receptors to the plasma membrane. 10 minutes following injection, immuno-

label also appears in low amounts in lysosomal structures, indicative of lysosomal degradation.

Since endothelial cells contribute to the uptake of both Ac-LDL and Ox-LDL and since two types of scavenger receptors are present on this cell type, we compared the internalization and processing of Ox-LDL by liver endothelial cells with that of Ac-LDL. At the electron microscopical level, immuno-localization of both ligands showed that similar structures were involved in the processing (chapters 2, 4). Using gold-conjugated Ac-LDL as a ligand, it could be established that at 30 minutes after injection the non-degradable gold marker strongly accumulated in the lysosomal compartment (chapter 4), which confirmed that the low amount of immuno-label noticed in the lysosomes reflected degradation of the modified LDL. Localization of Ox-LDL and Ac-LDL labeled with different fluorescent probes after simultaneous administration showed that the fluorescent probes appeared at the same spots, indicating that actually the same intracellular organelles were involved in the intracellular processing of both ligands in the liver endothelial cells.

The consequences of the involvement of different liver cell types in the uptake of Ox-LDL and Ac-LDL for the processing of the cholesterol moiety of these particles were studied (chapter 3). Ox-LDL labeled in its cholesteryl ester moiety was injected into rats which were permanently equipped with catheters in the heart, duodenum and bile. *In vivo*, the cholesteryl esters from [^{3}H]cholesteryl oleate labeled Ox-LDL are taken up rapidly from the circulation and almost quantitatively recovered in the liver (chapter 3). No differences were noticed in clearance and liver cell interaction of Ox-LDL labeled in its protein moiety or labeled in its cholesterol moiety. This indicates that Ox-LDL is internalized as an integral particle. At ten minutes after injection, unesterified cholesterol was already present in the liver indicating a rapid hydrolysis of the esterified cholesterol of Ox-LDL. This rapid hydrolysis is in agreement with the rapid appearance of Ox-LDL in the lysosomes as demonstrated by immuno-labeling techniques (chapter 2). At 1 h after injection of Ox-LDL the Kupffer cell associated radioactivity had declined to 32% of the maximal uptake value.

The rapid secretion of radiolabeled bile acids in the bile after injection of Ox-LDL, with a lag-phase of only 15 minutes, shows that cholesterol is rapidly transported from Kupffer cells to parenchymal cells. Since the biliary secretion of radioactivity from radiolabeled Ox-LDL up to 6 hours after injection was much higher than for radiolabeled Ac-LDL, we postulate that Kupffer cells transport the cholesterol to the parenchymal cells more efficiently than endothelial cells. Kupffer cells might utilize a more direct route to transport cholesterol to the parenchymal cells. Morphological examination of tissue used for autoradiography showed many contact areas between Kupffer cells and parenchymal cells which may enable such a rapid direct transfer of cholesterol (16).

Immuno-histochemical detection of Ox-LDL and localization of Ox-LDL by fluorescence microscopy showed that the same cell types and similar structures were involved in the uptake and processing of Ox-LDL in human liver as in the rat. The very consistent

fluorescent pattern observed in the different donors which differed in gender, age and health status, indicates that sufficient amounts of scavenger receptors are expressed on liver Kupffer and endothelial cells so that an efficient removal of this ligand is assured. It can therefore be concluded that Kupffer and endothelial liver cells form a highly effective, protective system against the occurrence of these atherogenic lipoprotein particles in the blood.

8.3 Uptake and processing of β-VLDL

β-VLDL is considered to be atherogenic, because *in vitro*, β-VLDL is able to induce an extensive accumulation of cholesteryl esters in macrophages leading to a foamy appearance (17). High levels of β-VLDL in the circulation of patients with type III hyperlipoproteinemia are accompanied by severe atherosclerosis at a young age (18).

Upon injection into rats, β-VLDL is rapidly cleared from the circulation by the liver, predominantly by liver parenchymal cells (1). β-VLDL can bind both to remnant- as well as to LDL receptors. Both receptors do recognize apoE which is abundantly present on β-VLDL. *In vivo*, the potential contribution of LDL- and remnant receptors to the uptake of β-VLDL is under debate, in the rat as well as in man. Furthermore, endogenous apoE, situated at the plasma membrane of parenchymal cells, was recently suggested to be involved in the rapid binding of β-VLDL (19). To study remnant receptor-mediated processes, lactoferrin was proposed as a very useful tool. Lactoferrin is able to inhibit the remnant receptor-mediated binding of β-VLDL and chylomicron remnants to parenchymal cells of normal rats (20).

Visualization of the localization of β-VLDL after injection into rats indicated an avid interaction with the parenchymal liver cells. This was observed by fluorescence microscopy and by immuno-electron microscopy (chapter 5). In accordance to previous biochemical data, Kupffer cells contributed only to a small extent to the uptake of β-VLDL (chapter 5). Pre-injection of lactoferrin clearly diminished the interaction of β-VLDL with the parenchymal cells, while the Kupffer cell interaction was unaffected, as was also observed in biochemical studies (20). Immuno-localization of lactoferrin showed a persistent presence of lactoferrin at the plasma membrane of the parenchymal cells up to 45 minutes after injection, suggesting that its presence on the microvilli of the parenchymal cells interferes with β-VLDL recognition. Since the amount of endogenous apoE on the parenchymal cells was not influenced by lactoferrin administration and no co-localization of lactoferrin and apoE was noticed excluding steric hindrance, we therefore concluded that the initial binding of β-VLDL by rat liver parenchymal cells is independent on the presence of apoE at plasma membrane.

To study the receptor specificity of the effect of lactoferrin, it was also applied in estradiol-treated rats. Estradiol-treated rats showed a selective up-regulation of 17-fold of the amount of LDL receptors on parenchymal liver cells (21). Administration of lactoferrin did

not effect the interaction of β-VLDL with parenchymal cells in estradiol-treated rats, while lactoferrin was present in similar amounts at the plasma membrane of the parenchymal cells as demonstrated by immuno-cytochemical staining. These data strongly suggest that in normal rats β-VLDL binds to the remnant receptor, while in estradiol-treated rats β-VLDL can circumvent lactoferrin inhibition by binding to an additional receptor, the LDL receptor.

Studies performed with human liver tissue blocks demonstrate that β-VLDL perfusion leads to a similar cellular distribution as was noticed in the rat. β-VLDL bound predominantly to the parenchymal cells and to a small extent to Kupffer cells (chapter 6). In order to study the relative involvement of the remnant- and LDL receptor in the human liver, tissue blocks were perfused with β-VLDL in the absence or presence of excess LDL and\or lactoferrin. Only addition of both excess LDL and lactoferrin was effective in inhibiting the interaction of β-VLDL with the parenchymal cells, suggesting that in human liver the LDL- and remnant receptor are capable to interact with β-VLDL. Immuno-localization of lactoferrin showed that this ligand was predominantly bound to the plasma membrane of the human parenchymal cells, which demonstrates the presence of a cell specific recognition site for lactoferrin, similarly as in rats. Immuno-localization of LDL receptors showed that in all human livers examined, variable, but significant amounts of LDL receptors were expressed on the parenchymal cells.

Interestingly, localization of fluorescently labeled β-VLDL in untreated and estradiol-treated rats differed with respect to initial distribution over the liver lobules and with respect to the time dependency of the intracellular appearance of fluorescence and the concomitant perisinusoidal disappearance (chapter 5). It is suggested that β-VLDL binds preferentially to LDL receptors, if LDL- and remnant receptors are simultaneously available. The rather slow appearance of fluorescence in the liver parenchymal cells of the estradiol-treated rats was in agreement with the lack of lipid accumulation in parenchymal cells, as was noticed in estradiol-treated rats following β-VLDL administration. It is, therefore, suggested that binding of β-VLDL to the LDL- or remnant receptor strongly effects the intracellular metabolism of β-VLDL. Regulation of the LDL- and remnant receptor might, therefore, have great consequences for the metabolic fate of β-VLDL. The LDL receptor on several cell types is regulated by intracellular cholesterol. β-VLDL is able to down-regulate the LDL receptor activity of the human parenchymal cells completely (22). The inhibitory effect noticed for the β-VLDL interaction with human parenchymal cells by physiological relevant concentrations of LDL (chapter 6) further indicates that the remnant receptor has to be present in order to clear atherogenic β-VLDL from the blood. Future research is needed to determine to what extent LDL- and remnant receptor levels are simultaneously regulated under high LDL conditions, and which factors influence this expression under normal, but also under pathological conditions.

8.4 *Reverse cholesterol transport and selective uptake*

According to the concept of Glomset (23), HDL transports cholesterol from peripheral tissues to the liver from where cholesterol can be excluded from the body by secretion into the bile. In an *in vivo* study (24), in accordance with this concept, evidence was provided that HDL can accept cholesterol from liver endothelial cells "pre-loaded" with Ac-LDL. Cholesterol was subsequently transported to the parenchymal cells and excreted into the bile as bile acids. Following injection of Ox-LDL labeled with ^{3}H-cholesteryl oleate a similar process was noticed, although Ox-LDL was predominantly internalized by Kupffer cells (chapter 3). Already at 10 minutes after injection of Ox-LDL, cholesteryl esters were hydrolyzed, and some ^{3}H-labeled unesterified cholesterol was already noticed in the circulation. Gradient centrifugation of the serum demonstrated that most of the radioactivity could be recovered in the HDL density range. The ratio of unesterified cholesterol to cholesteryl esters in the serum initially rapidly increased, but subsequently returned to lower values sustaining the uptake by HDL since HDL is the serum site of conversion of cholesterol into cholesteryl esters. The specific radioactivity of HDL's cholesterol was about 3.5 fold higher than for other lipoproteins, which supports the role of HDL as initial cholesterol acceptor. The very short lag-phase, of only 15 minutes, of the biliary secretion of radioactivity suggests, however, that apart from reverse cholesterol transport involving HDL, a more direct route is available for Kupffer cells to transport cholesterol to parenchymal cells (see 8.2).

In vivo, cholesteryl esters from HDL can be taken up by the liver in a so-called selective way which means that cholesteryl ester uptake exceeds that of the protein moiety. This phenomenon is only noticed in the parenchymal cells and not in liver endothelial and Kupffer cells (25). Since the characteristics of the binding sites on the liver cell types do not differ (26), it is clear that although the high affinity binding of HDL to cells may be a prerequisite, additional cellular properties are needed for selective cholesteryl ester uptake. Recently it was demonstrated that the liver secretes a neutral cholesteryl ester hydrolase into the circulation (27). It might be that this enzyme is involved in the preferential uptake of cholesteryl esters from HDL.

Light microscopic localization of the cholesteryl ester hydrolase revealed a strong immuno-staining of Kupffer cells and parenchymal cells (chapter 7). Localization of the enzyme in the cytosol of the parenchymal cells is in agreement with the synthesis and subsequent secretion of the bile salt-dependent cholesteryl ester hydrolase by this cell type. This should, however, be further evaluated at the electron microscopical level by localizing which intracellular organelles are labeled for this enzyme. It might also be that the enzyme in the parenchymal cells is involved in the intracellular processing of cholesteryl esters. Hydrolysis of cholesteryl esters of HDL appeared to be necessary for biliary secretion, since with ^{3}H-cholesterol oleyl ether labelled HDL the secretion of radioactivity into the bile was very slow (25).

The significance of the presence of cholesteryl ester hydrolase in Kupffer cells is even less clear. The ability of this cell type to process large amounts of cholesteryl ester-rich modified lipoproteins might be related to the presence of this enzyme, although also another very active cholesterol esterase with an acid pH optimum is present in Kupffer cells (28).

To study the fate of secreted cholesteryl ester hydrolase, radiolabeled cholesteryl ester hydrolase, obtained by recombinant DNA technology, was injected into the circulation. Electrophoresis of the rat serum demonstrated that the radiolabel became predominantly associated with HDL. However, cholesteryl ester hydrolase was rapidly cleared from the circulation and degraded, indicating that HDL only functions as a temporary serum carrier. The carrier function of lipoproteins might also explain the significant contribution of bone (20%) to the uptake of cholesteryl ester hydrolase, since significant amounts of chylomicron remnants are taken up by bone marrow macrophages (29). Further studies are required to evaluate the function of this enzyme in liver parenchymal and Kupffer cells, and in bone.

8.5 Conclusions

To study the different aspects of binding, internalization and processing of lipoproteins by the liver, a variety of complementary microscopical and biochemical techniques must be used.

Ox-LDL, which is predominantly taken up by Kupffer cells, is internalized by a highly complex membrane mechanism involving worm-like structures and lamellipodia. The presence of similar internalization structures in human and rat Kupffer cells sustains the general importance of this hitherto not described mechanism. An evaluation of the internalization and processing of modified LDL by liver endothelial cells indicated that, although several scavenger receptors might be involved, only one lysosomal directed pathway is present, characterized by four, ultrastructurally distinguishable, structures. Following internalization via coated vesicle formation, modified LDL is transported through an early endosomal and subsequently through a CURL-like structure into the lysosomal compartment.

Kupffer and endothelial cells are both capable to clear significant amounts of modified LDL which subsequently leads to lysosomal degradation of the apolipoproteins and secretion of the cholesterol moiety into the bile. Kupffer cells are equipped with a more efficient system to transport cholesterol to the parenchymal cells than endothelial cells.

Studies on the β-VLDL interaction with rat liver show that endogenous apoE as present at the plasma membrane is not involved in the initial recognition of β-VLDL by parenchymal cells. Furthermore, in rat the remnant receptor appears to be involved in the binding and uptake of β-VLDL while in man both the remnant- and LDL receptors are involved in the binding of β-VLDL as was evidenced from competition experiments. Although β-VLDL does preferentially bind to LDL receptors, the strong fluctuation noticed in the amount of LDL

receptors and the competition of physiologically relevant amounts of LDL indicate that also in man the remnant receptor may be highly relevant for the uptake of β-VLDL from the circulation.

In general it is ultrastructurally demonstrated that the liver contains a highly effective mechanism for the processing of atherogenic lipoprotein particles involving several receptors, cell types, internalization mechanisms and processing pathways, making it an important tissue for preventing atherosclerosis.

8.6 References

1. Harkes L, Van Duijne A, Van Berkel ThJC. Eur J Biochem 1989;180:241-48.
2. Wisse E. In: Wisse E, Knook DL. Kupffer cells and other liver sinusoidal cells. Elsevier/North Holland Biomedical Press Amsterdam, 1977:33-60.
3. Pastan I, Willingham MC. Trends Biochem Sci 1983;8:250-54.
4. Nagelkerke FJ, Barto KP, Van Berkel ThJC. J Biol Chem 1983;258:12221-27.
5. Kleinherenbrink-Stins MF, van der Boom J, Brouwer A, Van Berkel ThJC, Knook DL. Ultramicroscopy 1988;24:439A.
6. Renaud G, Hamilton RL, Havel RJ. Hepatology 1989;9:380-92.
7. Fodor I, Egyed A, Lelkes G. Eur. J Cell Biol 1986;42:74-78.
8. Reynolds GD, StClair RW. Am J Pathol 1985;121:200-11.
9. Goldstein JL, Ho YK, Basu SK, Brown MS. Proc Natl Acad Sci USA 1979;76:333-37.
10. Palinski W, Rosenfeld ME, Yla Herttuala S, Gurtner GC, Socher SS, Butler SW, Parthasarathy S, Carew TE, Steinberg D, Witztum JL. Proc Natl Acad Sci USA 1989;86:1372-76.
11. Kita T, Nagano Y, Yokoda M, Ishii K, Kume N, Ooshima A, Yoshida H, Kawai C. Proc Natl Acad Sci USA 1987;84:5928-31.
12. Van Berkel ThJC, De Rijke YB, Kruijt JK. J Biol Chem 1991;5: 2282-89.
13. Heinecke JW, Suits AG, Aviram M, Chait A. Arteriosclerosis and Thrombosis 1990;11:1643-1651.
14. Hoff HF, Cole TB. Lab Invest 1991;64:254-63.
15. Geuze HJ, Slot JW, Strous GJAM, Lodish HF, Schwartz AL. Cell 1983;32:277-87.
16. Pieters MN, Blauw B, Esbach S, Brouwer A, Knook DL, Van Berkel ThJC, Roholl PJM. submitted.
17. Goldstein JL, Ho YK, Brown MS, Innerarity TL, Mahley RW. J Biol Chem 1980;255:1839-48.
18. Frederickson DS, Levy RI, Lindgren FT. J Clin Invest 1969;47:2446-57.
19. Hamilton RL, Wong JS, Luke S, Guo S Krisans S, Havel RJ. J Lipid Res 1990;31:1589-1603.
20. Van Dijk MCM, Ziere GJ,, Boers W, Linthorst C, Bijsterbosch MK, Van Berkel ThJC. Biochem J 1991;279:863-70.
21. Harkes L, Berkel ThJC. FEBS letters 1983;154:75-80.
22. Kamps JAAM, Kuiper J, Kruijt JK, Van Berkel ThJC. FEBS Lett 1991;287:34-38.
23. Glomset JA. J Lipid Res 1968;9:155-67.
24. Bakkeren HF, Kuipers F, Vonk RJ, van Berkel ThJC. Biochem J 1990;268:685-91.
25. Pieters MN, Schouten D, Bakkeren H, Esbach S, Brouwer A, Knook DL, Van Berkel ThJC. Biochem J 1991;280:359-65.
26. Schouten D, Kleinherenbrink-Stins MF, Brouwer A, Knook DL, van Berkel ThJC. Biochem J 1988;256,615-21.
27. Winkler KE, Harrison EH, Marsh JB, Glick JM, Ross AC. Biochim Biophys Acta 1992;1126:151-58.

28. Van Berkel THJC, Kruijt K, Koster JF. Eur J Biochem 1975;58:145-52.
29. Hussain MM, Mahley RW, Boyles JK, Lindquist PA, Brecht WJ, Innerarity TL. J Biol Chem 1989;264:17931-38.

Summary

In the present thesis the uptake and processing of several atherogenic lipoproteins by the liver were studied. Special attention was given to the use of light and electron microscopical techniques to characterize the cell types and mechanisms involved in binding, internalization and processing.

In chapter 2 the cell types and processing mechanisms responsible for the Ox-LDL uptake by human and rat liver are described. Ox-LDL is considered to be highly atherogenic since several lines of evidence indicated that LDL modified by oxidation accumulates in atherosclerotic lesions. It was demonstrated that Ox-LDL is predominantly taken up by Kupffer cells and to a lesser extent by liver endothelial cells. Kupffer cells internalized Ox-LDL by a highly complex membrane mechanism involving worm-like structures and lamellipodia. Endothelial cells internalized Ox-LDL by coated vesicle formation. Uptake of Ox-LDL by both cell types led to a rapid lysosomal processing involving different kinds of endosomal structures. No differences were noticed in the processing of Ox-LDL in human and rat liver, indicating that both species exhibit an efficient mechanism to clear atherogenic particles from the circulation.

In chapter 3 the processing of the cholesteryl ester moiety of Ox-LDL was studied in rats equipped with permanent catheters in the heart, duodenum and bile. The cholesteryl esters were rapidly cleared from the circulation predominantly by the Kupffer cells leading to a rapid hydrolysis. Fifteen minutes after injection radiolabel appeared in the bile as bile acids, indicating that Kupffer cells are able to transport cholesterol very efficiently to parenchymal cells. HDL was demonstrated to function as a serum cholesterol acceptor for the radiolabeled cholesterol, but, another mechanism might also be involved in the rapid transport of cholesterol from Kupffer to parenchymal cells. The rapid processing of cholesteryl esters from Ox-LDL leads to a cumulative biliary appearance of almost 60% of the injected dose at 72 h after injection, indicating that uptake of Ox-LDL by the liver is efficiently coupled with biliary secretion.

In chapter 4 the internalization and processing of modified LDL by liver endothelial cells were examined. Although different scavenger receptors are involved in the binding of Ox-LDL and Ac-LDL, no differences were noticed at the ultrastructural level between the organelles involved in the uptake and processing of Ox-LDL and Ac-LDL. Double-labeling experiments with Ox-LDL and Ac-LDL, labeled with different fluorescent probes, indicated that actually the same organelles were involved in the processing of both ligands. It was concluded that the scavenger receptor-mediated uptake of modified LDL by rat liver endothelial cells involved four morphologically distinguishable stages (coated vesicle

formation, early and late endosomal processing, and lysosomal degradation) which represent a highly effective catabolic route.

In chapter 5 the interaction of β-VLDL with the rat liver was studied. β-VLDL appears to bind predominantly to parenchymal cells and to a lesser extent to Kupffer cells. The interaction of β-VLDL with the parenchymal cells was independent of endogenous apoE at the plasma membrane of the parenchymal cells, and, furthermore, could be modulated by estradiol treatment of rats. Estradiol treatment resulted in the selective up-regulation of LDL receptors on liver parenchymal cells. The inhibitory effect of lactoferrin, an inhibitor of the remnant receptor interaction, as evidenced in untreated rats, could not be demonstrated in estradiol-treated rats, indicating that in rats, under normal conditions, β-VLDL binds to remnant receptors, while in estradiol-treated rats β-VLDL is able to bind to LDL receptors. Uptake by the remnant receptor led to lysosomal degradation and a concomitant increase in the amount of lipid vacuoles, indicating that re-allocation of lipid, i.e. hydrolysis and re-esterification forms part of the processing route of β-VLDL in the liver parenchymal cells.

The involvement of remnant receptors and LDL receptors in the binding of β-VLDL was demonstrated in human liver in chapter 6 by *ex situ* competition experiments with excess lactoferrin and LDL, respectively. Since only simultaneous addition of excess LDL and lactoferrin resulted in a strong inhibition of the parenchymal cell interaction of β-VLDL, it is suggested that both the LDL- and remnant receptor must be blocked for an effective inhibition of the β-VLDL association with parenchymal cells. Immuno-staining for LDL receptors showed that parenchymal cells do express LDL receptors, although the amount of immuno-staining varies considerably. Immuno-localization of administered lactoferrin demonstrated that this ligand bound predominantly to the parenchymal cells, indicating a cell specific binding site. The importance of the remnant receptor in the uptake of β-VLDL in humans was indicated by the strong fluctuation of LDL receptors on the parenchymal cells and by the competition of physiological relevant LDL concentrations for the LDL receptor.

In chapter 7 the localization and fate of cholesteryl ester hydrolase were studied in the rat. The enzyme was demonstrated to be present in parenchymal and Kupffer cells. The function in the parenchymal cells could be related to the intracellular processing of cholesteryl esters or to synthesis and subsequent secretion. In the blood compartment cholesteryl ester hydrolase was associated with HDL. This might be a functional localization related to the preferential uptake of cholesteryl esters of HDL by liver parenchymal cells, or just a carrier function, since HDL is abundantly present in rat serum. Intravenously administered cholesteryl ester hydrolase is predominantly taken up by the liver, mainly by the Kupffer cells, and subsequently degraded, although unexpectedly, a significant amount of the enzyme was taken up by bone.

In chapter 8 the most important results are summarized and discussed in the framework of the role of the various liver cell types in the uptake and processing of atherogenic lipoproteins.

From the studies presented in this thesis it can be concluded that complementary morphological and biochemical techniques have to be applied to understand the highly complex mechanisms which are active in the liver. The liver internalizes and processes several lipoproteins very efficiently by the involvement of parenchymal, endothelial and Kupffer cells, by the expression of several receptors, and by the action of several internalization and processing mechanisms, thereby protecting the body against circulating atherogenic lipoproteins.

Samenvatting

De in dit proefschrift beschreven studies hadden tot doel om inzicht te verwerven in de opname- en verwerkingsmechanismen van lipoproteïnen in de lever. Er is met name gebruik gemaakt van licht- en electronenmicroscopische methoden om de celtypen en de mechanismen in de lever van de rat en de mens te karakteriseren.

Lipoproteïnen zijn bolvormige deeltjes die opgebouwd zijn uit vetten en eiwitten. De functie van lipoproteïnen is vetten te transporteren door het bloed en de lymfe. Om de vetten (cholesterol en triglyceriden) oplosbaar te houden in het waterige milieu van het bloed en de lymfe, worden ze omgeven door een mantel van fosfolipiden en eiwitten. Op basis van de dichtheid van de lipoproteïnen worden verschillende klassen onderscheiden. Uit bevolkingsonderzoek is gebleken dat met name cholesterol uit de lage dichtheidsklasse, het zgn. LDL, een belangrijke risicofactor vormt op de ontwikkeling van hart- en vaatziekten, terwijl cholesterol in de hoge dichtheidsklasse, het zgn. HDL, een beschermende werking lijkt te hebben. Dit hangt vermoedelijk samen met de functie van het LDL en het HDL. LDL verzorgt het transport van cholesterol vanuit de lever naar de rest van het lichaam, terwijl HDL, cholesterol in de periferie opneemt en vervolgens naar de lever transporteert, waar het cholesterol hergebruikt of uitgescheiden kan worden. De lever is het enige orgaan dat in staat is om cholesterol uit het lichaam te verwijderen. Naast HDL worden ook andere lipoproteïnen-klassen in de lever opgenomen, waarbij verschillende leverceltypen een rol spelen, te weten parenchymcellen, Kupffercellen en endotheelcellen.

In hoofdstuk 2 zijn de leverceltypen en de verwerkingsmechanismen beschreven die betrokken zijn bij de opname van geoxideerd-LDL (Ox-LDL). Ox-LDL wordt als zeer gevaarlijk beschouwd, aangezien verschillende onderzoeken hebben aangetoond dat Ox-LDL in de vaatwand ophoopt in zgn. atherosclerotische plaques. Met behulp van microscopische technieken werd in hoofdstuk 2 aangetoond dat Ox-LDL vnl. door lever Kupffercellen wordt opgenomen en voor een deel door de endotheelcellen. Kupffercellen namen Ox-LDL op via een zeer complex membraanmechanisme waarbij zgn. "worm-like structures" en lamellipodia betrokken zijn. Endotheelcellen namen Ox-LDL op via een reeds eerder beschreven mechanisme, de zgn. "coated vesicle" vorming. Opname van Ox-LDL door Kupffercellen en endotheelcellen leidde tot een snel transport via verschillende endosomale structuren naar de lysosomen waar de deeltjes vervolgens werden afgebroken. Er werden geen verschillen waargenomen tussen de verwerking van Ox-LDL in de rat en in de mens, wat duidt op het bestaan van een efficiënt mechanisme om schadelijke lipoproteïnen uit het bloed te verwijderen in de beide species.

In hoofdstuk 3 is de verwerking van het cholesterol deel van het Ox-LDL bestudeerd in de rat. Het gemerkte-cholesterol van het Ox-LDL werd na injectie snel uit het bloed verwijderd. Het grootste deel kwam in Kupffercellen terecht, waar het cholesterol omgezet werd van de opslagvorm naar vrij cholesterol. Al vijftien minuten na injectie, werd cholesterol in de gal waargenomen in de vorm van galzouten. Dat betekent op basis van de leverstructuur dat Kupffercellen in staat zijn om het cholesterol op zeer efficiënte wijze naar parenchymcellen te transporteren. HDL bleek in het bloed als tussengastheer voor het cholesterol uit de Kupffercellen te fungeren, hoewel daarnaast ook een ander mechanisme betrokken zou kunnen zijn bij het zeer snelle transport van het cholesterol van Kupffer- naar parenchymcellen. 72 uur na inspuiting van Ox-LDL werd 60% van de geïnjecteerde dosis in de gal aangetroffen, wat betekent dat de opname van Ox-LDL door de lever gekoppeld is aan een zeer efficiënte galuitscheiding.

In hoofdstuk 4 is de opname en verwerking van gemodificeerde LDL-partikels door de leverendotheelcellen onderzocht. Hoewel verschillende bindingseiwitten betrokken zijn bij de binding van geoxideerd en geacetyleerd-LDL (Ac-LDL), werden geen verschillen gevonden tussen de organellen die betrokken waren bij de opname en verwerking van het Ox-LDL en het Ac-LDL. Dubbel-labelingsexperimenten waarbij Ox-LDL en Ac-LDL gemerkt werden met verschillende fluorescerende merkers, toonden zelfs aan dat dezelfde structuren betrokken zijn bij de verwerking van de beide liganden. In de loop van de tijd verplaatste de gemodificeerde LDL-partikels zich door de leverendotheelcellen via 4 morfologisch onderscheidbare structuren, 1) "coated vesicles" 2) vroege endosomen 3) late endosomen en 4) lysosomen. Op basis van de snelheid waarmee de deeltjes werden afgebroken werd geconcludeerd dat de beschreven structuren tezamen een zeer efficiënte afbraakroute vertegenwoordigen.

In hoofdstuk 5 is de interactie van β-VLDL met de rattelever bestudeerd. β-VLDL is een deeltje dat voorkomt in mensen met een bepaalde genetische afwijking en in cholesterol-gevoede dieren. Vanwege de extreme vetophoping die β-VLDL kan veroorzaken, wordt dit deeltje als zeer schadelijk aangemerkt. β-VLDL kan door twee bindingseiwitten herkend worden, te weten de LDL- en de remnant-receptor. In hoofdstuk 5 werd met behulp van microscopische technieken vastgesteld dat β-VLDL vnl. aan de parenchymcellen bindt en slechts voor een klein deel aan Kupffercellen. Binding van β-VLDL aan de parenchymcellen bleek onafhankelijk te zijn van reeds aanwezig apoE op de plasmamembraan van de parenchymcellen. Bovendien bleek de interactie van β-VLDL met de parenchymcellen te beïnvloeden door ratten een hormoonbehandeling te geven met estradiol. Deze behandeling leidt tot een selectieve toename van LDL-receptoren op parenchymcellen. De remming door toevoeging van lactoferrine (een competatief deeltje voor de remnant-receptor) op de binding van β-VLDL aan de parenchymcellen in onbehandelde ratten werd niet waargenomen in estradiol-behandelde ratten. Dit wijst op het feit dat onder normale condities β-VLDL aan remnant-receptoren bindt, terwijl in estradiol-behandelde ratten β-VLDL aan de LDL-

receptor bindt. Opname via de remnant-receptor had een snelle lysosomale afbraak tot gevolg in de parenchymcellen, terwijl tegelijkertijd een toename werd waargenomen in het aantal vet-vacuoles. Dit wijst op de mogelijkheid dat de verwerking van de vetten van β-VLDL in de lysosomen en de daaropvolgende opslag in een ander deel van de cel, onderdeel vormen van de verwerkingsroute van β-VLDL in de leverparenchymcellen.

De betrokkenheid van remnant- en LDL-receptoren in de binding van β-VLDL in de humane lever is in hoofdstuk 6 aangetoond door competitie-experimenten uit te voeren met een overmaat aan lactoferrine en LDL. Aangezien alleen toevoeging van beiden, LDL en lactoferrine, de interactie van β-VLDL met de leverparenchymcellen blokkeerde, lijkt het erop dat beide receptoren, de LDL- en de remnant-receptor, geblokkeerd moeten worden voor een effectieve remming van de binding van β-VLDL aan de parenchymcellen optreedt. Aankleuring van de LDL-receptoren toonde aan dat parenchymcellen deze receptor inderdaad tot expressie brengen, maar bovendien dat de hoeveelheid receptoren sterk varieerde tussen de verschillende leverdonoren. Localisatie van het aangeboden lactoferrine toonde aan dat dit ligand voornamelijk aan de parenchymcellen bindt, wat duidt op een celspecifieke bindingsplaats. Het belang van de remnant-receptor in de opname van β-VLDL in de mens wordt aangegeven, ten eerste door de sterke fluctuatie die wordt waargenomen in het aantal LDL-receptoren op de parenchymcellen en ten tweede doordat een van nature voorkomende LDL-concentratie reeds in staat is om de interactie van β-VLDL met de LDL-receptor te verhinderen.

In hoofdstuk 7 wordt de localisatie en het lot van het enzym cholesterolesterase bestudeerd in de rat. De aanmaak van dit enzym in de lever is pas kort geleden beschreven en zou kunnen samenhangen met de opname van HDL-cholesterol in de lever. Het enzym werd met behulp van microscopische technieken aangetoond op Kupffer- en parenchymcellen. De functie in parenchymcellen kan samenhangen met de intracellulaire verwerking van cholesterol of met de eerder gesuggereerde aanmaak. In het bloed is het enzym gebonden aan HDL. Dit zou een functionele betekenis kunnen hebben in het licht van de verwerking van cholesterol uit HDL of slechts wijzen op het feit dat HDL in staat is om het enzym te transporteren, aangezien ook andere lipoproteïnen-klassen in staat zijn om dit enzym te binden. In het bloed toegediend cholesterolesterase wordt voornamelijk door de lever opgenomen door de Kupffercellen waar het vervolgens werd afgebroken. Onverwacht bleek dat ook een groot deel van het ingespoten enzym in botten terecht kwam. De functie in het bot is momenteel onbekend.

In hoofdstuk 8 zijn de belangrijkste resultaten samengevat en bediscussieerd in het kader van de rol van de verschillende leverceltypen in de opname en verwerking van schadelijke lipoproteïnen. Uit de in dit proefschrift gepresenteerde resultaten kan geconcludeerd worden dat elkaar aanvullende biochemische en morfologische technieken gebruikt moeten worden om de zeer complexe mechanismen in de lever te karakteriseren. Daarnaast bleek dat de lever in staat is om verschillende typen lipoproteïnen uit de circulatie op te nemen en te verwerken

via zeer efficiënte mechanismen. De betrokkenheid van verschillende celtypen, receptoren en opname- en verwerkingsmechanismen leidt tot een bescherming van het organisme tegen circulerende schadelijke lipoproteïnen.

Abbreviations

Ac-LDL	acetylated low density lipoprotein
apo	apolipoprotein
BSA	bovine serum albumin
β-VLDL	β-migrating very low density lipoprotein
CE	cholesterol ester
CURL	compartment of uncoupling of receptor and ligand
DAB	diaminobenzidine tetrahydrochloride
DiI	dioctadecyl-tetramethyl indocarbocyanine percholate
DiO	dioctadecyloxacarbo-cyanine perchlorate
EC	endothelial cell
FC	unesterified cholesterol
GA	glutaraldehyde
HDL	high density lipoprotein
HL	hepatic lipase
KC	Kupffer cell
LDL	low density lipoprotein
LPL	lipoprotein lipase
LRP	low density lipoprotein receptor-related protein
Ox-LDL	oxidized low density lipoprotein
PBS	phosphate-buffered saline
PC	parenchymal cell
PF	paraformaldehyde
PIA	polyinosinic acid
VLDL	very low density lipoprotein

Curriculum Vitae

De schrijver van dit proefschrift werd op 17 april 1963 geboren te Goirle. Na het behalen van het VWO-diploma aan de Rijswijkse openbare scholengemeenschap werd in 1982 aangevangen met de studie biologie aan de Rijksuniversiteit Leiden. Als differentiatierichting werd gekozen voor medische-biologie met als hoofdvak celbiologie. Doctoraalstages werden gelopen aan de Rijksuniversiteit Leiden, vakgroep celbiologie onder leiding van Dr. W. de Priester en aan het TNO Instituut voor Experimentele Gerontologie onder leiding van Dr. W. Seifert. Na het behalen van het doctoraalexamen werd in 1988 begonnen met een promotie-onderzoek aan het voormalige TNO Instituut voor Experimentele Gerontologie (sinds april 1991 gefuseerd met twee andere instituten onder de naam Instituut voor Verouderings- en Vaatziekten Onderzoek TNO, alg. directeur: prof. dr. D.L. Knook). Dit onderzoek werd uitgevoerd in samenwerking met de sectie Biofarmacie van de Rijksuniversiteit Leiden (hoofd: prof. dr. Th.J.C. van Berkel). In oktober 1993 is aangevangen met een opleiding tot logistiek specialist bij Siemens Nixdorf.